EFFECTS OF WEATHERING IN THE ROCK AND ROCK MASS PROPERTIES AND THE INFLUENCE OF SALTS IN THE COASTAL ROADCUTS IN SAINT VINCENT AND DOMINICA

XSA A. CABRIA
March, 2015

SUPERVISORS:
Assoc. Prof. H.R.G.K. Hack
Prof.V.G. Jetten

EFFECTS OF WEATHERING IN THE ROCK AND ROCK MASS PROPERTIES AND THE INFLUENCE OF SALTS IN THE COASTAL ROADCUTS IN SAINT VINCENT AND DOMINICA
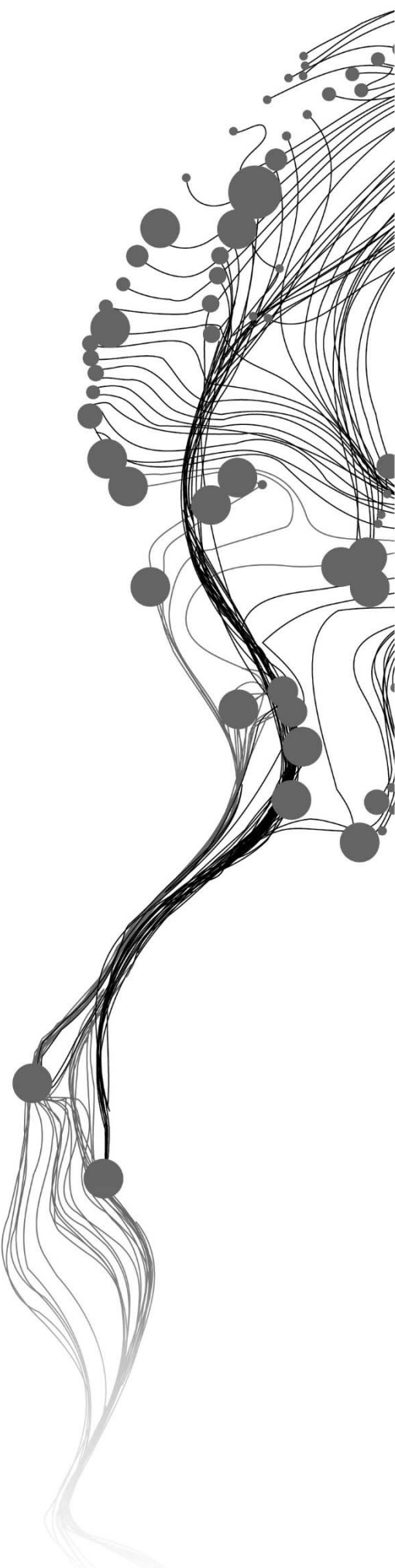
XSA A. CABRIA
Enschede, The Netherlands, March, 2015

SUPERVISORS:
Assoc. Prof. H.R.G.K. Hack
Prof.V.G. Jetten

THESIS ASSESSMENT BOARD:
Prof. Dr. F.D. van der Meer (Chair)
Dr. Ir. S. (Siefko) Slob (External Examiner, Witteveen and Bos, Engineering Consultancy Firm)

ABSTRACT

Weathering in man-made slopes, such as road cuts, is said to be accelerated by stress relief and the method of excavation and this will influence the rate at which the rock mass properties deteriorate in the engineering lifetime of the slope. It is shown in this study that the response of different volcanic rock and the associated volcanoclastic rocks respond to weathering differently, but still reflective of the weathering susceptibility dictated by their mineral composition. In general, the rocks show consistent reduction of the intact rock strength and conditions of the discontinuity. The discontinuity spacing however increases from moderate weathering degree to complete weathering degree.

Indicators of salt weathering are observed in some of the rock masses exposed in the coastal areas of Saint Vincent and Dominica. The matrix of the lahar deposits show indications of granular disintegration while andesite and dacite clasts exhibit disintegration through scaling. Honeycomb structures and the tafoni are seen in the andesite lava flow unit. In the ignimbrites and block-and-ash flow deposits, the presence of the hardened surface can also be attributed to the influence of salts. The estimated rate of cavity development in andesites is at 2.5 cm/year while the estimated rate of retreat of the matrix materials of the lahar deposits is 30 cm in 55 years.

ACKNOWLEDGEMENTS

TABLE OF CONTENTS

LIST OF FIGURES

LIST OF TABLES

1. INTRODUCTION

1.1. Research Background

The weathering phase is a preparatory stage of slope denudation wherein significant modification in the engineering properties of intact rocks and the rock masses occur (Dearman, 1974). These changes are dependent on the intrinsic properties of the rock materials and on the prevailing environmental conditions. (Hencher & McNicholl, 1995; ANON., 1995; Price, 1995; Hack et al., 2003; Huisman, 2006; Tating et al., 2013). Newly exposed rock masses resulting from engineering works, also referred to as man-made slopes, are subject to accelerated deterioration due to the release of confining pressure or stress relief, and general disruption of its quasi equilibrium state that leads to intensified weathering right after excavation (Hack & Price, 1997; Nicholson, 1997; Niini et al., 2001; Huisman, 2006). Despite the general knowledge that stress relief and weathering inevitably lead to rock decay and eventual slope failure, it is still poorly integrated in the formulation of geotechnical models and oftentimes overlooked as a cause of repeated failure (Hencher & McNicholl, 1995; Lee & Hencher, 2009). The limited understanding and appreciation, as well as the limited quantitative information, on stress relief and weathering are the main reasons why these processes are oftentimes neglected or given little consideration in slope designs (Tating et al., 2013).

The effects of stress and weathering are highly influenced by the composition of the rocks and on the prevailing environmental conditions. To gain more understanding on this field of study, this research focuses on the changes in the engineering properties due to stress relief and weathering of rock masses along in roadcuts in the Saint Vincent and Dominica. Both of these islands are underlain by young volcanic and volcanoclastic rocks and are located in a warm, humid environment. In addition, the main roads interconnecting most of the towns mainly traverse coastal areas. In a typical rocky coast profile, most of the coastal roadcuts are located in the sea spray zone and thus the rock masses are likely influenced by marine salts carried by sea sprays (Mottershead, 2013). Previous studies have shown the important role of salts in landscape development (Johannessen et al., 1982; Rodriguez-Navarro & Doehne, 1999; Hampton & Griggs, 2004; Lawrence et al., 2013) and their deleterious effects on rocks used as building and construction materials (Benito et al., 1993; Benavente et al., 2007; Zedef et al., 2007; Kamh, 2011). Therefore, the rock masses that are exposed to sea sprays are also investigated for any indications of salt influence and its implication in their engineering properties.

1.2. Research problem

Slope stability problems related to weathering results from the failure to recognize during site investigation and to consider in the design phase that a particular slope consists of zones with different degree of weathering and hence with varying engineering properties that also change as the rock mass further weathers through time (Hencher & McNicholl, 1995). Previous studies have shown the relationship of weathering with the degradation of the geotechnical properties of rock masses (e.g. Gupta & Rao, 2000;Tuğrul, 2004;Arıkan, 2007). These studies have generated a lot of information collected from extensive laboratory analyses. However, these laboratory tests are very expensive to conduct and the collection and transport of samples to ensure that these meet the criteria (e.g. enough volume, representativeness and whether disturbed of undisturbed etc...) of each test is quite challenging. Field observation and *in situ* assessments combined with empirical models are sufficient in the initial stages of site investigation.

Landslides in natural slopes and failures in man-made slopes are common in Saint Vincent and Dominica. More than conducting slope stability assessment in these islands, this research uses the slope stability parameters to determine the weathering dependent changes in the rock properties control the strength of the studied rock masses This is done using the empirically-derived weathering reduction parameter *(WE)* introduced by Hack (1998) and imbedded in the Slope Stability Probability Classification (SSPC). This classification allows for quantitative evaluation of changes in the intact rock and rock mass engineering properties from their undisturbed states to their current conditions. Using the same principle, the future values of these properties are also be estimated and incorporated to determine future slope stability scenarios.

In both islands, some of the road cuts are located very close to the sea and thus, are exposed to the influence of marine salts carried by sea sprays (Mottershead, 1989). Some of the features that are known to be associated with salt influence, such as honeycomb structures, tafone, scaling and pitting or rock surfaces, are also present in some of the exposures in the coastal areas in both islands. Previous studies have shown that salts have negative impact on the stability of coastal cliffs (Hampton et al., 2004; Lawrence et al., 2013). The presence of such features indicates that the rock masses are affected by salts and this is likely to have implications on their engineering properties.

1.3.   Constraints and limitations

The climatic and geologic settings of these two islands however provide constraints and limitations that can potentially become sources of data uncertainty.

- The extensive chemical weathering typical in young, volcanic terrains in tropical regions (Aristizábal et al., 2005; Jain, 2014), high erosion rate (Radet al., 2013) and the thick vegetation cover resulted to gaps in the observed weathering grades for most of the rocks.

- Because volcanism in these islands has been very active in the recent geologic times (Smith et al., 2013), most exposures consist of various facies of pyroclastic materials. These are highly heterogeneous and are hardly fitting in the existing weathering rock mass classification methods. Price (1995) stressed that before relating the weathering grade to the measured engineering parameters, it is important to note that a systematic description of the existing weathering conditions of the rocks is necessary. Furthermore, the heterogeneity also causes deviation from the general trends of the weathering-induced changes in the engineering properties of the rocks. The ubiquity of the pyroclastic materials makes the sampling points biased to this rock types over the others.

- Especially in the case of Dominica, the good rock exposures are located in high, steep slopes where rock fall is regularly occurring. This limits the ease and thus, accuracy in the level of observation.

1.4.   Objectives

The general objective of this research is to determine the effect of weathering on the geotechnical properties of rock masses and the possible influence of salts in the rock masses exposed in the coastal roadcuts in Saint Vincent and Dominica.

The specific objectives are:

- To determine the engineering parameters of rock masses in selected slopes using the Slope Stability Probability Classification (SSPC) method and relate this to the degree of weathering of the rock masses
- To describe the weathering-time relationship from trends exhibited by the results of the rock mass classification to the length of year the slope has been exposed
- To determine influence of salts and infer on the implications in the engineering properties of the rocks and rock masses in the coastal roadcuts

1.5. Research questions

- What is the applicability of the weathering classification recommended in BS5930 to the rock masses in Saint Vincent and Dominica?
- How are the values of the rock properties changing with increasing degree of weathering?
- What are the factors influencing the weathering intensity rate of the rock properties in the studied rock masses?
- How are the weathering classes distributed among the SSPC stability classes?
- What are the distinct features in the exposures influenced by sea sprays and what do these indicate?
- What are the implications of salt influence on the engineering properties of the affected rock masses?

1.6. Thesis structure

Chapter 1- Introduction: Provides the research background and the statement of the research problem, the objectives, and the questions addressed in the research.

Chapter 2 - Literature review: Provides a discussion of results and facts obtained from previous works related to the weathering process and its relationship with the engineering properties of the intact rock and rock masses, including presence of salt and salt weathering processes.

Chapter 3 - Description of the study area: Describes the topography, climate, location, and the general geology of Saint Vincent and Dominica.

Chapter 4 - Methodology: Describes the general approach of the research, the classification schemes used for weathering and strength, the SSPC parameter values, the laboratory procedures and the equations The equations are used calculating the geotechnical parameters and determining the slope stability (mostly from the SSPC method) and the weathering rates used and followed in the research.

Chapter 5 - Slope Descriptions and Characterizations: Presents samples of field characterization of slopes. The complete description included in Appendix 1.

Chapter 6 - Results and Discussion: Includes presentation and discussion of the results of the data analysis on the effects of weathering on the engineering properties of rock masses, weathering rate and stability probability classification (SSPC).

Chapter 7 - Discussion on influence of salts: Includes the field observation in exposures with indicators of salt influence observed in the field and their implication on the engineering properties of the affected rock masses.

Chapter 8 - Conclusions and recommendations: Answers to the research questions and recommendations for future research

2. LITERATURE REVIEW

2.1. Stress relief

The change in the stress regime following the removal of confining pressure is one of the most dominant deterioration mechanisms affecting man-made slopes upon excavation (Huisman, 2006; Tating et al., 2014). Stress relief can result to the opening of existing cracks and development of new ones within the intact rocks as illustrated in Figure 1 (Hack & Price, 1997; Price, 2009). As a result, the rock mass becomes further exposed to weathering as increased discontinuities allow more water to ingress and plant roots to reach a larger area of the rock mass (Price, 1995). Lateral stress relief upon excavation in over-consolidated clay materials cause outward movement (Waltham, 2002). Secondary stress relief is in the form of unloading after erosion where a set of discontinuities develops parallel to the ground surface (Gamon, 1983) or parallel to the erosion surface (Price, 1995).

2.2. Weathering process

Weathering is the *in situ* breakdown of intact rock and rock masses due to physical and chemical processes under the influence of atmospheric and hydrospheric factors (Hack, 2006) and this implies decay and change in state from an original condition to a new one (Price, 2009). It is an irreversible response of soil and rock materials to their natural or artificial exposure to the near surface engineering environment (Price, 1995). The changes resulting from weathering is a product of the interplay of structure and type of parent material, groundwater, climate, time, topography and organisms (Dearman, 1974). Through time, weathering can also be influenced by changes in land use and in the quality of the percolating groundwater as an effect of chemicals from sewage, fertilizers etc… (Hack & Price, 1997).

2.2.1. Physical or mechanical weathering

Physical or mechanical weathering is the disintegration of a rock material into smaller pieces without any change in the original property of the rock. It usually results from temperature and pressure changes. The main mechanisms for this type of weathering are wedging, exfoliation and abrasion. In the tropics, repeated drying and wetting results to heaving and eventual break down of the rocks. Exfoliation occurs when rock layers break apart due to the removal of confining pressure such as when slopes are excavated (Huisman et al., 2011) or eroded (Gamon, 1983). Abrasion is the physical grinding of rock fragments either by action of water or air. Several mechanical weathering processes, such as salt weathering (more details in Section 2.3), involve the growth of a solid substance along the confining space of a pore exerting tensile stress along the pore walls and which exceeds the tensile strength of the pore leading to splitting and eventual disintegration of the rocks (Wellman & Wilson, 1965; Matsukura & Matsuoka, 1996).

2.2.2. Chemical weathering

This process involves the formation of new minerals (clays and salts) when minerals react with water. This process is more favoured in warm, damp, climates. The most common processes of chemical weathering are dissolution, hydrolysis and oxidation. Dissolution mainly occurs when certain minerals are dissolved by acidic solutions and the most common example is the formation of caves in limestones due

to the dissolution of calcite by carbonic acid. Hydrolysis occurs when pure water ionizes and reacts with silicate minerals and it is assumed that the original
mineral is transformed to a totally new mineral. Oxidation or rusting involves the combination of certain metals with oxygen allowing electron transfer leading to the formation of crumbly and weak rocks(Colman & Dethier, 1986).

2.2.3. Biological weathering

Biological weathering encompasses weathering caused by plants, animals and microbes. For examples, some organisms release acidic and chelating compounds as well as inorganic nutrients that enhance chemical weathering. A species of lichens was found to cause incipient weathering of basalts by glass dissolution and precipitation of secondary carbonates and oxides (Meunier et al., 2014). Furthermore, microorganisms can oxidize organic or mineral compounds that they use as source of energy for their growth and reproduction(Lerman & Meybeck, 1988). The ability of large plants species like trees to thrive in rocky slopes that their roots and the associated mircroorganisms can potentially induce mineral weathering (Boyle& Voigt 1973).

2.3. Weathering intensity, rate and susceptibility of intact rock and rock mass

Weathering intensity refers to the degree of decomposition of intact rock and rock masses (Huisman, 2006). For rock mass mass classification purposes, standardized weathering classification schemes such as the BS5930 1981/1999) are commonly used. Other methods of describing weathering intensity are through measurement of mechanical index properties (Ceryan et al., 2007) of by using chemical indices (Gupta & Rao, 2001). The weathering intensity rate is the amount of change in the weathering intensity, or just a certain amount of change per unit time. Huisman (2006) presented studies suggesting that weathering intensity rates are decreasing with time as the rock mass attains equilibrium with its surroundings.

Weathering susceptibility in this context is the susceptibility to weathering of the rock or soil mass at the end of the slopes' engineering life span (Price, 2009). Figure 1 shows the general stability and weathering characteristics of common rock-forming minerals. Although not shown in the figure, gypsum, weather easily and its effect on the rock mass is observable within a short span of time after excavation. However, for rock masses with relatively resistant components, the susceptibility to weathering can be assessed based on exposures of the same rock type with known excavation date. This concept is important in slope stability because the changes in the geotechnical properties of the rock mass due to weathering can cause failure to occur even before slopes reach their designed lifetime. The accuracy on the estimation of weathering susceptibility is highly dependent on the experience of the worker and also on the rock mass factors such as regularity of weathering over the years, quantity of exposures in the area, exposure time, number of degree of rock mass weathering and the homogeneity of the rock mass (Hack, 1998).
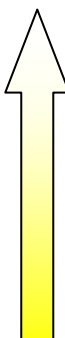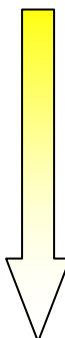
Fastest Weathering	Mineral	Least Stable
↑	Halite Calcite Olivine Ca-plagioclase Pyroxene Amphibole Na-plagioclase Biotite Orthoclase (K-feldspar) Muscovite Clays (various types) Quartz Gibbsite (Al-hydroxide)	↓
Slowest Weathering	Hematite (Fe-oxide)	Most Stable

Figure 1. General stability and weathering characteristics of common rock-forming minerals (modified from http://www.columbia.edu/~vjd1/weathering.htm, viewed 16 February 2015)

2.4.   Classification of weathered intact rock material and rock mass

The main purpose of having a mass classification scheme for engineering purposes, is "to provide short-hand descriptions for zones of rock of particular qualities to which can be assigned engineering characteristics within a single project" Anon.(1995). It is a means to transfer experience from one situation to another but keeping in mind that the effects of weathering varies from every rock type. A comprehensive summary and comparison of the existing weathering schemes used and recommended by researchers from 1955 to 1982 and from 1955 to 1995 as part of the effort to standardise characterization of weathered rocks and their engineering properties, were made by Gamon (1983) and Anon.(1995), respectively. The state of weathering is characterized by the degree of discoloration, decomposition and disintegration. In both papers, the authors agree that there is no single classification scheme that can encompass the complexity of weathering nor can classification be made based on a single material attribute. Hencher & McNicholl (1995) proposed a zonal weathering classification. This can be very helpful in determining which among the other existing classification methods, e.g., Anon.(1995), is applicable for a certain zone.

2.4.1.   The British Standards: BS5930:1981 and BS5930:1999

The weathering classification in the BS5930:1981 is among the commonly used rock mass classification schemes. However, many researchers regard it as over simplistic and often inappropriate (Anon., 1995). In a recent review by Hencher (2008), he commended that this scheme "doesn't work well in practice and conflicts with other well-established classifications" and it also lacks weathering classification on intact weathered rock samples while it is supposed to be used in geotechnical logging of boreholes. A revised version of the weathering classification scheme in BS5930:1981 was incorporated in the BS5930:1999 following the points raised by (Hencher, 2008). This new version consists of five approaches that cover uniform and heterogeneous materials. In this document, it is explicitly stated that the subclasses are rather

broad and thus its usage should be coupled by local experience, site-specific studies and by consulting other established schemes. Hencher (2008) found the 1999 version to be compatible with other schemes.

Hack (1998) proposed a comparison scheme for the application of the old and new versions (Table 1). This is with reference to the weathering factors incorporated in the Slope Stability Probability Classification (SSPC) (Chapter 2.6 and Chapter 4) which is based on the 1981 version. Based on the table, the description of the moderately weathered to completely weathered weathering grades in the BS5930:1999 are already encompassed by rock masses which are classified as moderately weathered in BS5930:1981 and the completely weathered degree of Approach 1 can be under the high weathering grade of BS5930:1981. If this classification is used, then there will a single reduction value for rock masses that are moderately weathered to highly weathered which is practically unlikely. Thus

Table 1 Comparison for the application of BS5930:1981 and BS5930:1999 (from Hack , 1998)

BS5930 1981		approach 2 Uniform materials (moderately strong or strong rock in fresh state)		Approach 3 Heterogeneous masses (mixture of relatively strong and weak material)		Approach 4 Material and mass (moderately weak or weaker in fresh state)	
Degree	Description	Grade	Description	Zone	Description (2)	Class	Description
I Fresh	No visible sign of rock material weathering; perhaps slight discoloration on major discontinuity surfaces.	I Fresh	Unchanged from original state	1	100 % grades I - III	A Unweathered	Original strength, colour, fracture spacing
II Slightly weathered	Discoloration indicates weathering of rock material and discontinuity surfaces. All rock material may be discoloured by weathering.	II Slightly weathered	Slight discolouration, slight weakening	2	> 9 0% grades III <10 % grades IV - VI	B Partially weathered	Slightly reduced strength, slightly closer fracture spacing, weathering penetrating in from fractures, brown oxidation
III Moderately weathered	Less than half of the rock material is decomposed or disintegrated to a soil. Fresh or discoloured rock is present either as a continuous framework or as core stones.	III Moderately weathered	Considerably weakened, penetrative discolouration Large pieces cannot be broken by hand	3	50 to 90 % grades I – III 10 to 50 % grades IV - VI		
		IV Highly weathered	Large pieces can be broken by hand Does not readily disintegrate (slake) when dry sample immersed in water				
		V Completely weathered	Considerably weakened Slakes in water Original texture apparent				
IV Highly weathered	More than half of the rock material is decomposed or disintegrated to a soil. Fresh or discoloured rock is present either as a discontinuous framework or as core stones.			4	30 to 50% grades I – III 50 to 70 - 100% grades IV - VI	C Distinctly weathered	Further weakened, much closer fracture spacing, grey reduction
V Completely weathered	All rock material is decomposed and/or disintegrated to soil. The original mass structure is still largely intact.			5	< 30% grades I – III 70 - 100% grades IV - VI	D de-structured	Greatly weakened, mottled, lithorelics in matrix becoming weakened and disordered, bedding

BS5930 1981		approach 2 Uniform materials (moderately strong or strong rock in fresh state)		Approach 3 Heterogeneous masses (mixture of relatively strong and weak material)		Approach 4 Material and mass (moderately weak or weaker in fresh state)	
Degree	Description	Grade	Description	Zone	Description (2)	Class	Description
							disturbed
VI Residual soil	All rock material is converted to soil. The mass structure and material fabric is destroyed. There is a large change in volume, but the soil has not been significantly transported.	VI Residual soil	Soil derived by in-situ weathering but having lost retaining original texture and fabric	6	100% grades IV - VI	E residual or reworked	Matrix with occasional altered random or apparent lithorelicts, bedding destroyed. Classed as reworked when foreign inclusions are present as a result of transportation

2.4.2. ISO 14689-1

This weathering classification scheme made a distinction between intact rock and rock masses shown in Table 2 (modified from Mulder et al., 2012). It adapts the BS5930:1981 weathering classification for rock mass but the notation for weathering grades was modified. In this classification, the fresh rock, which is noted as I in BS5930 is assigned a grade of 0 and the residual soil, which is noted as V in BS5930 is assigned a grade of 5. This move was highly criticized by Hencher (2008) as not very helpful and not usable in practice and that adjusting the weathering grade notation provides further confusion. He also warned against the poor practice of characterizing a small sample (e.g. core from borehole), even conducting laboratory tests, then translating the results to the whole rock mass.

Table 2. Weathering description and classification of intact rock material (modified from Tables 2 and 13 from (NEN-EN-) ISO 14689-1:2003 (modified from Mulder et al., 2012; excluded weathering classification of rock mass)

Classification	Description
Fresh	No visible sign of weathering/alteration of rock material
Discoloured	The colour of the original fresh rock material is changed and is evidence of weathering/alteration. The degree of change from the original colour should be indicated. If the colour change is confined to particular mineral constituents, this should be mentioned.
Disintegrated	The rock material is broken up by physical weathering, so that bonding between grains is lost and the rock is weathered/altered towards the condition of a soil in which the original material fabric is still intact. The rock material is friable but the mineral grains are not decomposed
Decomposed	The rock material is weathered by the chemical alteration of the mineral grains to the condition of a soil in which the original material is still intact; some or all of the mineral grains are decomposed.

2.5. Weathering effects on the geotechnical properties of intact rock and rock masses

2.5.1. Response of various rock types to weathering

Various rock types respond to weathering in various ways. For volcanic rocks, the reaction of water converts the volcanic glass into clay and this causes volumetric changes that would further promote physical and mechanical changes in the inter-granular structures (Yokota & Iwamatsu, 1999). Volcaniclastic rocks may generally behave like conglomerates with the matrix materials sometimes behaving as sandstones. Chigira & Sone (1991) studied the weathering profile of young sandstones and conglomerates and identified weathering zones of oxidation to dissolution through depth. The mechanical properties of the rock mass vary systematically with the change of the weathering zone. Gupta & Rao (2000) presented studies showing that in granites, the loss of strength from fresh to moderately weathered rocks reaches about 80%. For claystones, the tensile strength observed in fresh rocks is decreased by 75% in slightly weathered rocks because of the increase in microfractures. Results of petrographic analyses suggest that microfractures, pores and voids are the dominant factors that govern the strength of fresh rocks and not the mineralogy itself. Gurocak & Kilic (2005) studied the weathering effects on the properties of Miocene basalts in Turkey classified using ISRM weathering classification. Their results showed that UCS derived from Schmidt hammer tests, the compressive wave velocity and unit weight decrease while porosity and water absorption increase with increasing degree of weathering.

2.5.2. Weathering effects on discontinuities

Discontinuities can be mechanical or integral (Hack, 2006). Mechanical discontinuities are planes of weakness such as bedding planes and joints where the shear strength is significantly lower than the surrounding rock material. Integral discontinuities have the same shear strength as the surrounding materials such that it does not affect the intact rock strength. Discontinuities are also modified by weathering (Hack&Price, 1997). After stress relief where new cracks in the intact rocks can develop and existing cracks are opened, weathering subsequently weakens the discontinuity wall and infill materials. Further weathering will cause discontinuity planes to smoothen due to the loss of their asperities. Tating et al. (2014) noted new mechanical discontinuity sets formed thus a decrease in the spacing was observed with increasing degree of weathering in massive sandstones. However, Ehlen(2002) observed that some discontinuities disappear or become less persistent in more weathered granite and attributed this to the infilling of mineral grains in joint apertures, eventually obscuring the individual joints. This may lead to inaccurate rock mass classification such that careful assessment should always be practiced.

2.5.3. Changes in the strength parameters due to weathering

Weathering leads to the disruption of grain to grain bonding creating micro-fractures and new minerals. This inevitably results to modifications in the rock mass engineering properties (Gupta & Rao, 2000). These changes include decrease or loss of intact rock strength and rock mass strength, increase in their deformability and changes in the permeability depending on the nature of the rock and its stage of weathering (Hencher & McNicholl, 1995) and this usually leads to the deterioration and subsequently, slope failure (Huisman, 2006; Fan et al., 1999; Gupta & Rao, 2000; Calcaterra & Parise, 2010; Tating et al., 2013). Parameters that are highly affected by weathering as indicated by their good correlation with the degree of weathering include tensile strength (Arıkan et al.,2007), compressive strength and to some extent, elasticity modulus (Heidari et al., 2013). Index properties that change during weathering include dry density, void ratio, clay content and seismic velocity (Ceryan, 2007). These changes however occur after rocks reach certain weathering stage (Arıkan et al., 2007).

2.6. Weathering-time relation in rock mass classification

Rock mass classification schemes are widely used in slope stability assessment. These include the Rock Mass Rating (RMR), the Slope Mass Rating (SMR), Q-system, among others (Nicholson, 2004). These classification systems are difficult to apply to rock masses that are of very poor quality and in heterogeneous rocks such as flysch. The geological strength index (GSI) was formulated to address this as it would place greater emphasis on basic geological observations of rock-mass characteristics, reflect the material, its structure and its geological history and would be developed specifically for the estimation of rock mass properties (Marinos et al., 2005).However, these schemes focus on the attitude of discontinuity planes and less attention is given to the weathering state of the rocks.

Weathering classifications also exist (BS 5930, 1981,1999; Dearman, 1974; Ceryan et al., 2007;Arıkanet al., 2007) but these fail to treat weathering as a progressive process that affects salient geotechnical properties of the rock mass during the engineering lifetime of a cut slope. The inadequacy in considering weathering-time relation is addressed in the Slope Stability Probability Classification (SSPC) of Hack et al. (2003) and the Rockslope Deterioration Assessment (RDA) of Nicholson (2004).

The SSPC is specifically designed to address slope stability while the RDA addresses shallow weathering-related erosional processes and mass movements. SSPC involves a three-step approach that take into consideration the past and future weathering and the damage resulting from the excavation method which would indicate probable failure mechanisms (Hack, 2003). A modification of the 1998 version of SSPC was made by Lindsay et al. (2001). The main modification was the introduction of rock intact strength derived from the modified Mohr-Coloumb failure criterion adapted from varying moisture content,

weathering state and confining pressure. The RDA addresses shallow weathering-related erosional processes and mass movements. It likewise follows a step-wise approach to slope hazard assessment involving the application of ratings to assess rockslope deterioration susceptibility, review of the nature of the likely deterioration based on rock mass type and slope morphology and providing guidance and appropriate mitigation based on the findings in the two earlier stages (Nicholson, 2004).

Between SSPC and RDA, there are more published papers applying the weathering-time relation concept of SSPC than those that actually used the RDA. Tating et al. (2013) established relationship of intact rock reduction with exposure time in sandstone units and this can be used to predict further reduction within the serviceable time of slopes built in the said unit. Rijkers & Hack (2000) found that laboratory test results for friction angle, cohesion and natural slope angle correlate well with SSPC results for the pyroclastic deposits in Saba, Netherlands Antilles. Das et al. (2010) used SSPC for landslide susceptibility assessment and remarked that although it required extensive field data, it is more accurate than GIS-based quantitative modelling.

2.7. Influence of salt

The influence of marine salts makes the weathering process in the coastal environment distinct (Mottershead, 2013). Numerous studies have been conducted in natural environments and in simulated laboratory conditions to study the effect of these salts on rock materials. Results commonly show that in general, the influence of generally leads to the weakening and subsequent disintegration of rock materials (Lawrence et al. 2013). Thus, the term *"salt weathering"*. Salt weathering includes the physical process of salt crystallization with that results to rupturing of the rock thus it is an important mechanism in rock decay (Rodriguez-Navarro & Doehne (1999). It plays an important role in the development of many geomorphologic features in coastal environment (Mottershead, 1989; Goudie & Viles, 1997;Cardell et al., 2003; Rivas et al., 2003; Sunamura & Aoki, 2011; Lawrence et al.,2013;Hampton & Griggs, 2004) and in the degradation of many structures in archaeological sites (Kamh, 2011,2005; Mottershead at at.,2003; Lubelli et al., 2004; Sancho et al., 2003). Its damaging impact impact on engineering structures such as roads, highways, runways, dams and building foundations are shown by the studies of Benavente et al.(2007), Liu et al. (2014). Salt weathering can occur on a wide range of environment and most studies done in coastal environments in temperate regions (Lawrence et al., 2013) or arid regions (Wellman & Wilson, 1965; Brandmeier et al., 2011) . There is however, limited studies that were conducted in tropical areas (Wells et al., 2006; Bryan & Stephens, 1993) . The indicators of salt weathering have been collectively noted as cavernous cavities called honeycombs and tafoni depending on the scale; white salt efflorescence, contour scaling and stone surface exfoliation (Smith & McGreevy, 1988).

In general, the temporal variability in salt accumulation along the coastal area is governed by episodes of high winds, high surfs and precipitation. The spatial distribution of salt is controlled by the elevation above the shoreline, the aspect and the presence of shelters or buffers (Mottershead, 2013). The transfer of marine salt from the ocean involves three stages: the salt is released from the ocean to the atmosphere, it travels laterally through the atmosphere and finally it gets deposited on a land surface (Mottershead, 2013). The amount of salt transferred to the land through this mechanism is highly influenced by wind speed as suggested by the positive correlation between wind speed and salt concentration(Lewis & Shwartz, 2004 in Mottershead, 2013).

2.7.1. Mechanism of salt weathering

The most common mechanisms of salt weathering involve physical effects caused by the stress generated by crystal growth or moisture absorption by hygroscopic salts and chemical weathering resulting from the interaction of saline pore fluids and minerals (Mustoe, 2010). Other studies (e.g. Sperling and Cooke,

1984) also show that hydration of sodium sulfate can also induce rock deterioration but not as aggressive as the effect of crystal growth. The influence of salts to chemical weathering was explored by Mottershead et al., (2003) They attributed the formation honeycombs in sandstones as the result of accelerated weathering that takes place during chemical dissolution of grain boundaries under the influence of salts. The same remark is found in Goudie&Viles (1997) "Salts in general participate in chemical reactions, reacting with minerals and rock surfaces." However, because more authors support the idea of salt crystallisation as salt weathering mechanism, they tend to regard salt weathering as a physical weathering process and does not involve major chemical processes such as hydration, as implied by Kirchner (1996).

2.7.2. Rate of salt weathering

In terms of rate associated to salt weathering, Kamh (2011) measured a weathering rate of 0.42mm/year in sandstones used in ancient buildings in Aachen, Germany. This rate is said to be higher compared to 0.1mm/year previously measured in studies conducted in an area with similar climatic conditions. For long term weathering, salt weathering decelerates through time as suggested by the experiments of Sperling & Cooke (1984) and Wells et al. (2006) where material loss decrease after samples were subjected to a certain number of cycles. In addition, Wells et al. (2006) also showed that there is no significant difference in the weathering rate in schists between dry and wet seasons in a simulated tropical environment.

Matsukura & Matsuoka (1996) considered depth to be the most reasonable measure of growth because it increases gradually (exponential function) with time compared with the other dimensions due to the possibility of coalescence of adjoining tafoni. They computed rates ranging from 0.595 mm/year to 0.0108 mm/year. Motterhead (1982) calculated and annual weathering grate of 0.6mm/year for greenschists and this was attributed to salt weathering due to the crystallization of halite and not on chemical dissolution. Exceptional erosion figures measured from surface lowering associated with coastal salt weathering is >1mm/year and a maximum of 5.25 mm over 20 years in insoluble rocks (Mottershead, 2013).

2.7.3. Factors governing salt weathering

The factors influencing salt weathering come from the attributes of the material such as porosity, permeability, geochemistry and mineralogy of the rock (Mottershead, 2013; Kamh, 2011) and the properties of the salt including its composition and the concentration of the solution, viscosity, surface tension and vapour pressure. Environmental factors such as temperature, moisture content (Trenhaile, 2005), humidity and topography (Goudie & Viles, 1997) as well as, solar exposure (Mottershead, 2013) are also important. Sperling & Cooke (1985, in Kamh (2011)) found that hydration of sodium sulphate is effective in rock disintegration but significantly less effective than crystal growth (anhydrated versus hyrdrated (thenardite vs. mirabilite). The most disintegration occurs during extreme temperature and very low relative humidity.

The porosity and permeability of the rocks enable the water to enter, circulate and remain within the material. A comparative study was done on the salt weathering in sandstones, limestones and trachytes, rocks making up the St. Maria church in Cologne, Germany. The sandstones have high macropore content and interconnecting micropores encouraging crystallisation in the interstices which leads to granular disintegration.   The limestones have very fine, interconnected intergranular pores so crystallization occurs in the surface forming salt crusts which sometimes detach and pulling off some fragments. Trachyte has heterogenous pore system with fissures near weathered phenocrysts encouraging cracking and scaling of fragments (Goudie&Viles, 1997). In contrast, Auger (1990, in McLaren, 2001) noted that it is the rocks with lower porosities that are more prone to salt weathering. In porous rock, the pores allow solutions to move freely in and out of the rocks such that little weathering occurs.

For granites and probably applicable to other crystalline rocks such as basalts and andesites, salt weathering is linked with the increase in porosity resulting from the decomposition of the minerals through other weathering processes.

2.7.4. Cementing effect of salt

It was previously mentioned that salt crystallization in pore spaces under certain conditions depending on the nature of salts and the material porosity does not necessarily exert enough pressure in the walls to cause disruption or eventual weathering. Instead, this can increase cohesion among the particles through cementation. McLaren (2001) found that "in highly porous rocks (including sandstone and limestone) aeolianite deposits in the spray zone tend to be better cemented, have higher levels of secondary porosity, lower primary porosity and a lower unaltered allochemical content than the same formations that are not exposed to sea spray. However, note that the cementing effect of salt was only described in rocs that are inherently containing carbonates. The processes can be different rocks with low carbonate content such as volcanic rocks.

3.   STUDY AREA

3.1.   Location , topography and climate

Saint Vincent and Dominica are located in the east of the Caribbean Sea. Dominica has a land area 750 km² while Saint Vincent has 344km². Roseau is the capital city of Dominica and Kingstown for Saint Vincent. In both islands, these capital cities are located in the southwest part which is said to be relatively sheltered from hurricanes that regularly visit the region. The topography in both islands is typically characterized by a rugged, mountainous central part such that areas for settlements and road networks are only limited in the coastal region and in foot slopes (Anderson & Kneale, 1985). The central highland of Dominica is formed by MorneDiablotins (1421m) and other peaks with heights exceeding 1000 m. Volcaniclastic fans form most of the flat lands where settlements have been established. Similarly, the major topographic feature in Saint Vincent is a north-south trending chain of mountains from La Soufriere (1178 m) in the north to Mount St. Andrew (736m) to the south. Fifty percent (50%) of the total surface area has a slope of at least 30° and only less than twenty percent (20%) has a slope of less than 20°. Deep-cut valleys and steep coastal cliffs characterize the leeward side and wider and flatter valleys in the windward side (USAID, 1991). Both islands are characterized by a tropical climate. However, there is a significant difference in terms of rainfall. Dominica is significantly wetter with average annual rainfall frequently exceeding 5000 mm in the east coast and just 1800 mm in the west side. In the highlands, the annual rainfall can reach up to 9000 mm. The wettest months are from June through October. In Saint Vincent, the wettest months are from May to October where average annual rainfall is about 3800 mm inland and about 2000 mm in the coast. Humidity follows the trend of the rainfall

3.2.   Geology

Dominica and Saint Vincent belong to the chain of volcanic islands forming the Lesser Antilles island arc. It is the surface manifestation of the subduction of the North American Plate beneath the Caribbean Plate that was initiated as early lower Eocene (Smith et al., 1980; Bouysse et al., 1990; Rad et al., 2013). The general geology of both islands are described below and the maps are included in Appendix 9.1.

3.2.1.   Saint Vincent

The geology of Saint Vincent is characterized by basalts emplaced during the early phase of volcanic activity in the island and followed by the andesites that occur as dikes, domes or central plugs in the vents of some volcanic centres. Basalts are dominant in the south while andesites are abundant in the northern part of the island. The Southeast Volcanics consist of scoraceous basalts interbedded with massive well-jointed basaltic lava flows. It is intruded by dikes and mostly overlain by fine grained yellow ash associated with the tephra ejected by the Soufriere volcano. The Grand Bonhomme Volcanic Center is interpreted as a stratovolcano with interbedded sequences of block and ash pyroclastic flow deposits, ashfall deposits, lava flows and subordinate domes. These rocks form a heavily forested landscape with inaccessible interior composed of deeply weathered lavas and volcaniclastic deposits. The MorneGaru volcanic centre is in the north of Grand Bonhomme. The rocks exposed are lava flows, undifferentiated volcaniclastics, red scoria bombs and yellow ashfall deposits.

In the southeast and northern part of the island are poorly consolidated sequence of clast-supported, pumice lapilli airfall, scoria bombs and ash overlying old lava flows. The abundant scoria bombs that fell close to these centres formed thick and sometimes welded deposits. Ash and small projectiles deposited further from the vents produced discrete beds. Spatter cones are also exposed in the northern part of the

island consist of a thick sequence (>20 m) of interbedded grey lapilli-sized ash and red scoria overlain by yellow ash. The red scoria clasts are composed of olivine microphyric basalts but also contain angular basaltic-andesite. The Soufriere stratovolcano occupies the northern half of the island. It is the most active volcano in the Antilles arc. Its last five major eruptions occurred in 1718, 1812, 1902, 1971 and 1979 where basaltic lava domes were extruded in the crater area followed by a phreatomagmatic explosion that produced pyroclastic flows. Other major volcanic centers were identified but these have already become extinct (Heath et al., 1998). It is deemed that the volcanic activity in Saint Vincent is younger than the other islands. There were no deposits older than 2.8 Ma, though this may also indicate incomplete sampling.

3.2.2. Dominica

Dominica is underlain by sub-aerial lava flows and pyroclastics with minor Pleistocene to Holocene uplifted conglomerates and corals in the west coast of the island (Christian, 2012). A comprehensive K-Ar and carbon dating of the volcanic rocks resulted to the subdivision of the rocks into four units (Smith et al., 2013). The Upper Miocene dominated by mafic volcanism and make up the eastern part of the island. The Upper Pliocene to Lower Pleistocene unit forms two major stratovolcanoes (proto- Morne Diablotins and Cochrane-Mahaut) and two smaller Morne Concrod and Morne Bois) stratovolcanoes located in the eastern flank of Mount Diablotins. Lower to Upper Pleistocene forms two volcanic centers, Proto- Morne aux Diables in the north and Foundland in the south, and is the least extensive unit in the island. The Upper Pleistocene – Holocene is composed of seven volcanic centers in the island which marked the renewed volcanism producing andesites and dacites.

4. METHODOLOGY

4.1. General Approach

As indicated in the list of objectives, the purpose of the research is not to conduct slope stability assessment per se but rather to use the slope stability parameters to show how the initial stress relief and weathering are affecting the geotechnical properties, and consequently the stability, of the studied rock masses. The data obtained from the various slopes that are made up of different lithologies, with different weathering degree and with different number of exposure years, are systematically recorded and manipulated using empirical equations in the Slope Stability Probability Classification (SSPC) system (Hack, 1998). Because the degree of weathering is incorporated in the calibration of the SSPC system, it is still expected to reflect differences in the calculated stability of geotechnical units with broadly uniform conditions but with different degree of weathering (e.g. exposure of one lithology with varying weathering degree). However, the difference between the rocks types and the climatic condition in the Caribbean islands and that of the area in Spain where the model was calibrated from, may give unexpected results. These are discussed in the subsequent chapters.

Defining the relationship of weathering with time can be done in two ways as long as the exposure time is known. One is using the concept of Reference Rock Mass (RRM) and Slope Rock Mass (SRM) of the SSPC system and the other is to compare actual measurements from a particular geotechnical unit exposed in a certain year with those of its counterpart in a newly exposed slope (reference slope). Unfortunately, for this research, there is only one reference slope identified during the fieldwork (further discussed in Chapter 6).

In order to describe the influence of salts, the exposures along the coast were compared with the exposures found in the interior (roads traversing the forested highlands) parts of the islands. Some features that are commonly observed in areas affected by salts documented elsewhere were identified in the coastal exposures in both islands. The trend in the concentrations of salts in the samples with respect to the distance from the coast strengthens the hypothesis that these features indicate the influence of marine salts. The mechanisms of how salts are affecting the rock masses depending on the type of salt influence indicator observed are inferred using literature data. These secondary data were obtained from long term monitoring, e.g. 7 years in Mottershead (1989) of salt weathering in the natural environment and from simulations in specially designed laboratory climate rooms. Both methods are not doable in the given timeframe of this research. Nevertheless, by combining these data with the field data and limited laboratory analysis results obtained in this research, possible implications to the engineering properties of the affected rock masses can be inferred.

4.2. Desk study

The east Caribbean region, where Saint Vincent and Dominica are located, has been a subject of numerous projects on management and mitigation of natural hazards relating to hurricanes and volcanic activities. The reports generated from these studies contain a considerable amount of secondary information. A geological report is available for Dominica Smith et al., 2013) and a fair description of the geology of Saint Vincent can be found on the website of the Seismic Research Centre of the University of West Indies (http://www.uwiseismic.com/General.aspx?id=66). Sources of information on the geotechnical properties of the rocks in the islands are very limited. Most of the reports on geotechnical testing are for particular engineering projects, which mostly cover a limited area and contain few details.

4.3. Field survey

A reconnaissance survey was conducted to identify the location of particular slopes to be investigated. Among the considerations in selecting these locations include the representativeness in terms of lithology and weathering degree and the accessibility of the exposure. The distance to the base camp was also a factor given the limited time available for the fieldwork. Unfortunately, many good exposures are located in roadcut sections with high and steep slopes where rockfalls regularly occur and could not or only partially be assessed due to safety consideration.

4.3.1. Defining and naming geotechnical units (GU)

In the exposures, units with broadly the same geotechnical characteristics including the same weathering degree and fracture patterns are grouped as one geotechnical unit (GU). In all cases, one geotechnical unit consists of one lithologic type. In most of the exposures, several GUs were delineated within a single lithologic type. For example, 4 GUs were identified in an extensive exposure of pillow lava flow based on the differences in their weathering degree and block sizes. The names of the GUs include the assigned exposure identification code and the letter corresponding to the unit. For example, GU SV1A means geotechnical unit A in exposure SV1.

4.3.2. Assigning rock mass weathering grade

In the discussion of the various weathering classification schemes in Chapter 2, the two versions of the BS5930 classification systems were compared. Approach 3 appears to be fitting for the block-and-ash flow (BAF) deposits and tuff breccia rock masses. However, if the explanation of ANON. (1995) on the background of this classification is carefully considered, this cannot be used for the zoning of such deposits because these rocks did not originate from a homogenous unit but rather, these are intrinsically heterogeneous units even in their fresh state. This is where the relevance of the dominant component is considered. In clast-supported BAF, the rock mass weathering grade is based on the dominant weathering grade of the clasts but if it is matrix-supported, then the weathering grade assigned to the GU is based on that of the matrix. Based on Table 1, the weathering grade in BS5930:1981 and that of approach 3 is highly correlatable, thus the reduction values of the SSPC system yields the same result. Therefore, to be consistent with the SSPC system, BS5930:1981 was used in this research.

4.3.3. SSPC parameters for weathering (WE) and method of excavation (ME)

The SSPC parameter for weathering (Table 3) is proposed by (Hack, 1996;1998) as a method of quantifying weathering. This is embodied in the SSPC (Hack, 1996;1998) where the effects of weathering on the intact rock strength and the rock mass spacing and conditions of discontinuities are related to the degree of rock mass weathering classification in BS5930:1981. These reduction factors allow prediction of changes in these rock properties as weathering progresses for a certain slope.

Table 3. Reduction values per weathering grade by (H.R.G.K. Hack, 1996) as used by Huisman (2006)

Degree of weathering in slope (BS5930:1981)	SSPC WE
Fresh	1.00
Slightly weathered	0.95
Moderately weathered	0.90
Highly weathered	0.62
Completely weathered	0.35

The SSPC parameter for the method of excavation enables the exclusion of any influence of the method of excavation on the measured parameters. The correction values are in Table 4. According to the Ministry of Works (MOW) of both islands, there was no blasting and only excavators were used in the road sections investigated. Therefore the the ME value for all the slopes is 1.

Table 4. The SSPC correction values for the method of excavation

Method of Excavation	SSPC ME
Natural / hand-made	1.00
Pneumatic hammer excavation	0.76
Pre-splitting / smooth wall blasting	0.99
Conventional blasting with result:	
good	0.77
open discontinuities	0.75
dislodged block	0.72
fractured intact rock	0.67
crushed intact rock	0.62

4.3.4. Description of rock material and rock mass properties

The exposure characterization sheet of the SSPC is used to systematically record the field observations which mainly consist of the description of rock material and discontinuity properties. One sheet corresponds to one GU. The filled out sheets are in Appendix 1. The description of the exposures follows the format recommended in BS5930:1999. The complete slope description is included in Appendix 10.2.

4.3.4.1. Intact rock strength (IRS)

The intact rock strength (IRS) was estimated through crumbling by hand and by using the geologic hammer as recommended by Hack & Huisman (2002) and by referring to the scale in the BS 5930:1999 (Table 5).

Table 5. The BS5930:1999 classes for strength of rock material

Field definition	IRS estimate (MPa)
Crumbles in hand	<1.25
Thin slabs break easily in hand	1.25-5
Lumps broken by light hammer blows	5-12.5
Lumps broken by heavy hammer blows	12.5-50
Lumps only chip by heavy hammer blows (dull ringing sound)	50-100
Rocks ring on hammer blows. Sparks fly	> 200

For fresh and slightly weathered lava flows, rebound values were measured with an L - Type Schmidt hammer (serial no.: proceq L-9 5526) to estimate the Uniaxial Compressive Strength (UCS) as described by (Aydin, 2009). The conversion of the rebound values to MPa used the conversion method included in the operating manual published by the Schmidt Hammer manufacturer (Proceq, 2006).

4.3.4.2. Discontinuity spacing

The discontinuity sets were defined visually. Discontinuities with the same dip/dip direction are grouped as one set. The notation for discontinuity orientation used in the SSPC sheets is dip/dip direction. For example, J1 - 60/150 means Joint set 1 with dip of 60° and dip direction of 150°. Bedding planes are denoted as B and faults as F. Following BS5930:1999, the discontinuity spacing (DS) was measured perpendicular to the discontinuities. The minimum spacing was considered. Only the mechanical discontinuities are measured in detail in this research. The DS is used in the SSPC system to get the corresponding rock mass spacing parameter (SPA). Closely associated with the DS is the persistence of a discontinuity, which determines the possibilities of relative movement. The persistence was measured along dip and along the strike.

4.3.4.3. Condition of discontinuities

The conditions of discontinuities indicate the shear strength along the discontinuities. It is assumed that weathering will lead to the loss of roughness along the discontinuities and to the formation of clay infill materials. The results of these field data are included in the slope characterizations of the GUs in Chapter 5 and Appendix 10.2

a. Large-scale (Rl) and small-scale (Rs) roughness - The importance of the discontinuity surface roughness on the shear strength along the discontinuity planes depends on the stress configuration on the discontinuity plane and in the deformation characteristic of the discontinuity wall material and asperities (Hack, 1998). These are explained in detail in the SSPC System. The Rl and Rs were measured by assessing the wavelength and amplitudes of the discontinuity surface using the Figures 2a and 2b as reference. In the SSPC system, the ISRM profiles were modified for a new empirical relation consisting of a combination of tactile and visible roughness. The large-scale roughness is determined in an area larger than 20 cm x 20 cm but smaller than 1 m x 1 m. It is described in five classes namely wavy, slightly wavy, curved, slightly curved and straight. Tactile roughness is classified as rough, smooth and polished as distinguished by feeling the discontinuity surface with the fingers in an area of 20 cm x 20 cm. The small-scale roughness is described as stepped, undulating and planar.
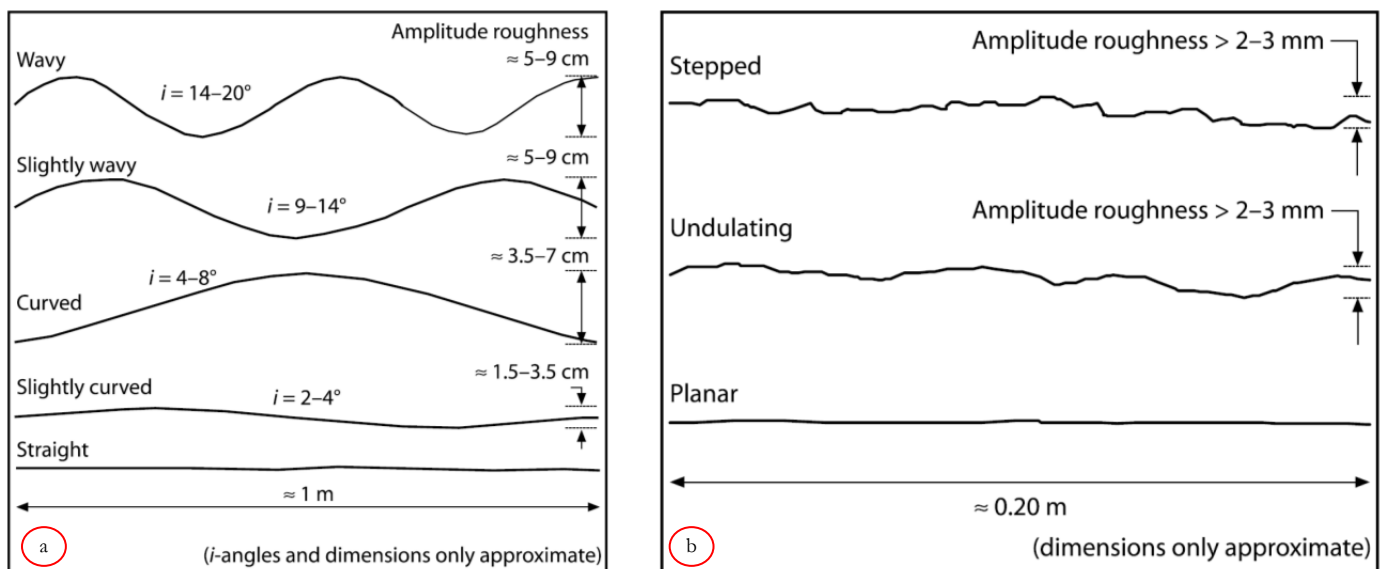
Figure 2. Description of large-scale (Rl) and small-scale (Rs) roughness of discontinuities;(a) Rl is determined in 1 m x 1m area; (b) Rs is determined in 20 cm x 20 cm area of the discontinuity plane (Hack, 1998)

b. Discontinuity infill material (Im) - The type of infill material in between discontinuity walls and whether the discontinuity walls are in contact or not during shearing have a very strong influence in the shear strength characteristics along the discontinuities. The materials are described as cemented, non-softening and softening when subjected to the influence of water, deformation or shear displacement.

C. Karst (Ka) - The open cavities are known to considerably weaken the rock mass. In the study area, the open cavities encountered are not from karstifcation but rather as a result of the gradual removal of unconsolidated pumice and scoria surrounded by a more competent rock unit. In the SSPC system, the rating is either 1 or 0.92 which only rates the presence or absence regardless of size of the cavity.

4.3.5. Sampling

Samples were collected for clay mineral identification, determining the indications of salt enrichment and for grain size analysis. Unfortunately, not all the weathering grades for all the rock types encountered were sampled mainly because no representative outcrop was observed or investigated. One of the major constraints in the quantity of samples brought back to the laboratory for analyses is related to logistics involving the strict regulations on transporting soil and rock materials from the study areas to ITC.

4.4. Laboratory Analysis

The laboratory analysis including all the necessary preparatory works were conducted in the ITC laboratory.

4.4.1. Grain size separation and analyses

Grain size separation through sieving was conducted during the sample preparation to separate the <56 microns grain fraction of the samples the for clay mineralogy analyses. Samples of matrix materials of the lahar deposits were also subjected to sieve analyses to determine their granularity and nature of their porosity.

4.4.2. Clay mineralogy

Clay mineralogy was conducted by X-ray Diffraction (XRD) to determine clay minerals that may give indications in the weathering conditions of the source GU as an augmentation to the weathering degree determined by visual assessment. It was also conducted to determine the presence of expanding clays which are relevant to slope stability. A Bruker D2 Phaser X-ray Diffractometer was used in the analysis following standard procedures.

4.4.3. Water extractable salts

The concentrations of water extractable salts were measured to determine the variation in the salt concentrations in the GU exposed to sea sprays and to see how these vary with distance from the coast. Because the islands are relatively small and sea sprays can be distributed all over the island, samples taken from exposures in the interior of the island were also analysed and the concentrations are regarded as baseline or background values of the salts. The concentrations of $NaCl$, $MgSO_4$, $CaCO_3$ and $Fe(OH)_3$ were stoichiometrically derived from the measured Na^+ Mg^+ Ca^{+2} and Fe^{+3} levels. Figure 3 shows the sample preparation set-up. The general steps involved in the analysis are the following:

Ten (10) grams of sample (about 2.5 mL) was soaked in 97.5 mL de- ionized water in 100 mL beakers, stirred regularly and were left to stand overnight. The next morning, 10 ml of solution was decanted, centrifuged and analysed by Inductively Coupled Plasma Optical Emission Spectrometer (ICP-OES - Varian Liberty II Model). Ten (10) mL of HCl (1:3 diluted) was added to the remaining 90 mL, stirred regularly then left to settle overnight after which 10 mL was analyzed by ICP-OES for Ca and Fe.

Figure 3. The set-up for the water extractable salts experiment. (a) Solution after stirring and (b) after being left overnight to settle (photos by de Smeth, 2015)

4.5.   Data analysis

The calculation for the strength parameters (and slope stability probability) of the rock masses entirely follows the SSPC system. This SSPC system differs from other rock mass classification systems because it involves a three-step approach. Three rocks masses are considered, namely: the exposure rock mass (ERM) representing the conditions at the time of investigation, the theoretical fresh reference rock mass (RRM) corrected using the SSPC reduction factors of weathering (Table 2) and excavation on the values of the ERM and; the slope rock mass (SRM) where the actual stability assessment is conducted. Using empirical equations, the cohesion angle, internal friction angle and the stability probability were calculated. This approach allows inferences to be made on the weathering induced- strength reduction in the rocks making up the geotechnical units and thus can be taken into account in designing future road improvement measures.

4.5.1.   Reference Intact Rock Strength (RIRS)

For the intact rock strength, the adjustment formula to obtain the Reference Intact Rock Strength (RIRS) is:

$$RIRS = \frac{IRS\ (MPa)}{WE} \qquad (1)$$

where IRS is the field estimate and WE is the correction for weathering. If IRS > 132 MPa, then RIRS is 132 MPa. The maximum value of 132 MPa is taken as the cut-off value "above which the influence of the IRS on the estimated slope stability is constant" (Hack, 1998).

4.5.2. Overall discontinuity spacing (SPA) and Reference Overall Discontinuity Spacing (RSPA)

Oftentimes, the stability of rock masses is not only controlled by a single set of discontinuities but rather it is influenced by all the discontinuity sets. In order to include possible influence of all the discontinuity sets present in a rock mass, the SSPC system adapted the SPA for a maximum of three discontinuity sets developed by Taylor (1980). The SPA is given by the formula:

$$SPA = factor\ 1 * factor2 * factor\ 3 \tag{2}$$

where SPA is the spacing parameter and the factors are obtained from Figure 4.
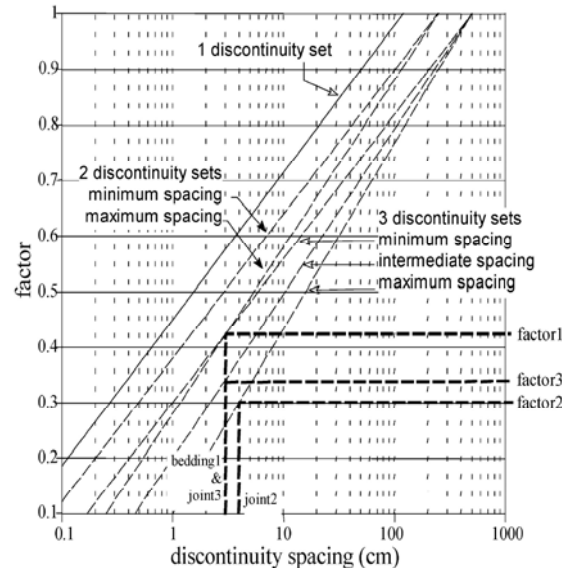
Figure 4. Discontinuity spacing factors (from Taylor (1980) in Hack (1998))

The RSPA is given by:

$$RSPA\ = \frac{SPA}{WE * ME} \tag{3}$$

where RSPA is the spacing parameter for the RRM, SPA is the existing spacing parameter, WE is the correction parameter for weathering and ME (Table 3) is the correction factor for the method of excavation. In this research, there are exposures with maximum of five sets of discontinuities in which case the minimum, median and maximum spacing were considered.

4.5.3. Condition of discontinuities

This parameter includes the condition of individual discontinuity set (TC), reference condition of discontinuity set (RTC), overall condition of discontinuities (CD) and reference overall condition of discontinuities (RCD). The condition of each discontinuity set (TC) does not make any distinction between continuous and abutting discontinuities.

TC is the product of the large scale (Rl) and small scale (Rs) roughness, infill material (Im) and karst (Ka):

$$TC = Rl * Rs * Im * Ka \tag{4}$$

The TC corrected for the weathering parameter (RTC) for each single discontinuity set is given by:

$$RTC = \frac{TC}{\sqrt{1.452 - 1.220e^{-WE}}} \tag{5}$$

The SSPC system provides a formula that derives the weighted overall condition (CD)of a number of discontinuity sets in the rock mass exposure unit. This is important because similar with the parameter for discontinuity spacing, the strength of the rock mass is not only governed by the condition of only one discontinuity set.

$$CD = \frac{\frac{TC1}{DS1} + \frac{TC2}{DS2} + \frac{TC3}{DS3}}{\frac{1}{DS1} + \frac{1}{DS2} + \frac{1}{DS3}} \tag{6}$$

RCD is CD divided by the parameter for rock mass weathering (WE).

4.5.4. Reference rock mass friction angle (RFRI) and cohesion (RCOH)

These rock mass strength parameters friction angle and cohesion are estimated by optimising the Mohr-Coloumb failure criterion with the IRS, CD and SPA. For the reference rock mass, the RFRI and RCOH are calculated using the values corrected for weathering (i.e., RIRS, RCD and RSPA). The equations are:

$$RFRI = (RIRS * 0.2417) + (RSPA * 52.12) + (RCD * 5.779) \tag{7}$$

$$RCOH = (RIRS * 94.27) + (RSPA * 28629) + (RCD * 3593) \tag{8}$$

4.5.5. Slope rock mass properties (SRM) and slope geometry

The concept of SRM is meant to address slope stability as well as the future stability scenarios of a slope that has yet to be excavated until the end of its engineering lifetime. The geotechnical properties of the (SRM) are obtained by correcting the properties of the RRM geotechnical units for the damage due to the method of excavation (SME) and for the deterioration due to future weathering (SWE). However, for this research where the slopes studied are already existing, the SWE is the same as the observed WE, following the detailed explanation of Hack (1998). As previously mentioned, the method of excavation gives a rating of 1 in all the GU. The following equations are used to determine the slope intact rock strength (SIRS), slope overall discontinuity spacing (SSPA), slope overall condition of discontinuities (SCD) and the strength parameters (SFRI and SCOH) of the existing rock mass exposures.

$$SIRS = RIRS * SWE(weathering\ slope) \tag{9}$$

$$SSPA = RSPA * SWE * SME(method\ of\ slope\ excavation) \tag{10}$$

$$SCD = RCD * SWE \tag{11}$$

$$SFRI = (SIRS * 0.2417) + (SSPA * 52.12) + (SCD * 5.779) \tag{12}$$

$$SCOH = (SIRS * 94.27) + (SSPA * 28629) + (SCD * 3593) \tag{13}$$

The SSPC system requires that the dip, dip-direction and the height of the slope (from the bottom of the GU to the top of the slope) are broadly uniform. This means that if the dip direction of the slope is varying laterally, the stability of the slope should be assessed in different vertical section wherein each section has a broadly uniform dip direction. Likewise, a slope with vertically varying slope angle should be assessed in different horizontal sections where the slope dip is uniform. For a slope rock mass which consists of several GU, such as most of the case of this research, slope stability is assessed per GU.

4.5.6. Slope stability probability

The SSPC system considers both orientation dependent and orientation independent stability of the rock slopes. In orientation dependent stability, the failure in a rock slope is dependent on the orientation discontinuity in relation to the orientation of the slope and shear strength of the discontinuity. The failure modes related to the shear displacement along the discontinuities are sliding and toppling. The sliding criterion is based on the relationship of TC (Equation 4) and the apparent angle (AP) of the dip of the discontinuity

$$AP = \arctan(\cos \sigma) * \tan dip_{discontinuity}$$

if AP > 0° then AP = apparent discontinuity dip in the direction of the
slope dip

if AP < 0° then the absolute value = apparent discontinuity dip in the
direction opposite the slope

$$\sigma = dipdirection_{slope} - dip_{discontinuity}$$ (14)

The boundary condition for sliding in slopes and sliding occurs when

$$TC < 0.0113 * AP$$ (15)

The SSPC toppling criterion is

$$TC < 0.0087 * (-90 - AP + dipdirection_{slope}$$ (16)

The values for probability of sliding probability and toppling stability are determined from Figure 5a and 5b, respectively.
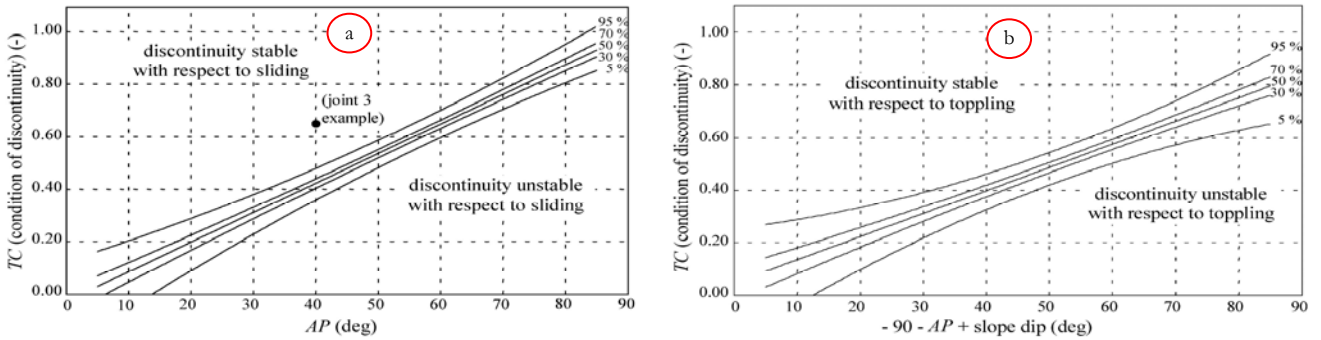
Figure 5. Probability for orientation dependent slope stability. (a) sliding criterion; (b) toppling criterion

However, a large number of slopes are still unstable even if they are stable with respect to the orientation dependent stability criteria. From the analysis of Hack (1998), these are likely unstable because of the combination of the intact rock strength, spacing and conditions of discontinuities and is therefore referred to as orientation independent stability. If SFRI is smaller than the slope dip, the maximum possible slope height (Hmax) for the slope is calculated using the formula:

$$Hmax = 1.6 * SCOH * \sin(slope\ dip) * \cos\frac{SFRI}{1 - \cos(slope\ dip - SFRI)}$$ (17)

The ratio of the computed Hmax and the Hslope (Hmax/Hslope) and the ratio of the SFRI and the slope dip angle (SFRI/slope dip) are used to determine the probability to be stable for orientation independent stability using Figure 6. If SFRI > slope dip, the probability of the slope to be stable is 100%.
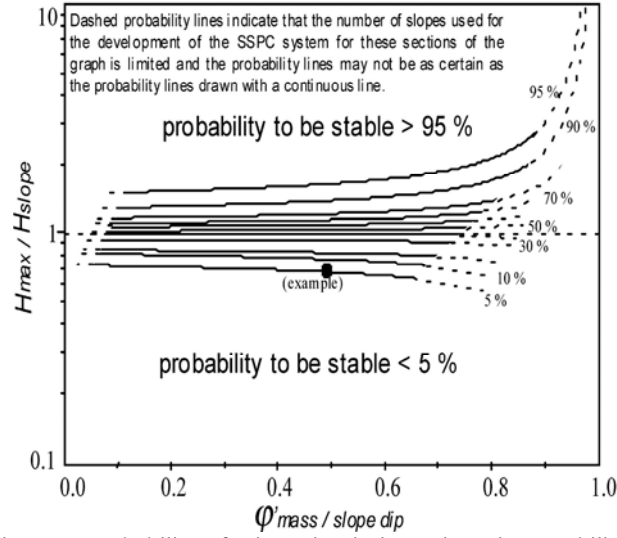
Figure 6. Probability of orientation independent slope stability. Percentage values indicate the probability of the slope to be stable (from Hack, 1998)

4.5.6.1. Estimating the apparent weathering intensity rate

The weathering intensity rate is used to describe the ratio of the changes in the state of weathering and a function of time required for that change to take place (Huisman, 2006). Using the difference of the rock properties of the RRM and the SRM and the number of exposure years, the apparent rate of e.g. IRS, can be determined using the formula in Tating et al. (2013):

$$R_{IRS}^{app} = \frac{IRS_{init} - IRS_t}{log\,(1\,+\,t)} \tag{18}$$

where IRS_{init} is the value from RRM (RIRS) and IRS_t is the IRS of the SRM (SIRS) and t is the number of exposure years. For the GUs with available reference slopes, IRS_{init} is the IRS value in the reference slope, IRS_t is the value for the older slope, and t is the number of years that elapsed between the times the two slopes were excavated. The formula can be used for SPA, CD, FRIC and COH.

4.5.6.2. Estimating salt weathering rate

The formula to determine the rate of salt of weathering is proposed by Matsukura & Matsuoka (1996). This was derived from their study in the development of tafoni or the cavities associated to salt weathering in Japan. This was also used by Kamh (2011) to determine the rate of deterioration in the sandstone dimension stones in ancient buildings in Germany. This formula is adapted in this research to determine the rate in the development of the same structures found in Saint Vincent and to estimate the retreat rate of the matrix of the lahar deposits in Dominica. The rate is given by:

$$R_w = \frac{D_w}{T_e} \tag{19}$$

where R_w is the rate of weathering, D_w is the depth of the cavity and the estimated amount of retreat of the matrix with respect to a reference clast and T_e is the year of exposure. T_e in this research is the same as the t in Equation 15.

5.   SLOPE CHARACTERIZATION

5.1.   Introduction

The fieldwork covered ten exposures in Saint Vincent and fourteen exposures in Dominica (Appendix 9.2).   One location in each island is described in detail in this chapter. The descriptions of the other locations, including the map showing all the locations, are included in Appendix 1. The slopes in these locations consist of andesites, basalts and pyroclastic deposits and lahar deposits.   The andesites and basalts occur as pillow and massive lavas. The pyroclastic rocks are block-and-ash flows, tuff breccia, tuff lapilli and ignimbrites. These rocks are common in both islands, except for the ignimbrites and the lahar deposits which are only seen in Dominica.

5.1.1.   Exposure SV1 in Saint Vincent

Exposure SV1 is along the Windward Highway in the vicinity of the new airport in Argyle. The total size of the exposure is 60 m length with a maximum height of about 9 m. Based on the geologic map (Figure 42 in Appendix 10.1), this area is underlain by the "lava flows, domes and associated deposits" rock group. Four geotechnical units (GUs) are identified in this exposure (Figure 7b).
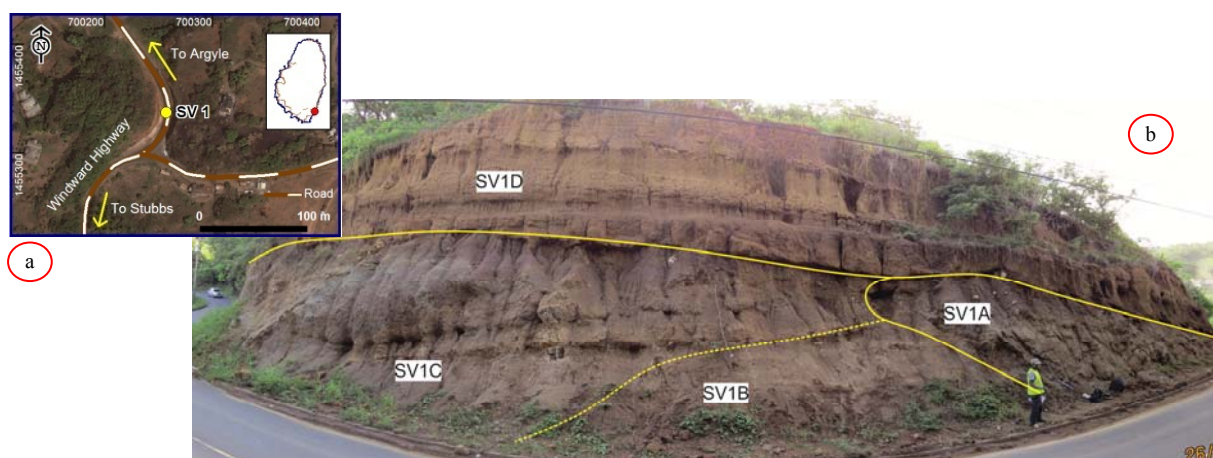
Figure 7. Exposure SV1 along the Windward Highway in Saint Vincent. (a) Location indicated by yellow dot in small map and general location shown by red dot in inset map; (b) Four geotechnical units are identified in the exposure. Map projection: UTM Zone 20 N, datum: WGS84, source: Google Earth.   (photo by XAC, 2014)

5.1.2.   GU SV1A

GU SV1A is a moderately weak (intact rock strength (IRS) = 8.75 MPa) greenish-light grey basalt lava, with inclusions of fresh, strong (IRS =   175 MPa) greenish dark-grey, vesiculated, coarse-grained core stones (Figure 8a). It is highly weathered. Three major discontinuity sets were observed: J1 – 60/050 with discontinuity spacing (DS) of 0.4 m, persistent within the unit, large-scale roughness slightly curved, small-scale roughness smooth undulating, with clay infill material, dry;   J2 – 66/068 has DS of 0.3 m, terminating against the contact with the overlying unit (Figure 8b), slightly curved, smooth undulating, filled with clay material, dry;   J3 – 8/080 has DS of 0.9 m, terminating against other discontinuities, curved, polished stepped, with clay infill material. No seepage observed and all discontinuities are dry.

Figure 8. Highly weathered basalt in GU SV1A. (a) greenish-grey, vesiculated cores stones; (b)most joints are abutting in the contact with the overlying unit. (photos by XAC, 2014)

5.1.3. SV1B

GU SV1B is a tuff breccia deposit. The matrix is moderately weak (IRS = 8.75 MPa), yellowish-brown tuffaceous material containing very few strong, light-grey, coarse grained andesite clasts. It is highly weathered as shown in Figure 9. There are three major discontinuity sets: J1 - 60/050 with DS of 0.12 m and terminating within the unit, slightly curved, polished undulating, filled with clay. J2 - 85/174 has DS of 0.02 m, abuts against the contact with the overlying unit, slightly curved rough undulating and filled with soft sheared fine material. J3 - 39/286 with DS of 2 m, terminating outside the unit, slightly curved, rough planar with only staining in walls. The surface material is very friable.

Figure 9. Highly weathered pyroclastic flow deposit in GU SV1B. Yellow line is the contact with the overlying unit and red circles outline the clasts. (photo by XAC, 2014)

5.1.4.   GU SV1C

GU SV1C is a block-and-ash flow (BAF) deposit with clasts of boulders and cobbles of andesite (Figure 10a), as well as blocks of tuff (Figure 10b). These are imbedded in a weak (IRS = 3.125 MPa) orange-brown to buff, medium to fine-grained tuff matrix. Both clasts and matrix have very friable surfaces (Figure 5b) probably due to baking and chilling. There are three major discontinuity sets   :J1 - 80/126, DS is 1.6 m, terminating within the unit, slightly curved, rough undulating, infilled with coarse soil. J2 - 80/204 has DS of 1.5 m, terminating within the unit, slightly curved, rough undulating. J3 - 30/314 with DS of 0.1 m, terminating against discontinuities, curved rough, undulating with clay infills. J4 - 10/070 with DS of 0.02 m, terminating against other discontinuities, slightly curved, smooth undulating with clay infill material. All the discontinuities are dry.

Figure 10. Block-and-ash flow (BAF) deposits in GU SV1C. (a) the clasts are cobbles and boulders of andesite; (b) highly friable surface of boulder-sized tuff clast (photos by XAC, 2014)

5.1.5.   GU SV1D

GU SV1D overlies all the three units previously described. It is a very weak, thinly, (top of exposure) to thickly (edge of exposure) bedded, brown, tuff . It is generally highly weathered and friable. Four layers are separated by dark brown weathering horizons shown in dashed yellow lines in Figure 11a. Three discontinuity sets are recorded: Bedding plane - 39/286 DS of 0.2 to 1 m, persistent throughout the exposure; J1 - 80/223 has DS of 0.5 m, terminating within the unit and against other discontinuities, straight, rough planar with clay infills. J2 - 90/296, DS is 0.5 m, terminating against other discontinuities, including the contact with the other layers, curved, rough planar, infilled with clay. Some joints appear to be widened or caused by rill erosion (in yellow arrow in Figure 11b).

Figure 11. Tuff overlying the other GUs in GU SV1D. (a) layers separated by weathering horizons shown in dashed yellow lines; (b) some discontinuities appear to be widened or caused by rill erosion. (photos by XAC, 2014)

5.2.   Exposure D10 in Dominica

Exposure D10 is a benched roadcut along a straight section of the Imperial Highway near Canefield (Figure 12a). The exposure is about 80 m in length and about 30 m high. The mapping, however, only covered the first bench or the lowermost 8 m part of the slope mainly because of its accessibility. Based on the variation in the discontinuity pattern and rock mass weathering, the slope was subdivided into five GUs (Figure12b).
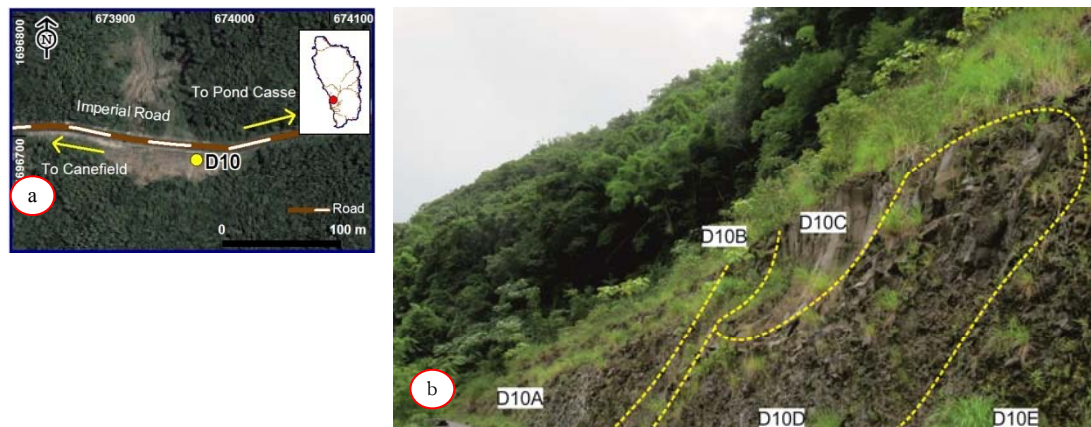
Figure 12. Exposure D10 . (a) location of the exposure along the Imperial Road; (b) Five geotechnical units based discontinuity patter and rock mass weathering. Map projection: UTM Zone 20 N, datum: WGS84, source: Google Earth.   (photos by XAC, 2014)

5.2.1.   GU D10A

GU D10A consists of very strong, greenish dark grey pillow basalts. It is slightly weathered and highly jointed. Joints form small polyhedral blocks (Figure 13a). The discontinuity sets are: J1 – 55/018 with DS of 0.06 m, J2 – 80/272 with DS of 0.3 m and J3 – 45/158 with DS of 0.3 m. These sets terminate against other discontinuities or at the top of the bench, straight, rough undulating and infilled with non-softening

fine material. J4 –62/226 with DS of 0.2 m, terminating against other discontinuity sets, straight, rough undulating; with non-softening fine infill material. J5 – 25/032 with DS of 0.02 m, terminating against other discontinuities, straight, polished stepped with coarse soft sheared infill material. The whole exposure is wet; a small flow emanated from the top of the slope. Amorphous precipitate on the surface of some discontinuities suggests regular or prolonged water flow (Figure 13b). Small plant species grow along some joints.

Figure 13. Discontinuities in GU D1A. (a) the discontinuities for polyhedral blocks (1 m tape in red circle) ; (b) amorphous deposits on the surface of discontinuities indicate trace of water flow path. (photos by XAC, 2014)

5.2.1.1. GU D10B

GU D10B has the same rock material and rock mass and weathering condition as GU D10A. Five discontinuity sets form medium to large columnar blocks (Figure 14a). J1 – 75/322 with DS of 0.1 m, slightly curved, rough stepped. J2 - 80/104 with DS of 0.3 m, straight, rough stepped. J3 – 70/360 with DS of 0.1 m, slightly curved, rough stepped. J4 – 36/192 with DS of 0.15 m, straight, smooth undulating. Most discontinuities are open and filled with soft sheared medium material. J5 – 65/084, DS of 0.7, straight, smooth planar, filled with soft sheared, coarse material. All joints terminate against other joints planes. The whole exposure is wet from water dripping out of some discontinuities.

5.2.1.2. D10C

The rock material and rock mass (Figure 14b) in D10C is the same as in D10A and D10B. Four discontinuity sets form columnar blocks. The discontinuity sets are: J1 – 60/312 with DS of 0.1 m, slightly curved, rough stepped; J2 – 65/038 with DS of 0.5 m, also slightly, curved rough stepped; J3- 50/112 with DS of 0.3 m, slightly curved, rough undulating. J1, J2, J3 abut on top of the bench and on the slope face. J4 – 80/161 with DS of 0.1 m, straight polished, undulating, terminating against other discontinuities. The infill material is medium soft sheared for J1 and J4 and clay for J2 and J3. A small flow emanated out of some discontinuities.

Figure 14. Columnar blocks formed by the discontinuity sets (a) in GU D10B (yellow tape in red circle is 1 meter) and (b) curved discontinuities (in yellow plane) in GU D10C

5.2.1.3. GU D10D

In GU D10D, the basalt is moderately strong (IRS = 31.25 MPa) and brownish dark grey in colour. It is moderately weathered. The discontinuity sets form very small polyhedral blocks (Figure 15a). The discontinuity sets are: J1 – 85/260 with DS of 0.6 m, straight, polished undulating, terminating at the top of the bench. J2 – 27/003 with 0.1 m DS. J3 – 42/050 with 0.07 m DS. J4 – 53/197 with 0.08 m DS. J2, J3 and J5 are straight, smooth planar; J1 and J2 have fine, sandy infill material while J3 and J4 are filled with clay. Discontinuities terminate against each other. A small water flow coming out from some discontinuities.

5.2.1.4. GU D10E

The basalts in GU D10E is moderately weak (IRS = 8.75 MPa) and brownish-grey in color. The matrix is coarse to fine-grained, yellowish-brown material and includes sub-angular to sub-rounded fragments with average block size of 2 cm x 2 cm. The rock mass is highly weathered and has no observable joints (Figure 15b). The exposure is generally wet.
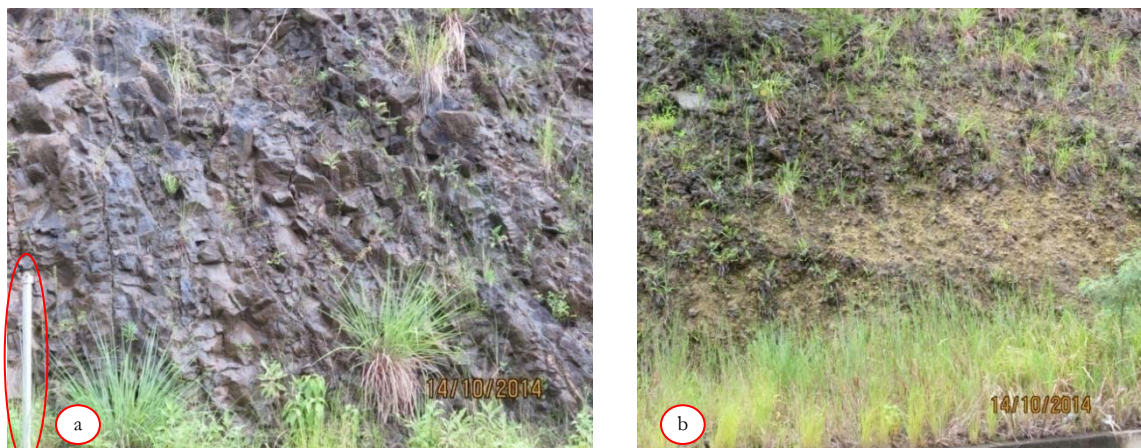
Figure 15. Smaller blocks formed by discontinuities in GUs D10D and D10E. (a) the rock mass in GU is moderately weathered in GU D10D and (b) highly weathered in GU D10E. (photos by XAC, 2014)

6.   RESULTS AND DISCUSSION

The deformability of rock masses is controlled by the properties of both intact rock and discontinuities (Hoek, 1983; Hack, 1998; Price, 2009) and these parameters have been shown to be affected by weathering (ANON., 1995; Hencher & McNicholl, 1995; Fan et al., 1996; Hack & Price, 1997; Gupta & Rao, 2000; Huisman; 2006; Tating et al., 2014). This chapter presents the changes in these properties based on the data gathered from the volcanic and volcaniclastic rocks in Saint Vincent and Dominica.

6.1.   Changes in the intact rock and rock mass properties with weathering degree

The intact rock and rock mass properties relevant to this research were previously introduced in Chapter 4. These include the properties that were estimated and measured in the field such as the intact rock strength (IRS) and the discontinuity spacing (DS), and the parameters obtained using the SSPC system namely, discontinuity spacing (SPA), condition of single discontinuity set (TC), and overall condition of discontinuities (CD). As described in Chapter 3.2, massive lava flows and pyroclastic deposit flows are common in both Saint Vincent and Dominica. The geotechnical units (GU) identified in these rocks did not show significant differences in properties between Saint Vincent and Dominica. Hence, the data of the two islands are combined in the analysis regardless of location. In addition to this, it has to be noted that both andesite and basalt occur as pillow lavas and massive flows. For the basalts, the pillow basalts (BP) and massive basalts (BM) are separated in the analysis because of the large difference in the density of the discontinuities. The GUs comprising both groups have different weathering degrees and thus comparison of their properties is possible. In the case of andesites, the GUs defined in the exposures are all classified fresh and so the andesites (AP) included in the succeeding graphs only refer to the pillow andesites.

The average values of the rock properties obtained from the GUs belonging to the same rock type and the same weathering classification (BS5930, 1999) (in Table 1, Chapter 2) are plotted against increasing degree of weathering to show the changes in these properties as weathering progresses. For clearer illustration, the average values are used in the graphs. The meaning of the abbreviations and notations used in the graphs (Figures 1-3, 9-10, 12-16) and in the texts describing them are explained in Table 6. The dotted lines indicate high uncertainty due to a limited number of observation points. For the data of individual GUs, refer to the scatter plots (rock properties versus SSPC WE values) in Appendix 9.3.

Table 6. Abbreviations and notations used in Figures 1-3, 9-10, 12-16

Lithology (details in Chapter 3)		Weathering degree (BS5930, 1981)		SSPC WE
AP	Andesite	I	Fresh	1
Bslt	Basalt	II	Slightly weathered	0.95
BP	Pillow basalts	III	Moderately weathered	0.9
BM	Massive basalts	IV	Highly weathered	0.62
Vlcs	Volcanoclastics (block-and-ash flow	V	Completely weathered	0.35
	(BAF) and (tuff breccias and lapilli)			
Tuff	Tuff			
Mtrx	Matrix of Vlcs			

6.1.1.   Intact Rock Strength (IRS)

The average IRS values are plotted in Figure 16. For this parameter, the GUs are grouped according to the lithologic types. The IRS values obtained from BP and BM are combined because there is no significant difference in the values of GUs within the same weathering grade. The graph shows that for all the rocks

types, the average IRS generally decreases as the weathering degree increases. The consistent reduction in the IRS from fresh to highly weathered GUs reflects the effect in the modification of the original structure of the intact rock during weathering which causes the bonding between mineral crystals and grains to disrupt. This creates microfractures and voids, and thus rocks become soft, friable and generally weakened (ANON., 1995; Gupta & Rao, 2000). This is in agreement with the study of Tugrul & Gurpinar (1997) that showed a significant increase in the porosity, a decrease in density, and a decrease in the Uniaxial Compressive Strength (UCS) in highly weathered basalts because 60% of the mineral composition of this rock decomposes in this weathering grade.

Weathering is an irreversible process (Price, 1995) and although the whole range of weathering grade is not represented in all the rocks investigated, it is expected that the reduction is consistent, although at a different rate, throughout the weathering spectrum provided that no cementation or any alteration has affected the rock masses. Except for the limited exposure of cemented tuff beds, there are no indications of other mineral alteration processes, for example, silicification which usually results in a decrease in porosity and an increase of IRS of the altered rock (Sibson, 1998 in Zuquim & Rowland, 2013; Pola et al., 2014). The absence of these processes makes the degradation of the rock masses due to weathering a straightforward process.
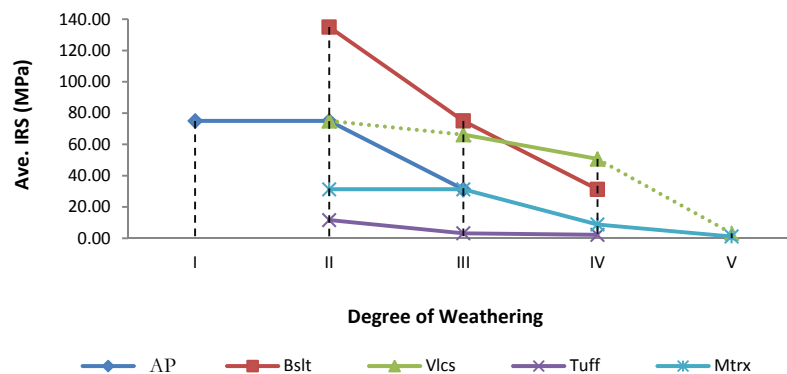
Figure 16. Average Intact Rock Strength (Ave. IRS) vs. degree of weathering. The IRS generally decreases with increasing degree of weathering. (Markers indicate average values from multiple GUs; the lines between the markers have no meaning, these are for identification and indication of data uncertainty only: solid lines indicate low uncertainty and dotted lines indicate high uncertainty. Refer to Table 5 for the explanation of the abbreviation and notations).

The rebound values of the Schmidt Hammer yielded IRS values that range from 40 to 60 MPa in the slightly weathered BM and 39 to 48 MPa for the slightly weathered BP. These values are lower than the 75 MPa estimated using the geologic hammer. Based on the strength classification in the BS5930 (1999) (Table 4, Chapter 4) the Schmidt Hammer values classify the BM as strong to moderately strong and the BP as moderately strong, whereas these are strong based on the value from geologic hammer. The Schmidt Hammer values fall in the upper limit of the moderately strong class and lower limit of the strong class and thus, still comparable to the classification based on geologic hammer estimate. This difference can be attributed to the various factors affecting the measurements in both methods. The size and shape of lumps, surface on which lumps rests when hammered, and the strength of the operator affect the IRS values obtained using the geologic hammer (BS5930, 1999). It is likely, however, that the inconsistencies in the measurements caused by these factors are minimized as the investigator gains experience as the fieldwork progresses. Although the Schmidt Hammer is recognized as a reliable tool for surface hardness measurements, among its limitations are the tendency to be affected by the discontinuities behind the measured surface (Hack, 2002) and the roughness of the impact surface (Goudie, 2006). Note that in the study area, all the rock masses have discontinuities and almost all the rock surfaces are coated with weathering skin making the surface generally rough. These complications in using the Schmidt Hammer is one of the reasons why using simple means (using hand and geologic

hammer) in estimating the strength of the intact rock for rock mass classification purposes is more recommended (Hack, 1998; BS5930,1999; Hack & Huisman, 2002).

6.1.2. Spacing of Discontinuities

The discontinuities recognized in the exposures include joints and bedding planes. The pronounced discontinuities in the exposures of the crystalline volcanic rocks (AP, BP, BM) and Tuff are mostly cooling joints. Bedding structures are also present in the Tuff. Most of the Vlcs exposures do not show distinct discontinuities that are as defined and clear as the discontinuities in the lava flows and in the tuff. In some exposures however, the alignment of clasts, which is indicatives of the flow direction during deposition, may be considered as an integral discontinuity that may become a plane of weakness in the future depending on the changes in the tectonic stress regime or the overall changes in the rock mass properties due to weathering.

The change in the average discontinuity spacing (DS) with increasing degree of weathering is shown in Figure 17. The average DS in the AP and the BP is consistently decreasing from fresh to highly weathered GUs. In the BM, Vlcs and Tuff, the average DS values show an initial decrease from slightly to moderately weathered GUs followed by an increase from moderately to completely weathered GUs. This trend is also reflected in the graph of average SPA in Figure 18, which indicates that block size is also decreasing from fresh to moderately and is increasing from moderately to highly weathered GUs. It has to be noted that the values of the slightly weathered and highly weathered Vlcs are derived from single GUs (thus the dotted line) and thus the uncertainty is high

.
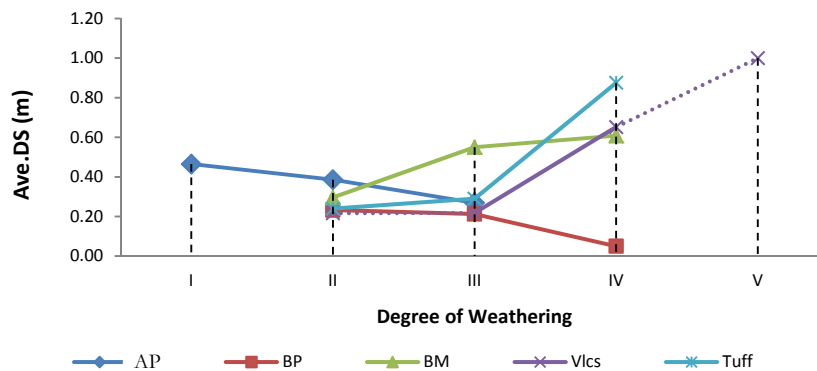
Figure 17. Average discontinuity spacing (Ave. DS) vs. degree of weathering. The Ave. DS is decreasing with increasing degree of weathering for AP and BP GUs and generally increasing with increasing degree of weathering in the BM, Vlcs and Tuff GUs. (Markers indicate average values from multiple GUs; the lines between the markers have no meaning, these are for identification and indication of data uncertainty only: solid lines indicate low uncertainty and dotted lines indicate high uncertainty. Refer to Table 5 for the explanation of the abbreviation and notations).
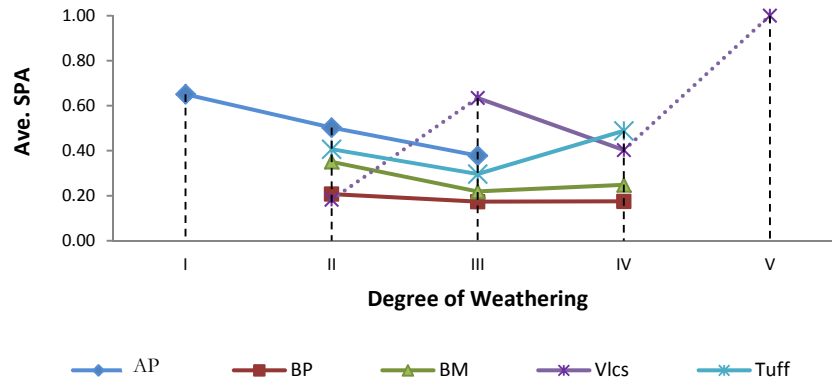
Figure 18. Average SPA (Ave. SPA) vs. degree of weathering. The Ave. SPA is generally decreasing from fresh to moderately weathered GUs of most of the rock types and generally increasing from moderately weathered to completely weathered BM and Tuff GUs (with the exception of the slightly weathered Vlcs GU). (Markers indicate average values from multiple GUs; the lines between the markers have no meaning, these are for identification and indication of data uncertainty only: solid lines indicate low uncertainty and dotted lines indicate high uncertainty. Refer to Table 5 for the explanation of the abbreviation and notations).

The general decrease in the SPA with increasing degree of weathering results from the opening of existing discontinuities, making them more visible and thus measureable (Hencher & McNicholl, 1995; Tating et al., 2013) as seen in Figure 19a. The same can also be applied to the clast-matrix interface in the volcaniclastics (Figure 19b).

Figure 19. Apertures of discontinuities in highly weathered rocks. (a) Discontinuities become more visible in tuff breccia when the discontinuity aperture increases as result of increasing degree of weathering ;(b) increased opening along the matrix-clast interface in the Vlcs (photos by XAC, 2014, Saint Vincent (a); Dominica (b))

The increase in the values of average DS and average SPA from moderately weathered to highly weathered BM GUs is reflected in Figures 20a to 20c. Figures 20a and 20b are photos of GU SV2A whereas Figure 21c is GU SV2C (description in Appendix .2 for slope description). The red line (Figure 20a) outlines the persistent and sharp discontinuities. As the degree of weathering increases, the trace of the discontinuities appear to fade out (outlined by dashed red lines). This apparent disappearance of joints occurs when the clay minerals produced during the earlier stage of weathering expand and induce further microcracking and expansion in the rock fabric. In crystalline rocks where mineral crystals are interlocking, the expansion can only be accommodated along the joint openings and the expansion leads to the narrowing of the apertures and eventual "*healing*" along the discontinuities making these less visible (Figures 20b and 20c) (Ehlen, 2002).
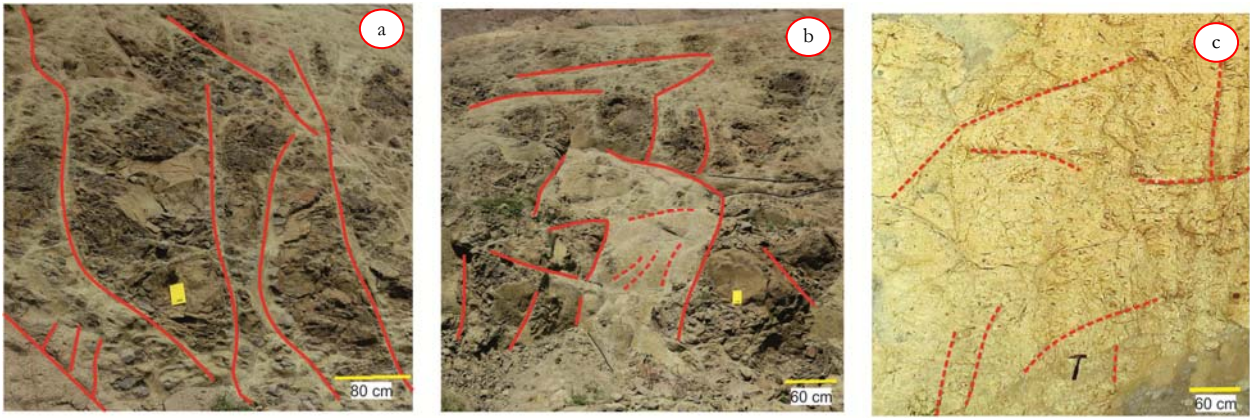
Figure 20. Joints becoming less evident with increasing degree of weathering. (a) persistent cooling joints in moderately weathered BM GU; (b) widened distance between joints with increasing weathering of core stones; (c) faint traces of joints in highly weathered BM GU (photos by XAC, 2014; SV2, Saint Vincent)

The value for the completely weathered Vlcs GU in Figures 17 and 18 is from a single observation point (D11) in Dominica (refer to Appendix 9.2 for location and slope description). However, the investigated exposure is very extensive and it exhibits the same characteristics seen in other exposures of the same material in other areas in Dominica. The rock mass in D11 appears to be massive (Figure 21a) and this explains the very high value of DS and SPA. The opening of the discontinuities is tight, likely as a result of the mechanism explained by Ehlen (2002) combined with clay infilling, such that the discontinuity traces cannot be easily observed even from a closer view (Figure 21b). These discontinuities can actually be persistent. Even on the microscopic scale, the healing effect by clay inflilling in discontinuities in the more advanced weathering grades results to the decrease in the density of microfractures as observed by Basu et al. (2008). The high SPA values are contributed by the clast-supported volcanoclastics. The spaces between the clasts are enough to accommodate internal stresses due to weathering thus no new joints are opened. For illustration, Figure 21c shows how discontinuities in the matrix-supported part of a highly weathered tuff breccia (GU SV7A) (Appendix 9.2) appear to terminate in its contact with the clast-supported part.
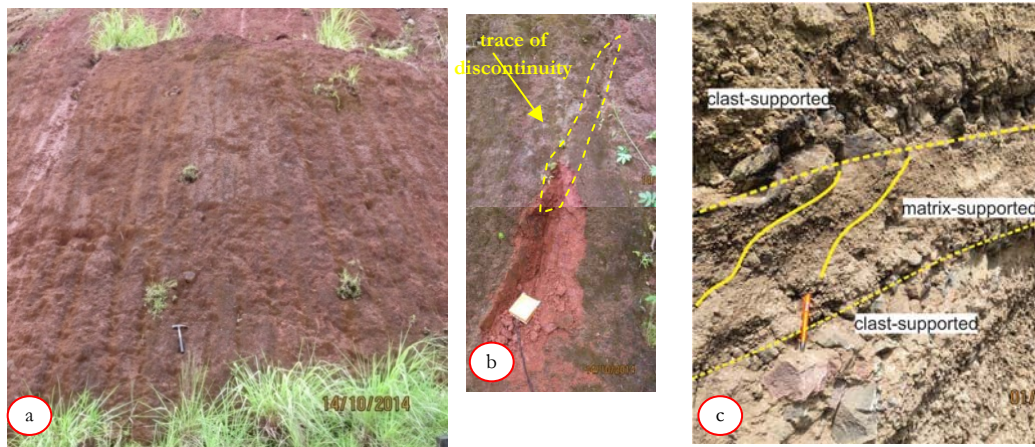
Figure 21. Discontinuities in completely weathered exposure and highly weathered Vlcs GUs (a) Apparently massive rock mass (b) very faint surface manifestation of a persistent discontinuity; (c) Discontinuities in clast-supported and matrix-supported tuff breccia. Fewer joints in the clast supported highly weathered tuff breccia (SV7A) suggesting that spaces between the clasts are enough to accommodate internal stresses caused by weathering. (photos by XAC, 2014; a, b: Dominica; c: Saint Vincent)

Discontinuities that are parallel or sub-parallel to the slope are common in highly weathered GUs (Figures 22a and 22b). These are steeply dipping joints and in most cases, the apertures are open and further widened by plant roots. These may be unloading joints that correspond to integral discontinuities that became mechanical discontinuities due to the combined effect of weathering and stress relief. ANON. (1995) describes unloading joints usually parallel to the erosional surface and these joints are expected to decrease with depth.
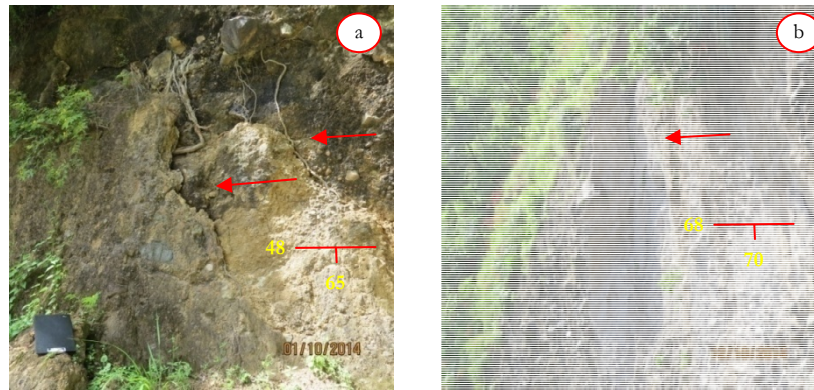
Figure 22. Unloading joints resulting from combined weathering and stress relief. (a) Joints parallel to sub-parallel to the slope correspond to unloading joints seen in block-and -ash flow deposits in SV8, Saint Vincent and (b) in lahar deposits in D7, Dominica. (red lines point to strike of joint planes) (photos by XAC, 2014)

6.1.3. Condition of Discontinuities

The average total condition of individual discontinuity sets (TC) is plotted in Figure 23. The graph shows that for all the rocks, the average TC is decreasing with increasing degree of weathering. The same trend is reflected in the graph of the average overall condition of discontinuity CD (Figure 24). The reduction in these values generally reflects the compound effect of the decreasing parameter values for the large-scale (Rl) and small-scale (Rs) roughness of the discontinuity plane, an increasing frequency of clay infill materials (Im) along discontinuities with increasing weathering degree, and the lack of cementation along these discontinuities (parameters explained in Chapter 4.3.4).

There are cases when the expected reduction in the Rl values with increasing degree of weathering is difficult to observe. This is because the waviness or shape of the discontinuities which dictates the parameter values for Rl is highly influenced by the type and density of discontinuities. For example, the discontinuities in the fresh to moderately weathered GUs are usually straight (therefore low Rl value) and the discontinuities (including unloading joints) in the highly weathered Vlcs GUs are wavy (high Rl value). The reduction in the Rs values reflects the smoothening effect of weathering along the discontinuity walls as also observed by Tating et al. (2014). Rs, therefore, appears to be more representative of the weathering effect in the discontinuity surface roughness.
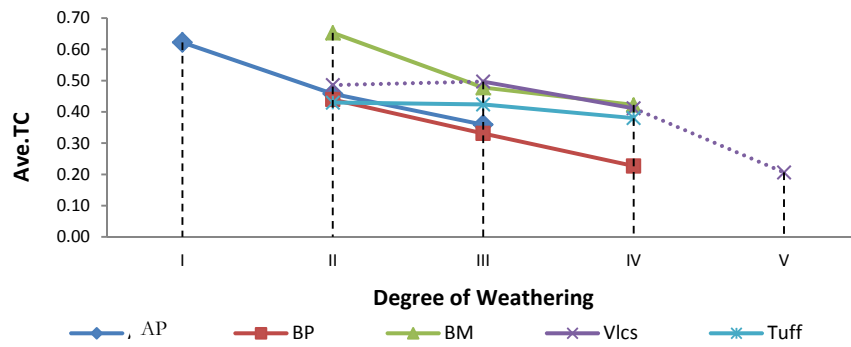
Figure 23. Average TC (Ave. TC) vs. degree of weathering. The average TC values in all rock types are consistently decreasing with increasing weathering degree. (Markers indicate average values from multiple GUs; the lines between the markers have no meaning, these are for identification and indication of data uncertainty only: solid lines indicate low uncertainty and dotted lines indicate high uncertainty. Refer to Table 5 for the explanation of the abbreviation and notations).
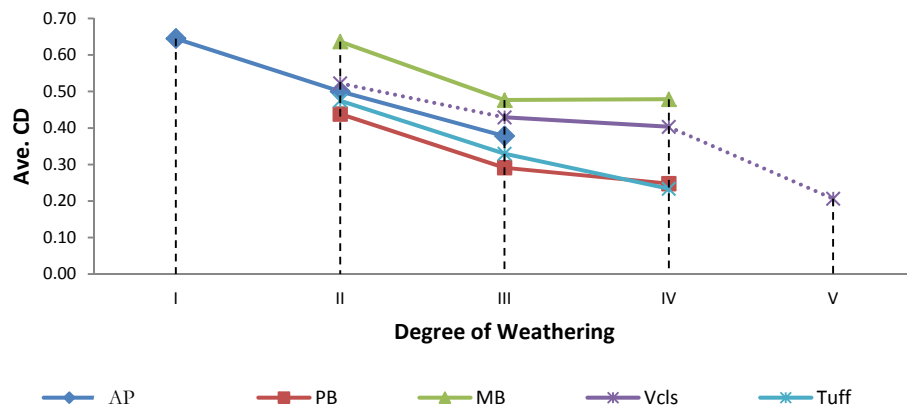
Figure 24. Average CD (Ave. CD) vs. degree of weathering. The average CD values in all rock types are decreasing with increasing degree of weathering. (Markers indicate average values from multiple GUs; the lines between the markers have no meaning, these are for identification and indication of data uncertainty only: solid lines indicate low uncertainty and dotted lines indicate high uncertainty. Refer to Table 5 for the explanation of the abbreviation and notations).

The Im in the studied GUs does not only consist of secondary minerals. The scoria that are interbedded with the cemented Tuff (Figure 25) particularly in GU SV5A in Saint Vincent (Appendix 9.2) are classified as "flowing" infill material (Hack, 1998) with very low Im value. Because these layers are bounded by the cemented and thus less permeable materials, the resulting poor drainage condition makes moisture to be retained for a longer period leading to enhanced weathering and loss of cohesion of the materials (Hay, 1981).

Figure 25. "Flowing" Im in tuff beds. The unconsolidated scoria in between tuff beds in SV5, Saint Vincent is classified as flowing infill materials that gives a very low Im value in the SSPC system (photo by XAC, 2014)

6.2. Rock mass friction angle (FRI) and cohesion (COH)

The friction angle and cohesion are among the strength parameters used to describe the deformation characteristics of rock masses (Hoek et al., 1983). In the SSPC system, the IRS, SPA and CD are used to empirically derive the FRI and COH for the RRM (RFRI) and SRM (SFRI) as described in Chapter 4. The average values of the friction angle and cohesion for the SRM (solid and dotted lines) and RRM (dashed lines) are plotted in Figures 26a and 26b and Figures 27a and 27b, respectively. The difference in the values represents the general effect of weathering in these parameters. As mentioned in Chapter 4, the excavation of the roadcuts investigated only utilized the bucket of an excavator. This is not expected to cause considerable damage to the rock mass and thus the influence of the method of excavation (ME) is given the value of 1 (Table 4, Chapter 4). The small difference of the average values of the RRM friction angle and the SRM friction angle in fresh to highly weathered AP and BM GUs suggests that weathering has not significantly affected these parameters in these GUs. The effect of weathering is more pronounced in the moderately weathered BP GUs. The difference in the average values of RRM and SRM in the Vlcs and Tuff also show that compared with the AP and BM, weathering has a higher effected in the friction angle and cohesion of these GUs. The graph further suggests that for the Vlcs, the effect of weathering leads to an increase in the average friction angle and cohesion. As mentioned in the previous section, the value of the highly weathered GU only represents a single observation point and the data uncertainty may be high. However, the presence of the very few discontinuities in the exposure and the visual stability assessment of possible "small problems" appear to agree with this. Generally, it appears that the change in friction angle and cohesion is more sensitive to SPA than to IRS and TC, as these consistently reflect similar trends with SPA.
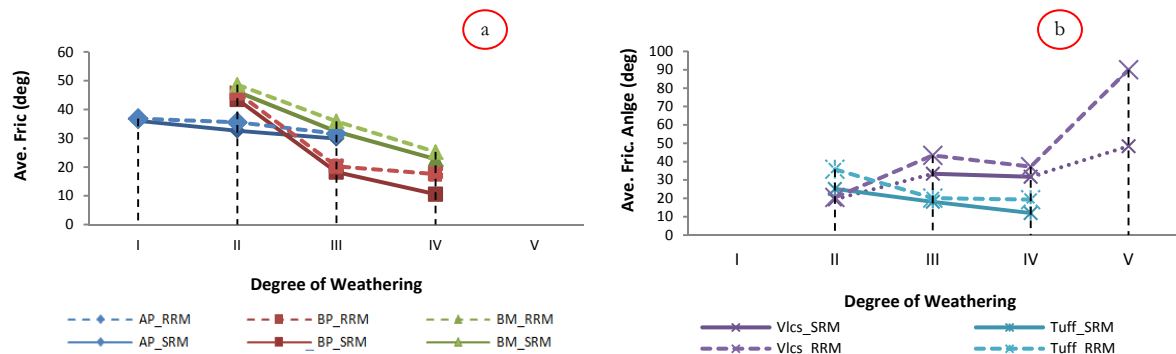
Figure 26. Average Friction Angle (Ave vs. degree of weathering. (a) The difference in the average values of SRM (solid and dotted lines)and RRM (dashed lines) represents the effect of weathering in the AP, BP and BM; (b) and in the Vlcs and Tuff. (Markers indicate average values from multiple GUs; the lines between the markers have no meaning, these are for identification and indication of data uncertainty only: solid lines indicate low uncertainty and dotted lines indicate high uncertainty. Refer to Table 5 for the explanation of the abbreviation and notations).
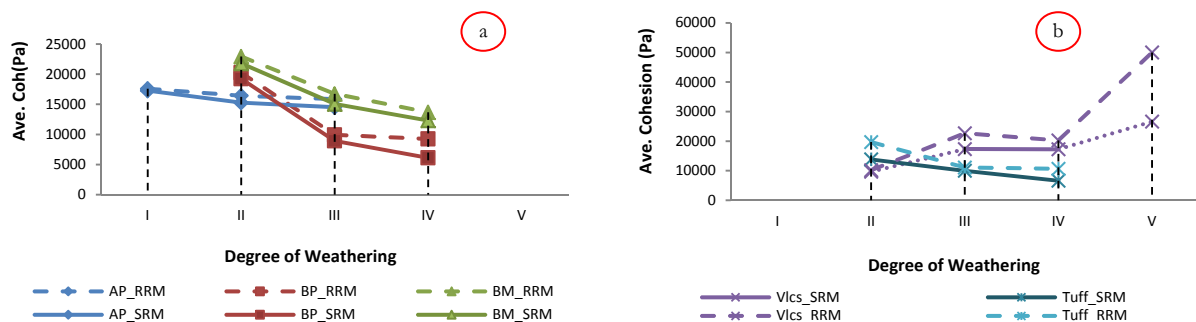
Figure 27. Average Cohesion (Ave. Cohesion) vs. degree of weathering. (a) the difference in the average values of SRM (solid and dotted lines) and RRM (dashed lines) values represents the effect of weathering in the AP, BP and BM (b) in the Vlcs and Tuff. (Markers indicate average values from multiple GUs; the lines between the markers have no meaning, these are for identification and indication of data uncertainty only: solid lines indicate low uncertainty and dotted lines indicate high uncertainty. Refer to Table 5 for the explanation of the abbreviation and notations).

6.3. Weathering intensity rate

The change in the rock properties over the the amount of time needed for the change to occur is the "*weathering dynamic rate*" (Huisman, 2006). This can only be accurately described if a time series of observation on the amount of change is available. This is not the case in this in this research as the data only consist of single and independent observations for each GU. Therefore, only the "*apparent weathering intensity rate*", can be determined and it is represented as the amount of reduction in the rock properties from its "undisturbed" state (RRM) to its current state (SRM) over a logarithmic function of the amount of time the rock masses are exposed.

The weathering reduction factors in Table 3 (Chapter 4) were derived from granodiorites, limestones, dolomites, shales, sandstones and conglomerates in an area in Spain that has a typical Mediterranean climate. Although it is generally accepted that the weathering rate in tropical regions is high, it may not be necessarily true that the actual weathering rate in the studied rock masses in Saint Vincent and Dominica is higher than in Spain. On one hand, the cyclic freeze and thaw, as well as wetting and drying brought about by the high variability of temperature and precipitation during the summer and winter in Spain may be very efficient in weathering the rocks especially the clastic types. On the other hand, the volcanic glasses in the crystalline rocks and in the volcaniclastics in the two islands are highly prone to chemical weathering which is further favoured by the generally, all year round high rainfall and warm, humid climate coupled with the influence of salts in the case of the coastal exposures (as discussed in Chapter 7). Given this balance in the two scenarios, it is possible that the SSPC derived reduction rates are applicable in the study area albeit up to a limited degree of certainty.

Applying Equation 18 (Chapter 4) on the rock properties, the average apparent rate for the rock types studied were calculated. The average values are shown in Table 7. Except for the IRS, the Vlcs and Tuff generally have higher reduction rates in all properties compared to the other rock types. Between the crystalline rocks, the basalts (BM and BP) have higher reduction rates than andesites (AM and AP). In basalts, the pillow lavas (BP) have higher reduction rates than the massive type (BM). For the andesites, the values for the AP are slightly lower than the AM but the difference is not as high as the difference between BP and BM. These differences generally indicate the weathering susceptibility of the various rocks to the weathering process.

Table 7. The apparent rate of weathering expressed as reduction in the rock properties obtained by subtracting the values in the SRM from the values of the RRM divided by a logarithmic function of time

Lithology	IRS	SPA	CD	FRIC	COH
Basalt pillow lavas (BP)	8.37	0.05	0.08	5.23	2583.27
Massive basalts (MB)	6.10	0.05	0.10	4.53	2295.48
Andesite pillow lavas (AP)	3.14	0.01	0.02	2.34	987.49
Massive andesites (AM)	3.70	0.01	0.03	1.63	768.14
Volcaniclastics (Vlcs)	4.03	0.37	0.18	16.84	9172.07
Tuff lapilli (Tuff)	1.34	0.10	0.07	10.82	5562.35

*Massive andesites (AM) were also investigated but because these are all classified as fresh, it is not possible to compare the rock properties with GUs with different degrees of weathering. These are now included in the discussion hereafter.

These differences in the response of the various rocks to weathering can be generally attributed to the difference in their composition and discontinuity characteristics. The heterogeneity of the Vlcs and Tuff as a result of the contrast in the properties of the crystalline clasts and ash- and volcanic glass-bearing matrix

materials may lead to differential weathering in these rock masses. The pyroxene and olivine in the basalts are known to be more susceptible to weathering compared with the plagioclases and hornblende minerals present in the andesites. In addition, the basalts are generally vesiculated. The BP have higher reduction rate because of the inherent high density of cooling joints that makes the rock mass easier to weather compared with the less fractured BM. The opposite is observed in the andesites. The reduction rate is higher in the AM than in the highly jointed AP. This possibly reflects the influence of salts in the studied AM exposure (discussed in Chapter 7). Because most of the rock masses are already weathered before being excavated, it implies that the calculated reduction rates (Table 7) only reflects the reduction of properties since the time when it was freshly exposed not during the time when it was deposited or emplaced.

Another way of determining the amount of change in the rock properties that can occur in a given period of time is by comparing a certain GU to its counterpart exposed in a reference slope, as recommended by Price (2009). In Saint Vincent, the exposure SV2 is used as reference for the exposure in SV1. The slope in SV2 was excavated in 2013 whereas SV1 was in 2006 (refer to Chapter 5 for location and Appendix 1 for complete slope description). GUs SV2C and SV2B are the reference of GUs SV1A and SV1B, respectively. Note however that there is no change in the weathering degree for both rock types, i.e., both GUs are highly weathered in both slopes. The values of reference GUs are used as the initial values in Equation 15 (Chapter 4). The apparent weathering rate computed using both approaches are shown in Table 8. GU SV1B (Vlcs) shows a consistent degradation in terms of all the parameters considered. GU SV1A (BM) shows a "gain" particularly in terms of SPA. This is previously explained in Section 6.1, as an effect of the advanced weathering of the discontinuity wall materials. Nevertheless, the expected reduction is reflected in the condition of discontinuities. As expected, the volcaniclastic deposits show higher reduction rate than the basalts owing to their mineralogical composition and fabric that make them more susceptible to weathering.

Table 8. Estimated rate of reduction in the rock properties of the GUs in SV1 using the reference slope approach and the RRM-SRM concept

Lithology	Years elapsed*	IRS		SPA		SCD		FRIC		COH	
		Ref. Slope	RRM-SRM	Ref. Slope	RRM-SRM	Ref. Slope	RRM-SRM	Ref. Slope	RRM-SRM	Ref. Slope	RRM-SRM
Massive basalt (SV1A)	8	No change	1.479	-0.17	0.056	0.26	0.06	-11.04	3.63	-5907	1964.7
Volcaniclastic (SV1B)	8	No change	5.620	0.31	0.113	0.05	0.223	12.55	8.55	8382	4575.4

* with reference to the year of excavation of the reference slope

The reduction in the values of the rock properties through time is however, not clearly reflected in the graphs (Appendix of the rock properties versus the exposure time. The resulting correlation coefficient (R^2) ranges 0.468 to 0.018. This can be explained by the presence of of highly weathered GUs in recently excavated exposures and the lava flows which are slightly to moderately weathered are in old exposures. Tating et al. (2014) made the same remark for the sandstones in Sabah, Malaysia. However, his observation points were substantial enough to give a clear relationship in the changes in IRS, friction angle and cohesion with time and this allowed him to back calculate the rock properties at $t = 0$.

The rates obtained from the reference slope approach would have given more realistic values, the unavailability of more observation points during the time of the fieldwork makes the results uncertain and Nevertheless, it still indicates that there is an appreciable change in the rock mass properties in a short span of time.

6.4. Weathering degree of GUs in the slope stability classes

The SSPC probability for orientation independent stability (OIS) and orientation dependent stability (ODS) is used in this research to demonstrate the implication of the weathering degree in the stability of the studied rock masses. The relevant equations and classification methods using the values of the rock calculated friction angle and cohesion and other inputs are shown in Section 4.5.6 in Chapter 4 with reference to Hack (1996; 1998) and Hack et al., (2003). The interval used in the classification initially followed the classes in the SSPC form (i.e. <%5, 10%, 30%, 50%.....>95%). However, the GUs are not evenly distributed over these classes so the the interval is hereby modified for the sake or clear presentation (Table 9). In general, GUs with >50% probability to be stable with respect to OIS and to the sliding and toppling criteria of the ODS are higher than those with probability of stability ranging from <50%. Although landslides generally plague the two islands, the visual assessment of stability in the investigated roadcuts identified mostly "small" problems.

Table 9. Summary of results of the probability of OIS and ODS stability classification

	Probability of OIS			
Probability to be stable:	≤5%	7% - 49%	50% - 94%	≥95%
Percentage of GU under each OIS classification *(n = 53)*	23%	21%	9%	47%
	Probability of ODS			
Probability to be stable:	≤5%	30% - 70%	≥95%	
Percentage of GU in each ODS - sliding criterion classes *(n = 49)*	45%	8%	47%	
Percentage of GU in each ODS - toppling criterion classes *(n = 49)*	37%	6%	57%	

Because the degree of weathering is incorporated in the calibration of the SSPC system, it is expected that the probability of stability will reflect the influence of the weathering degree of the classified GUs. The GUs consisting each of the stability classes are subdivided according their weathering degree and these are presented as percentages in Figures 28 to 30. In terms of the OIS, the moderately to highly weathered GUs are dominant in the class with ≤5% probability to be stable whereas slightly weathered GUs are dominant in the class that has ≥95% probability to be stable (Figure 29). Highly weathered GUs are dominant in the classes with 7%-49% and 50%-94% probability. With respect to the ODS-sliding criterion, the GUs that are classified to be ≤5% probability to be stable are dominantly highly weathered whereas the GUs classified to have ≥95% probability to be stable are dominantly fresh to moderately weathered (Figure 30). In the ODS-toppling criterion, the slightly weathered to highly weathered GUs are almost uniformly distributed in the ≤5% and ≥95 probability classes of stability. Slightly weathered GUs are also more dominant in the stability class of 30% - 70% probability to be stable (Figure 31). Note that the SSPC system also considers slope stability factors that are not influenced by weathering, such as slope height, slope angle, and the orientation of the discontinuities with respect to slope geometry.
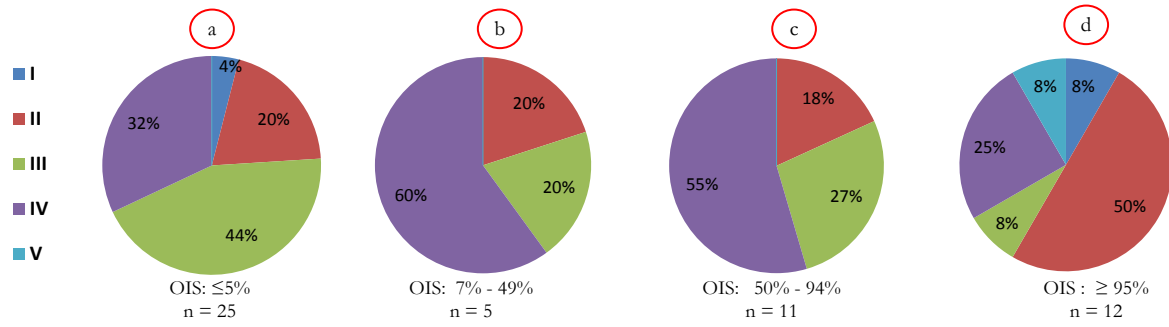
Figure 28. Degree of weathering of the GUs in the OIS stability classes. The class with ≤5% probability to be stable are dominantly moderately weathered whereas the classes with ≥95% probability are slightly weathered. Highly weathered GUs are dominant in the classes with 7%-49% and 50%-94% probability of stability.
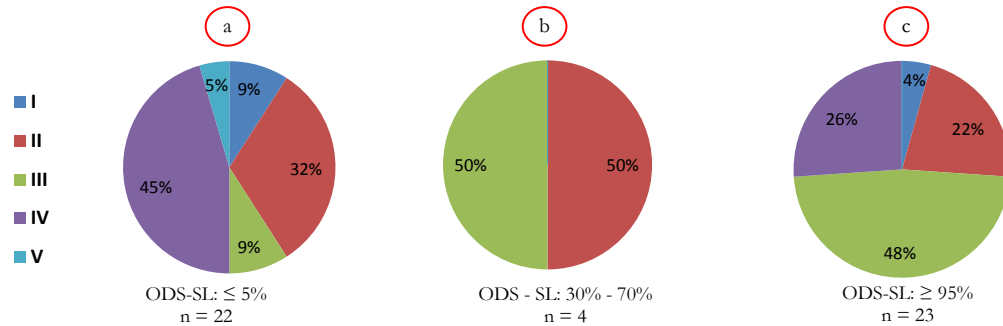
Figure 29. Degree of weathering of GUs in the ODS-sliding criterion classes. Highly weathered GUs are dominant in the class with ≤5% probability to be stable whereas moderately weathered GUs are dominant in the class with ≥95% probability to be stable
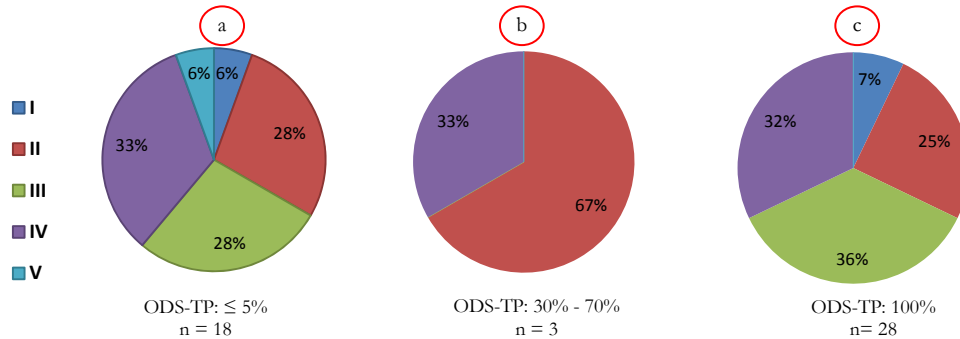
Figure 30. Degree of weathering of GUs in the ODS-toppling criterion classes. The the slightly weathered to highly weathered GUs are almost uniformly distributed in the ≤5% and ≥95 probability classes of stability. Slightly weathered GUs are also more dominant in the 30% - 70% probability of stability class

6.5. Summary

The results of the data analyses show a generally consistent reduction in the average values of intact rock strength (IRS) and in the average values of the parameters for the condition of individual discontinuity sets (TC) and the overall condition of discontinuities (CD). The average values of the parameter for discontinuity spacing (SPA) and the average of measured discontinuity spacing (DS) are generally decreasing for the andesite (AP) and pillow basalt (BP) GUs. The massive basalt (BM) GUs however follow the trend of the volcaniclastics (Vlcs) and tuff lapilli (Tuff) that show increasing SPA with increasing weathering, contrary to the expected reduction in this parameter with weathering. This is explained by the development of secondary minerals along the discontinuity walls that decreases their visibility. The changes in these properties are reflected in the calculated rock mass friction angle and

cohesion. Generally, it appears that the change in friction angle and cohesion is more sensitive to SPA that to the IRS and TC, as these consistently reflect similar trends. The difference of the computed RRM properties and the existing slope properties (SRM) can only be attributed to weathering and stress relief method the method of excavation is not considered to cause significant damage.

The apparent weathering rate is calculated as the change in the properties of the reference rock mass (RRM) and the Slope Rock Mass (SRM) over a logarithmic function of time. In order of decreasing apparent weathering rate, the various rock types considered in this research are arranged in the following order: Vlcs, Tuff, BP, BM, massive andesites (AM), and AP. The same order can also be used to describe their weathering susceptibility. Note that in both islands, there are no fresh outcrops of the volcaniclastics and tuff even in newly excavated slopes. The heterogeneity of the clastic rocks as a result of the contrast in the properties of the crystalline clasts and ash- and volcanic glass-bearing matrix materials may lead to differential weathering in these rock masses. The pyroxene and olivine, coupled with the abundant vesicles of the BM, makes the basalts generally more susceptible to weathering than andesites, which contain plagioclases and hornblende. The inherent high density of cooling joints in the pillow basalts lavas makes these rock mass easier to weather compared with the massive unit, although the opposite is shown by the andesites. By comparing the properties of a GU in BM and Vlcs in exposures with different excavation time in an area in Saint Vincent, it is observed that there is an appreciable reduction in the rock properties a span of 8 years. This is however based on single GU of the two rock types and an extensive study is needed to establish more accurate weathering factors to give better reduction rate estimates for the rocks in this area.

Using the SSPC probability for OIS and ODS, it is been shown that GUs with >50% probability to be stable with respect to OIS and to the sliding and toppling criteria of the ODS are higher than those with <50% probability to be stable. This generally agrees with the field assessment where most of the slopes were mostly visually assessed to have small problems. The results of the slope stability assessment are used to demonstrate the overall influence of the weathering degree to slope stability. Although the relationship is not distinctively clear, it can still be observed that in the OIS, the percentage of moderately to highly weathered GUs is generally high in the ≤5% stability class whereas, the slightly weathered GUs are dominant in the class with ≥95% stability probability. In the sliding criterion of the ODS, the GUs that are classified to have ≤5% probability to be stable are dominantly highly weathered whereas GUs in the ≥95% probability of stability class are mostly fresh to moderately weathered. In the ODS-toppling criterion, the slightly weathered to highly weathered GUs are almost uniformly distributed in the ≤5% and ≥95 probability classes of stability. Although it has been shown that the weathering degree of the rocks masses are correlated to IRS, CD and SPA, the whole SSPC system considers other factors that are not affected by weathering such as slope height, slope angle, and the orientation of the discontinuities.

7. INFLUENCE OF SALTS IN THE ROCK MASSES ALONG COASTAL ROADS IN SAINT VINCENT AND DOMINICA

7.1. Introduction

As mentioned in Chapter 2, the influence of salt can be through salt weathering, which generally leads to the weakening and subsequent disintegration of rock materials (Lawrence et al. 2013) through filling up of the pores which aids in holding the grains of porous rocks together (McLaren 2001). The objective of this chapter is to describe the indicators of salt influence in the rock masses exposed to sea spray. Based on these, it is investigated whether it is possible to infer the influence of salts on the geotechnical properties of these rock masses.

7.2. Characteristics of rock masses exposed to sea spray

7.2.1. Andesites

Among the exposures investigated in Saint Vincent, SV10 and CM2 are very close to the sea. Both are along the Windward Highway in the eastern side of the island. The complete slope description is in Appendix 9.1. Location SV10 is between Fancy and Owia (Figure 31a). The road is about 10 m to 12 m above the average sea level.   The andesite in this exposure is strong, dark to light-gray, and prophyritic. It is generally fresh and cut by numerous discontinuity sets. Evidence of rock disintegration through spalling and cavernous structures called honeycomb and tafoni (Chapter 2.7) are present (Figure 31b and 31c). Honeycombs are from millimetres to centimetres in size while tafoni occur on the scale of centimetres to meters (Pye & Mottershead 1995). The honeycomb structures were observed to be more developed along blocks with planar surfaces facing the sea. The cavities are 1 cm deep, on average. Two poorly developed tafoni are present, one is 2 m long and 3 cm deep (Figure 31b). If fragments are chipped off from the fresh surfaces cavities are revealed about 3 mm deep from the original surface.   These cavities are surrounded by brown discoloration that is not visible at the original surface (Figure32a). These cavities may be at the incipient stage weathering resulting to the structure in Figure 32b.

Figure 31. Indicators of salt weathering in Exposure SV10. (a) location of the exposure; (b) honeycomb structures; (c) tafoni and scars from spalling. Map projection: UTM Zone 20 N, datum: WGS84, source: Google Earth (photos by XAC,2014)
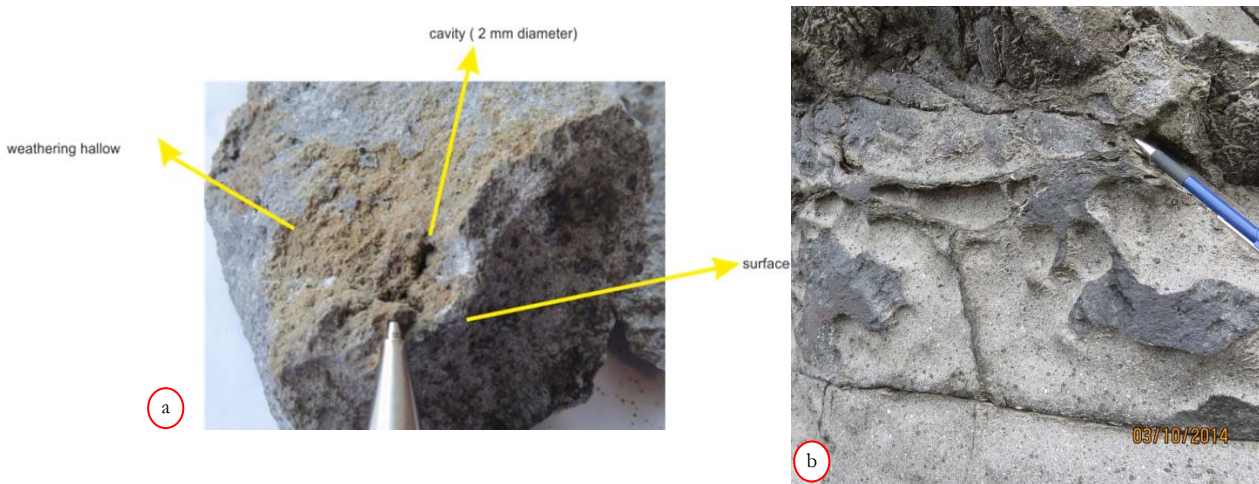
Figure 32. Cavities probably caused by salt weathering in the andesites. (a) chipped off fragment from the exposure reveal cavities that are surrounded by brown discoloration that is not visible in the original surface. (scale: tip of pen at centre bottom, diameter about 1 mm). (b) closer view of the cavities forming the honeycomb structures that could have resulted from the cavities shown in b. Map projection: UTM Zone 20 N, datum: WGS84, source: Google Earth (photos by XAC,2014; Saint Vincent)

Exposure CM2 (see note in photo caption for data ownership) is in between Argyle and Biabou (Figure 33a). The road in this section of the highway is about 20 m above the shoreline. The andesite in this location is moderately strong, brownish-grey. It is slightly weathered. Although these are not as well-developed as in SV10, the honeycomb structures are still evident.
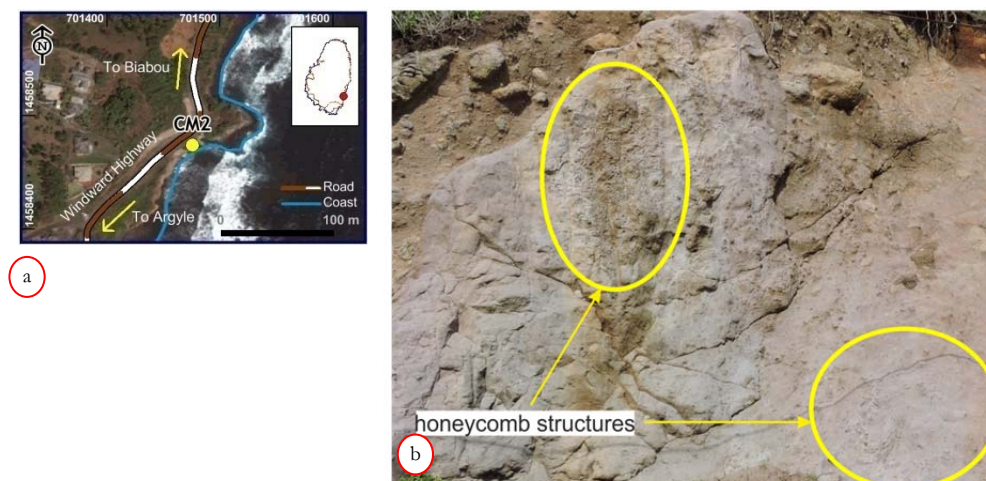
Figure 33. Honeycomb structures in exposure CM2. (a) Exposure CM2 indicated by black arrow in inset map of island; (b) poorly developed but still visible honeycomb structures; Map projection: UTM Zone 20 N, datum: WGS84, source: Google Earth *(photo direction 340° from the yellow dot on the map; by CM; 2014; note: exposure investigated by CM, used only by this author to show salt weathering influence; not included in the investigation of rock properties)*

For comparison, other exposures of lava flows investigated in both islands are shown below. Figure 34a is the part of the fresh andesite exposure in SV10 (Figure 31a) geotechnical unit (GU) SV10A where the slope direction is not parallel to the coast. Figure 34b is a slightly weathered andesite pillow lava unit (Exposure D9 in Appendix 9.2) in the leeward side of Dominica. This exposure is 30 m away from the coast at elevation 20 m above mean sea level. Figure 34c is a basalt lava flow in the windward side of Dominica. The exposure is about 100 m away from the coast and elevated to about 30 m. The salt weathering features shown in Figures 31 and 34 are obviously lacking in these exposures.

Figure 34. Examples of lava flow exposures in Saint Vincent and Dominica that do not exhibit visible indications of salt weathering   (a) GU SV10A in the exposure SV10 with slope not directly facing the Atlantic Ocean; (b) andesite pillows in exposure D14 in Dominica. Map projection: UTM Zone 20 N, datum: WGS84, source: Google Earth *photo direction 050° from the yellow dot position;* (c) basalt in exposure D14 in Dominica. *(photo direction 90° from the yellow dot position. photos by XAC, 2014)*

7.2.2.   Lahar deposits

The investigated exposures of lahar deposits are in Dubuc (D2 - D7) in the southeastern side of Dominica (Figure 35a).   These are along an 800 m stretch of the Dubuc - Fond St. Jean Road where the road is at the base of a 100 m high cliff with slope angle ranging from 80-88° (Figure 35b). Locations D2 to D5 are along the first 500 m stretch where the road width is about 8 m and the seawall is about 5 m high. Exposures D6 and D7 are also near the sea but are on a higher elevation of about 15 m above the mean sea level.

Figure 35. Exposures of lahar deposits in the southeastern side of Dominica(a) location of the lahar deposits (D2-D5) and ignimbrites exposures (D12); (b) coastal road in the area showing high cliffs and the road alignment very close to the sea *(from D12 in map, photo direction 040°, photo by XAC, 2014)* Map projection: UTM Zone 20 N, datum: WGS84, source: Google Earth

In general, the clasts of the lahar deposits are strong, brownish-grey to grey porphyritic andesites and strong, light-grey, porphyritic dacites. These are dominantly sub-angular and sub-rounded, boulder to cobble-sized and fresh to slightly weathered. The matrix is granular but dense. Based on sieve analysis, the matrix grains are dominantly medium-sized with a very little percentage of finer materials that may fill the voids in between the grains. The surface of the rock mass is generally uneven and rough because the clasts are protruding from the slope.

Salt crystals are present in the lower 3 m part of the slope (Figure 36a). These are generally thicker and thus more visible in the matrix-supported part of the slope. Scaling is also evident in some of the andesite clasts (Figure 36b) and some also appear to be cut off from the matrix (Figure 36c). Powdery materials, probably rock meals produced from granular disintegration of the matrix, cover the exposure.

The lahar deposit in exposures D6 and D7 is matrix-supported with dominantly cobble-sized clasts. Few lenses are present and only a single discontinuity is visible. These slopes have relatively thicker vegetation cover than the in exposures D2 to D5 and and the matrix materials is more weathered. In D6, water was observed dripping from a height of 30 m from the base of the slope. The features earlier described for D2 and D5 were not observed in these two locations.
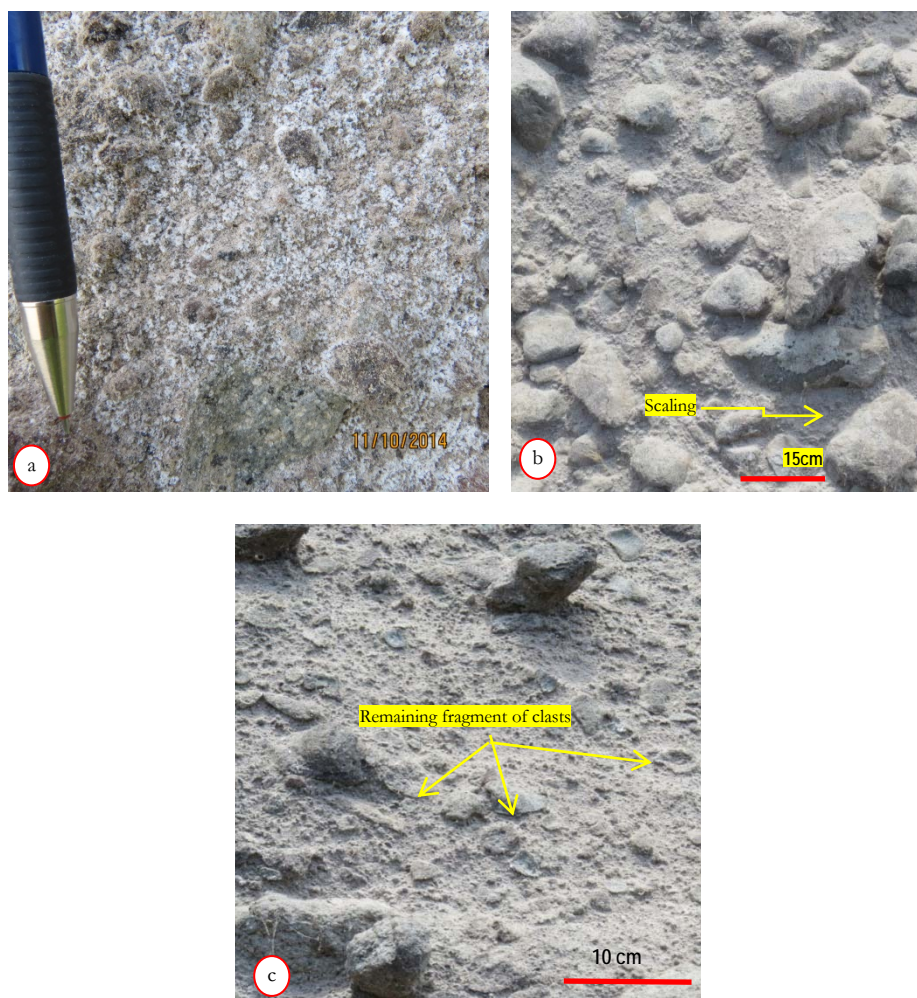
Figure 36. Indicators of salt weathering in the lahar deposits. (a) Salt crystals in the surface of the slope; (b) scaling in the andesite clasts; (c) fragments left by a dislodged clasts, the slope surface is generally covered by powdery material that probably correspond to rockmeals rock meals (photos by XAC, 2014)

7.2.3. Block-and-ash flow deposits and ignimbrites

The ignimbrite is exposed in a benched roadcut in exposure D12 (Figure 37a). The slope is 10 m away from the edge of the 6 m high sea wall. The slope is about 15 m high and was cut to 60° at the bottom and about 80° towards the top. The clasts are dominantly cobble to gravel-sized, sub-angular to sub-rounded, moderately strong pumice and a few cobble-sized, angular, strong, vesicular, porphyritic andesites and basalts. The pumice clasts are slightly weathered while the andesites and basalts are fresh. The matrix is dense, coarse pumice and with finer quartz crystals. The base of the slope is dark-grey to black and this is covered by a 1-mm thick hard crust. The freshly exposed surface is light-grey (Figure 37b). There are no visible discontinuities.

The investigated exposure of block-and-ash flow (BAF) deposits is along the Edward Oliver Leblanc Highway (D13) (Figure 37c). The slope is about 10 m (width of the road) from the edge of the 6 m high seawall. The clasts consist of angular, dominantly cobble-sized, strong, light-grey to grey, vesicular, porphyritic dacites and andesites. The matrix material is light-yellow to light-orange, gravelly coarse sand. A 1 mm thick hard coating (Figure 37d) gives a dark-gray to black discoloration in the lower part of the exposure. Behind the coating, clasts and matrix are poorly consolidated.
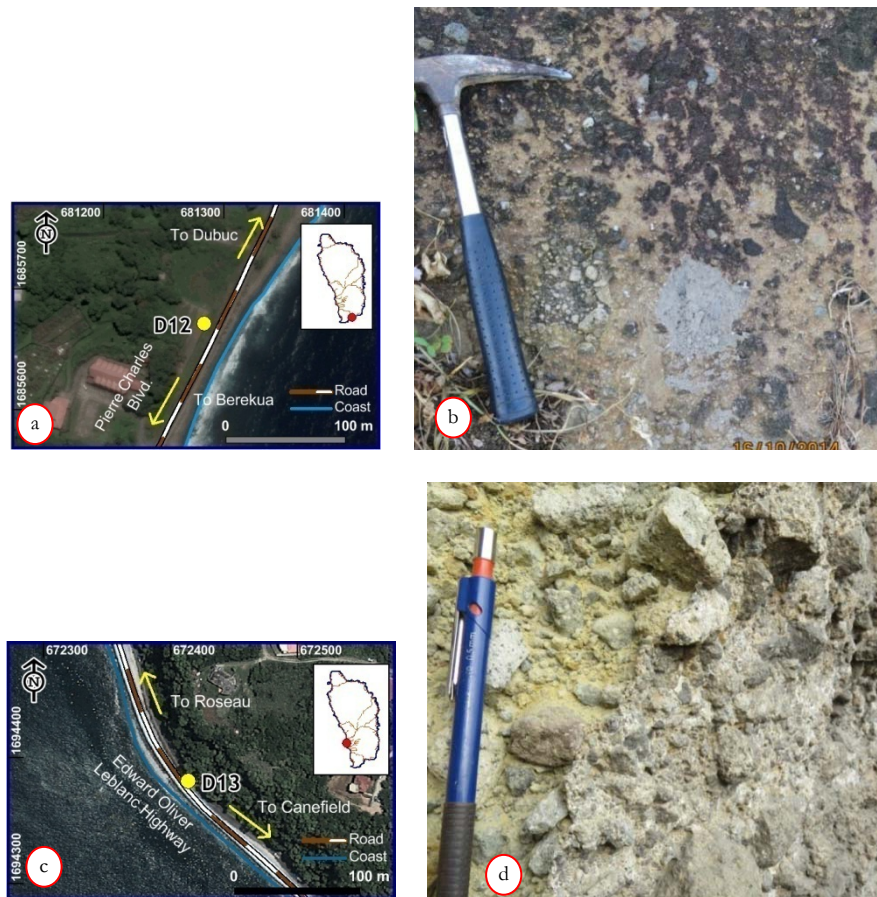
Figure 37. Hardened surfaces probably due to salt influence on the the ignimbrite and BAF deposits de(a) Location of exposure D12; (b) dark-grey coating and light-grey fresh surface of the ignimbrites in exposure D12; (c) location of exposure D13; (d) light-grey surface and poorly consolidated materials behind in the BAF deposits id exposure D13. Map projection: UTM Zone 20 N, datum: WGS84, source: Google Earth (*photo XAC, 2014*)

BAF deposits with the same characteristics as in exposure D13 are exposed in a quarry in Pennvile (Figure 38a) in the interior and mountainous part of Dominica. The surface is generally damp. The discoloration and the hardened crust in D13 is not present in this exposure (Figure 38b).
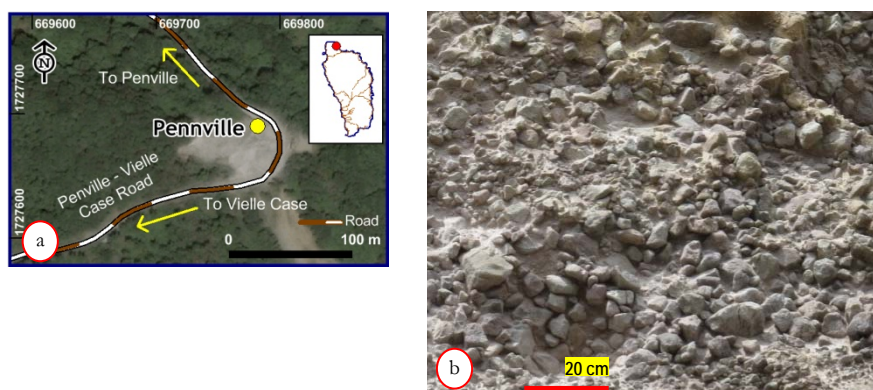
Figure 38. BAF exposure in a quarry in Penville, Dominica (a) Location of the quarry. (b) The hard surface coating in exposure D13 is absent in the surface of the BAF exposure in this quarry (yellow dot on the map indicates camera position, photo direction looking 230°; photo, by XAC, 2014) Map projection: UTM Zone 20 N, datum: WGS84, source: Google Earth

7.3. Results of water extractable salt experiment

NaCl and $MgSO_4$ are the most dominant salts crystallizing from seawater (Mottershead, 2013). The water extractable concentrations of these salts were determined in samples obtained from exposures previously described in Section 7.1. Control samples (D1 and SV7) from inland slopes were also analysed. Exposure D1 is in Marigot along the Dr. Nicholas Liverpool Highway in Dominica and Exposure SV7 is along the Leeward Highway in Troumaca, Saint Vincent (refer Appendix 9.2 for location). These exposures were selected as controls because they are located in deep valleys such that the likelihood of influence from sea sprays is minimized by the geomorphologic and vegetation barriers. As expected, the samples with observed salt crystal accumulation in the surface yielded the highest NaCl concentrations (Table 10). The concentrations are decreasing with increasing elevation from the mean sea level (msl) (Figure 39). The salt levels in D6 and D7 are almost comparable with those in Troumaca although their relative elevation elevation is not significantly different from D2 and D12. Note however, that vegetation that may be acting as a buffer, is present in D6 and D7.

Table 10. Concentration of water extractable salts in samples from various exposures with different estimated elevation above msl

Sample Location	NaCl	$MgSO_4$	Rel. Elevation	Buffer
	ppm	ppm	m	Y/N
D1	187	621	50*	Y
SV7	304	284	50*	Y
D7 (matrix)	309	203	15	Y
D8	349	288	20	Y
D7 (coating)	501	171	15	Y
SV10	970	639	10	N
D13 (behind coating)	3618	1533	10	N
D12 (matrix)	8640	4274	7	N
D12 (coating)	9288	2125	7	N
D2 (lens)	54879	16358	5	N
D2	60496	13970	5	N

*Note The elevation value only indicates the relative elevation, thus only the vertical distance. The exposures are actually farther from the coast if the horizontal distance is considered
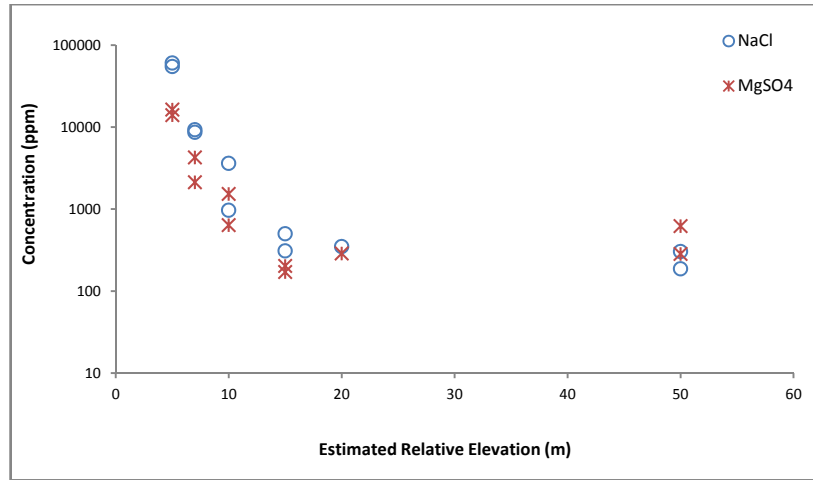
Figure 39. Estimated elevation (m) vs. salt concentration (ppm). The concentrations of NaCl and MgSO$_4$ are decreasing with increasing estimated relative elevation from msl

7.4.   Discussion

The scaling/spalling scars, honeycomb and tafoni and the presence of powdery materials or rock meals, are indicative of salt weathering (Smith & McGreevy, 1988; Frenzel, 1989; Bryan & Stephens, 1993; Matsukura & Matsuoka, 1996; Goudie & Viles, 1997; Mottershead, 2013). The hardened coating on the pyroclastic deposits shows the cementing effect of salts (McLaren, 2001). In the study areas, these features are only present in exposures that are very close to the sea with no vegetation that can serve as buffers or protection from sea spray. Although the analyses for water extractable salts were done in a limited number of samples, the results show that the accumulation of NaCl and MgSO$_4$ is dependent on the elevation of the exposures with respect to the shoreline and influenced by vegetation cover. Doehne (2002) stressed that salt accumulation does not automatically indicate that there is salt weathering. However, the fact that the high salt concentrations are in exposures exhibiting structures associated with this process is a clear indication that it is occurring in these rock masses.

As mentioned in the Literature Review (Chapter 2), the factors that influence salt weathering can be generalized as: the properties of the rocks, the properties of the salt and the prevailing environmental factors. The environmental factors refer to humidity, temperature and solar exposure. The experiment of Wells et al. (2006) showed that small differences in the rock properties can override the effects of changes in the environmental conditions. Among these three, the salt influence as observed in the field is dependent on the differences in the rock properties and the location and orientation of the exposure with respect to the sea. Thus, these are the focus of the following discussion. Determining the specific kind of salts and their properties is not within the scope of this report. In addition, the variation in the influence of temperature and humidity is not expected to be significantly high because the study areas are within the same region such that they are exposed to the same wetting and drying cycle and overall temperatures.

7.4.1.   Influence of rock properties

The porosity and tensile strength of the rock materials were found by previous researchers to be the important rock properties that influence salt weathering (Wellman & Wilson, 1965; Matsukura & Matsuoka, 1996; Benavente et al., 2007). The relationship of porosity to crystallization pressure is given by:

$$P = \frac{4\sigma}{d} \qquad (20)$$

where p is the crystallization pressure, σ is the interfacial tension of the salt solution and d is the diameter of the pore. Apart from the pore size, the pore network also influences how rocks respond to salt attack (Goudie & Viles, 1997; Labus & Bochen, 2012. This explains why the observed indicators of salt influence are different in each of the rock types as explained hereafter.

The high granularity of the outermost few centimetre of the lahar matrix material suggests that the pores are interconnected. This encourages salt crystallization (Benavente et al., 2007) that leads to granular disintegration (Goudie & Viles, 1997). In contrast, the porosity of the crystalline rocks is given by the vesicles and fissures in the phenocryst-groundmass boundary and this results in a heterogeneous pore system. Disintegration in rocks with such pore system is in the form of cracking and scaling (Goudie & Viles, 1997). Pye & Mottershead (1995) observed that granular disintegration is not favoured in rocks with interlocking crystalline texture. As indicated by the thin peels of clasts left attached to the matrix, the clasts were dislodged from the slope because scaling has significantly decreased the tensile strength along the matrix-clast interface. However, the formation of the honeycomb structures may be due to the combination of salt weathering with other weathering processes. It is possible that the relatively rapid physical disintegration by the salts enhances the chemical weathering or vice versa (Goudie & Viles, 1997).

The tensile strength of the materials measures their resistance to the disruptive effect of crystal growth during salt crystallization (Matsukura & Matsuoka, 1996). The crystallization pressure of salts is related to the tensile strength of the material by the weathering susceptibility index (WSI) through the equation:

$$WSI = \frac{P}{S} \qquad (21)$$

where P is the crystallization pressure and S is the tensile strength. In this research, the tensile strength was not measured. However, the intact rock strength (IRS) of the rocks was estimated in the field and this can be used as an estimate of the unconfined compressive strength (UCS) following the arguments presented by Hack & Huisman(2002). Using the IRS values of andesite and the matrix materials lahar and BAF, the tensile strength was computed using the correlation function of UCS and Brazilian Tensile Strength (BTS) of Nazir et al.(2013):

$$UCS = BTS^{0.947} \qquad (22)$$

The results are shown in Table 11 including the range of laboratory tested values taken from literature. An attempt was made to use tensile strength using the RocLab program but the resulting values are those of rock masses. In the context of this study, the attack of salt weathering is more on the intact rock than on the rock mass via discontinuities as far was possible to determine. Hence, the tensile strength of intact rock is more applicable. The tensile strength values are less than the crystallization and hydration pressures of the NaCl and MgSO$_4$ (Table 12) though these are only indicative values. It is thus, not unlikely that intact rock breaks under these pressures.

Table 11. Computed tensile strength of the investigated rocks and values from literature

Rock	IRS (MPa)	BTS (MPa)	Range of typical BTS values (MPa)
Andesite	75	9.118	5 – 11*
Matrix Dubuc	31.25	3.617	0.14 – 0.9**
Matrix Dubuc	8.75	0.943	0.14 – 0.9**
Matrix Canefield	3.125	0.305	0.14 – 0.9**

*Sari & Karpuz (2008)
**(Tommasi et al., 2015)

Table 12. Pressure produced by salt processes (after Goudie & Viles, 1997)

Salt processes	Pressure (MPa)
Crystallization pressure of NaCl	5.54 to 373.7
Hydration pressure of MgSO$_4$	Up to 42

The BAF is clast-supported with very coarse matrix material and thus the porosity is likely to be high. In the ignimbrites, the highly vesicular nature of the pumice clasts and matrix also suggest high porosity. The

high porosity of these rocks may result to their response to the influence of salt. Rossi-Manaresi & Tucci (1991 in Goudie & Viles, 1997) observed that when the pore system does not favour mechanical failure during salt crystallization, surface hardening takes place instead of disintegration. For example, halite crystallization may actually increase cohesion between particle grains instead of exerting pressure against the pore walls (McLaren, 2001). This implies that this condition is favoured in big pores, such as the case of these pyroclastic deposits. It has to be noted that in order for salt weathering to occur, the solution should not freely pass through the host (Goudie & Viles, 1997). $CaCO_3$ is also found to be high in the hardened surface in exposure D13 indicating that the crust is formed by the combination of the two salts with other compounds.

7.4.2.   Influence of distance from the coast, presence of buffer and slope direction

The indicators of salt influence are only present in rock faces of exposures that are directly facing the sea, with no barriers such as vegetation. The reducing concentration of NaCl and $MgSO_4$ with increasing elevation also suggests that the influence of salt is becoming weaker with increasing distance from the shoreline. This is seen in the lahar exposures in Dubuc where the salt weathering indicators seen in the exposures in D2 to D5 are absent in the exposures in D6 and D7.

In exposure SV10, GU SV10A does not contain the cavernous structures seen in the rock faces in GUs SV10B and SV10C directly facing the Atlantic Ocean. One reason may be that there are more discontinuities in GUs SV10B and SV10C which make these units more permeable. However, the distribution of the spalling scars and the honeycomb structures do not show that they favour parts with closely spaced discontinuities. This suggests that in this case, the slope direction is controlling the influence of salt. This is similar to the observations of Mottershead (2013) from which he concluded that slope orientation is more important to salt accumulation than the proximity to the sea.

7.4.3.   Estimates on the rate of development of salt weathering associated structures

In the coastal environment, Matsukura& Matsuoka (1996) reported exponential rate in the initial stages of tafoni development and a later decline through time.   The decline is caused by the decreasing surface area exposed to salt spray as the cavities grow deeper. This is quite similar with the general behaviour of the whole weathering processes as described by Huisman et al. (2011).

It is not certain how much of the andesite in exposure SV10 was already exposed or what is the configuration of the original slope was like before it was excavated in 2010 during road construction. However, it is a common observation that during road improvement particularly in rock slopes, excavation is usually conducted at the bottom part of the slope and the top portion may be left untouched. If such is the case for the said exposure, the upper part of the slope where the more developed honeycomb structures and the bigger tafone are seen may be already exposed before 2010. Therefore, the cluster of cavities located in the lower 2 m of the exposure may be more representative of the salt weathering since 2010. Taking the 1 cm average depth of these cavities, a development rate of about 2.5 mm/year is estimated using Equation 19 (Chapter 4).

In the lahar deposits, the present protrusion of the clasts can be used to infer the rate of matrix retreat. It is likely that the matrix and the clasts are almost at the same level right after road construction in the early 1960s. Measurements however, can be only done in the accessible parts of the slope (e.g. Figure 40). Based on the exposed part of the big clasts, the maximum rate of matrix retreat is about 30 cm in 55 years. It has to be noted that the clasts are also being weathered and some of the previously exposed clasts were already dislodged from the slope. Therefore, it is deemed to be more logical to base the estimate retreat rate on the big clasts.
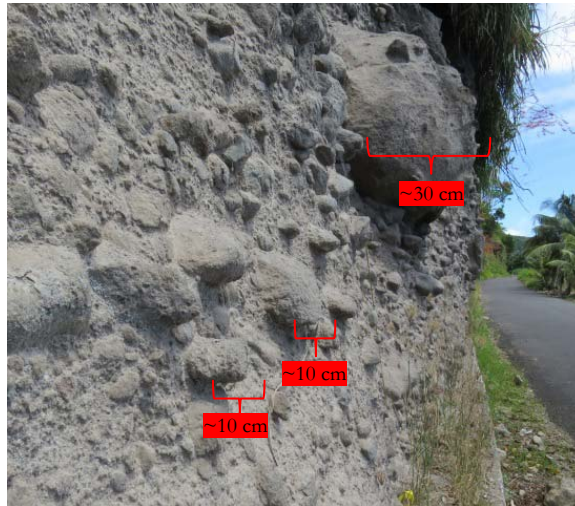
Figure 40. Estimating rate of salt weathering. The protrusion of clasts is used as estimate of the rate in the retreat of matrix that maybe attributed to the granular disintegration mechanism of salt weathering (*photo, XAC, 2014*)

The rates assumed in the development of the cavities in the andesites in SV10 and the retreat of the lahar matrix materials are very high compared with field measurements done by previous researchers in coastal weathering. For example, Bryan & Stephens (1993) computed a retreat rate of only 3 to 6 cm in 25 years in basaltic tuff cliffs, which is comparable to consolidated sandstones, in Hawaii; Matsukura & Matsuoka (1996) measured tafoni growth rate of 0.1 to 1 mm/year in tuffs and 0.01 mm/year for granite and basalt in Japan; and Mottershead (1989) measured a denudation rate of 0.3 to 1.5 mm/year in greenschist bedrocks in Devon, UK. Except for Hawaii, the rest of the studies were conducted in temperate areas while Saint Vincent and Dominica are in a warm, humid, tropical region where the weathering rate is generally high (Rad et al., 2013; Jain, 2014). Certainly, there is a very high uncertainty in the available data to arrive at a conclusive rate of salt weathering such that the high rates cannot be only attributed to the difference of the rock type and climate.

7.5. Implications of salt influence on the engineering properties of the affected rock masses

Salts generally accelerate weathering. Mottershead et al. (2003) recorded a difference in the weathering rate by a factor of 1.59 by comparing sandstone blocks of a church with the same sandstone unit in the source quarry. Topal & Sözmen (2003) conducted accelerated weathering test by wetting-drying, freezing-thawing test, and salt crystallization in two tuff units that have slightly different porosity. Among the rock properties they measured after the experiment, the UCS showed the highest reduction by about 40% for the more porous unit and about 28% in the less porous unit.

By combining secondary data with the field observations obtained in this research, it is possible to link the observed indicators of salt influence with the engineering behaviour of the affected rock masses. It is however, important to note that in reality, other weathering mechanisms such as swelling and shrinking of clays may be active in the study area. The results of the XRD analysis showed that kaolinite is the only dominant clay mineral in the matrix material of the lahar deposits. This clay mineral has a very small swelling potential (Warkentin & Yong, 1960) thus, it is unlikely that it has a more significant effect than that of the salts.

The accelerated weathering and more intensive erosion in the matrix material of the lahars, coupled with the "wick effect" and scaling of the clasts, reduce the tensile strength along the clast-matrix interface. This mechanism may be one of the causes on the regular rockfalls occurring in the Dubuc-Stowe area, as well as in the other coastal road cuts where the rocks are massive and failure is likely to be controlled by

strength of the clast-matrix interface. However, it has to be noted that this may only be true in the lower part of the cliff where salt weathering is actually observed to be active. In the upper part of the slopes (above ~20m) the vegetation is thicker and more regular (not just occurring as patches) indicating that soil has developed. Although it has not been proven by this study, it is likely that chemical weathering is the more dominant weathering mechanism in this part of the slope which may or may not be affected by sea sprays.

Prior to granular disintegration, the volumetric change that occurs when salt crystals exert pressure on the pore walls in the matrix material of the increases the the porosity in the materials and may result to the reduction of the IRS. It is not certain, however, at what depth the salt solution can penetrate towards the slope for salt crystallization to influence the IRS. High moisture content is retained in the rock masses covered with the hardened surface layer, enhancing the weathering of the materials behind the crust.

The cavities seen 3 mm underneath the rock surface (discussed in section 7.1.1) can serve as nucleation point for chemical weathering. The lack of surface manifestation of these cavities increases the risk of overestimating the stability of these geotechnical units. There are indications that discontinuities can develop from the individual cavities as seen in some of the slope face of the andesite (Figure 41a) . These discontinuities correspond to the wavy and tight, non-persistent discontinuity sets (indicated by dotted yellow circles) shown in Figures 41b and 41c. These can be differentiated from the cooling joints, which usually have straight traces (traced in yellow solid lines). The development of these discontinuities increases porosity of the rocks leading to the reduction of the strength parameters of this rock mass.
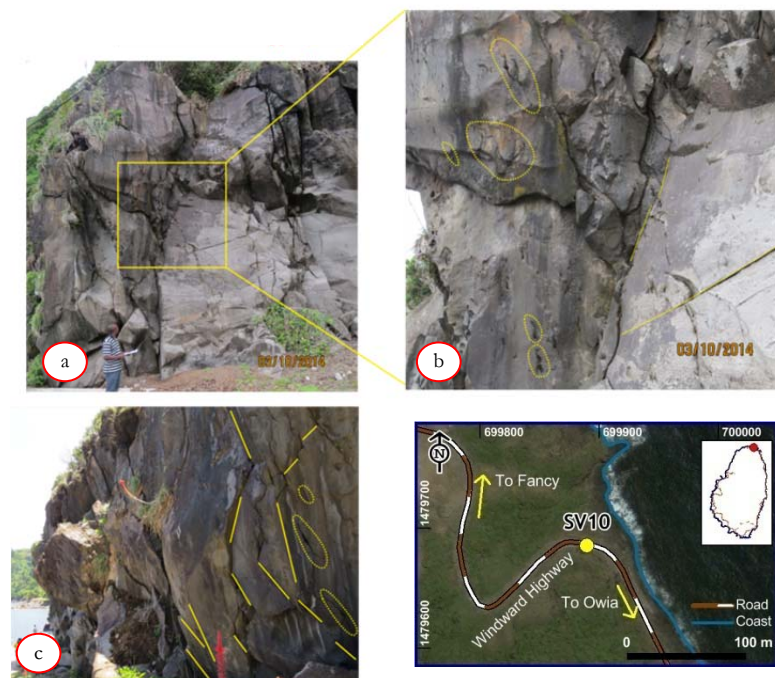
Figure 41. Incipient development of new discontinuity sets in Exposure SV10 due to salt weathering. (a) highly jointed part of the andesite exposure; (b) wavy and short discontinuities (in dotted outlines) appear to develop from interconnecting cavities (c)straight traces of cooling joints versus the developing discontinuities (solid lines). *(Photos by XAC, 2014)*

7.5.1. Summary

Structures that are closely associated with salt influence are evident in the exposures along the coastal roads in Saint Vincent and Dominica. The concentrations of NaCl and $MgSO_4$ are also high in these

exposures. These indicators generally differentiate rock masses from those that are in the more interior parts of the islands, or those that are not exposed to sea spray. The different rock types exhibit different different salt influence indicator and this reflects the influence of the rock properties particularly porosity and tensile strength on the mechanism of salt influence. The matrix materials of the lahar deposits show indications of granular disintegration. The crystalline rocks disintegrate through scaling and spalling. The development of the tafoni and honeycombs in the andesite lava flows are however assumed to be a result of the combination of physical disintegration by scaling/spalling followed by chemical weathering. The dominant mechanism of salt weathering is related to the rate of rock disintegration. Between the crystalline and clastic rocks, the granular disintegration in the clastic rocks gives a high retreat rate of the matrix compared with the clasts that disintegrate through scaling. The estimated rate of retreat of the matrix material in the lahar deposits is 30 cm in 55 years while the development of the cavities in the andesites is 2.5 mm/year. These values are generally high compared with the results of previous studies although these studies were done in in different rocks and in different climatic setting. The more porous pyroclastic deposits exhibit surface hardening that developed from salts in combination with other compounds.

8. CONCLUSIONS AND RECOMMENDATIONS

1. **What is the applicability of the rock mass weathering classification recommended in BS5930 to the rock masses in Saint Vincent and Dominica?**

   The weathering classification of BS5930:1981 can be applied to uniform rock masses such as the andesites, basalts, and lapilli tuff in a straightforward manner. It does not, however, differentiate between materials that are inherently fragmented and consisting of fresh but non-cohesive individual fragments. Therefore, Approach 3 of the BS5930:1999 is more appropriate and easier to apply in the classification of highly heterogeneous volcaniclastic.

2. *How are the rock properties changing with increasing degree of weathering?*

   The intact rock strength, the condition and spacing of discontinuities, as well as the rock mass friction angle and cohesion, are generally reducing from fresh to moderately weathered rock masses. However, the spacing of discontinuities increases from moderately weathered to highly weathered volcaniclastics, massive basalts, and tuffs. The values of some weathering classes are derived from single geotechnical units and/or few available exposures causing a relatively high uncertainty of the assessed changes in the rock properties.

3. **How are the rock properties changing with increasing amount of exposure time?**

   Based on available data, there is a weak correlation of exposure time with the rock properties. The large spread of the data set and the limited number of observation points cannot be used to establish an equation that best describes their relationship to predict future values could not be established. In addition, most of the rocks are already weathered prior to exposure such that the degree of weathering recorded during the fieldwork cannot be directly correlated to the amount of time that the rock mass is exposed.

4. *How do the computed weathering intensity rates relate with the general knowledge on weathering susceptibility of rocks as a function of their composition?*

   The volcaniclastic rocks (block and ash flow, tuff breccia and tuff lapilli) exhibit higher reduction rates than the crystalline rocks (andesite and basalts). Basalts have higher reduction rate than andesites. The pillow basalts have higher reduction rate than the massive basalts. There is no significant difference in the reduction rates of pillow and massive andesites. This sequence agrees very well with the generally known weathering susceptibility of the rocks as published in the literature (Chapter 2.3). Aside from the composition of the intact rock material, the density of discontinuities also influences the weathering intensity rate.

5. *How are the weathering classes distributed among the stability classes derived using the SSPC system?*

   Moderately to highly weathered geotechnical units (GUs) are dominant in the ≤5% probability of stability class whereas the slightly weathered GUs are dominant in the class with ≥95% probability of stability for the orientation independent and orientation dependent stability. However, this is not always the case for all the stability classes indicating that the slope stability is also controlled by other factors such as slope orientation, slope height and orientation of discontinuities that are not influenced by the degree of weathering of the rock mass.

6. **What are the distinct features in the exposures influenced by salts and what do these features indicate?**

    Features associated with salt weathering such as tafone, honeycomb structures, salt crystals, rock meals, disintegration by scaling and highly pitted surfaces are present in the andesites and lahar deposits that are directly exposed to sea sprays. Aside from these, the hardened surfaces in the pyroclastic deposits are also closely associated to salts. These features differentiate the rock masses from those that are not directly exposed to sea sprays due to the distance of their locations from the coast and due to the presence of buffers such as vegetation.

7. **What are the implications of salt influence to the engineering properties of the affected rock masses?**

    Salt weathering generally accelerates the weathering process as a whole. In the andesites, some cavities develop along a preferred orientation forming new discontinuities. The cavities create voids that result in an increase in the porosity of the rocks. The tactile roughness, is increased because of the protruding phenocrysts as the groundmass appears to be preferentially weathered. In the lahar deposits , the granular disintegration in the matrix accelerates retreat of the matrix compared to the clasts leaving the clasts protruding out of the slope. Scaling in the clasts lead to the loss of tensile strength between the clast and matrix interface. This implies that the matrix-clast boundaries do not have to weather through chemical processes before the clasts get dislodged from the slope to produce rockfalls. The estimated rate of cavity development in the andesites is about 2.5 mm/year and the retreat of the matrix materials in the lahar deposits is estimated to be 30 cm in 55 years.

Based on the experience gained in this research on how variable each of the volcanic and volcaniclastic rocks respond to weathering, it is recommended that further research be conducted to establish reduction factors for each for the rock types in a tropical environment. More exposures in the same rock type with the same weathering degree and same time of exposure should be compared (Chapter 6.3)

The increase in the discontinuities in the andesites due to interconnecting cavities caused by salt weathering and the retreat of the matrix materials in the lahar deposits, as well as the scaling in the clasts imply that the the strength properties of these rock masses are relatively rapidly reduced. It is therefore recommended that the effect of salt weathering be also considered in the planning of coastal slopes. (Chapter 7.4.3).

REFERENCES

Anderson, M.G. & Kneale, P. E. (1985). Empirical approaches to the improvement of road cut slope design, with sepcial reference to St. Lucia, West Indies. *Singapore Journal of Tropical Geography*, *6*(2). doi:10.1111/j.1467-9493.1985.tb00163.x

ANON. (1995). The description and classificatioin of weathered rocks for engineering purposes. *Quarterly Journal of Engineering Geology and Hydrogeology*, *28*(3), 207–242. doi:10.1144/GSL.QJEGH.1995.028.P3.02

Arıkan, F., Ulusay, R., & Aydın, N. (2007). Characterization of weathered acidic volcanic rocks and a weathering classification based on a rating system. *Bulletin of Engineering Geology and the Environment*, *66*(4), 415–430. doi:10.1007/s10064-007-0087-0

Aristizábal, E., Roser, B., & Yokota, S. (2005). Tropical chemical weathering of hillslope deposits and bedrock source in the Aburrá Valley, northern Colombian Andes. *Engineering Geology*, *81*(4), 389–406. doi:10.1016/j.enggeo.2005.08.001

Aydin, A. (2009). ISRM Suggested method for determination of the Schmidt hammer rebound hardness: Revised version. *International Journal of Rock Mechanics and Mining Sciences*, *46*(3), 627–634. doi:10.1016/j.ijrmms.2008.01.020

Basu, a., Celestino, T. B., & Bortolucci, a. a. (2008). Evaluation of rock mechanical behaviors under uniaxial compression with reference to assessed weathering grades. *Rock Mechanics and Rock Engineering*, *42*(1), 73–93. doi:10.1007/s00603-008-0170-2

Benavente, D., Martínez-Martínez, J., Cueto, N., & García-del-Cura, M. a. (2007). Salt weathering in dual-porosity building dolostones. *Engineering Geology*, *94*(3-4), 215–226. doi:10.1016/j.enggeo.2007.08.003

Benito, G., Machado, J., & Sancho, C. (1993). Sandstone weathering process damaging prehistoric rock paintings at the Albarracin Cultural Park, NE Spain. *Environmental Geology*, *22*, 71–79. doi:10.1007/BF00775287

Bouysse, P., Westercamp, D., & Andreieff, P. (1990). BIOLOGICAL WEATHERING SILICATE MINERALS., *110*.

Boyle, J.R. & Voigt, G. K. (1973). BIOLOGICAL WEATHERING SILICATE MINERALS. *Plants and Soils*, *38*, 191–201. doi:10.1007/BF00011226

Brandmeier, M., Kuhlemann, J., Krumrei, I., Kappler, a., & Kubik, P. W. (2011). New challenges for tafoni research. A new approach to understand processes and weathering rates. *Earth Surface Processes and Landforms*, *36*(6), 839–852. doi:10.1002/esp.2112

Bryan, W. B., & Stephens, R. S. (1993). Coastal bench formation at Hanauma Bay , Oahu , Hawaii. *Geological Society of America Bulletin*, *105*, 377–386. doi:10.1130/0016-7606(1993)105<0377:CBFAHB>2.3.CO;2

BS5930. (1999). *British Standard Code of practice for site investigations. British Standards Instituition, London.* (pp. 1 – 192. ISBN:0 580 33059).

Calcaterra, D., & Parise, M. (2010). Weathering as a predisposing factor to slope movements: an introduction. *Geological Society, London, Engineering Geology Special Publications*, *23*(1), 1–4. doi:10.1144/EGSP23.1

Cardell, C., Rivas, T., Mosquera, M. J., Birginie, J. M., Moropoulou, a., Prieto, B., … Van Grieken, R. (2003). Patterns of damage in igneous and sedimentary rocks under conditions simulating sea-salt weathering. *Earth Surface Processes and Landforms*, *28*(1), 1–14. doi:10.1002/esp.408

Ceryan, S., Tudes, S., & Ceryan, N. (2007). A new quantitative weathering classification for igneous rocks. *Environmental Geology*, *55*(6), 1319–1336. doi:10.1007/s00254-007-1080-4

Chigira, M., & Sone, K. (1991). Chemical weathering mechanisms and their effects on engineering properties of soft sandstone and conglomerate cemented by zeolite in a mountainous area. *Engineering Geology*, *30*(2), 195–219. doi:10.1016/0013-7952(91)90043-K

Christian, M. (2012). A geological outlook on geothermal explorations in Dominica. *GHC Bulletin*, (August 2012).

Colman, S. M., & Dethier, D. P. (Eds.). (1986). *Rates of chemical weathering of rocks and minerals. Sedimentary Geology* (Vol. 52, pp. 1 – 603). Retrieved from http://linkinghub.elsevier.com/retrieve/pii/0037073887900674

Das, I., Sahoo, S., van Westen, C., Stein, A., & Hack, R. (2010). Landslide susceptibility assessment using logistic regression and its comparison with a rock mass classification system, along a road section in the northern Himalayas (India). *Geomorphology*, *114*(4), 627–637. doi:10.1016/j.geomorph.2009.09.023

Dearman, W. R. (1974). Weathering classification in the characterisation of rock for engineering purposes in British practice. *Bulletin of the International Association of Engineering Geology*, *9*(1), 33–42. doi:10.1007/BF02635301

Doehne, E. (2002). Salt weathering : a selective review, *205*(1), 51–64. doi:10.1144/GSL.SP.2002.205.01.05

Ehlen, J. (2002). Some effects of weathering on joints in granitic rocks. *Catena*, *49*(1-2), 91–109. doi:10.1016/S0341-8162(02)00019-X

Fan, C.-H., Allison, R. J., & Jones, M. E. (1996). Weathering effects on the geotechnical properties of argillaceous sediments in tropical environments and their geomorphological implications. *Earth Surface Processes and Landforms*, *21*(1), 49–66. doi:10.1002/(SICI)1096-9837(199601)21:1<49::AID-ESP541>3.0.CO;2-2

Frenzel, G. (1989). The tafoni weathering of granites. In A. Barto-Kyriakidis (Ed.), *Weathering; its products and deposits. Volume 1. Processes* (pp. 1 – 462).

Gamon, T. I. (1983). A comparison of existing schemes for the engineering description and classification of weathered rocks in Hongkong. *Bulletin of the International Association of Engineering Geology*, *28*.

Goudie, A. S. (2006). The Schmidt Hammer in geomorphological research. *Progress in Physical Geography*, *30*(6), 703–718. doi:10.1177/0309133306071954

Goudie, A. S., & Viles, H. A. (1997). *Salt Weathering Hazards* (pp. 1– 256). ISBN: 978-0-471-95842-0. Retrieved from http://eu.wiley.com/WileyCDA/WileyTitle/productCd-0471958425.html

Gupta, A. S., & Rao, K. S. (2000, May). Weathering effects on the strength and deformational behaviour of crystalline rocks under uniaxial compression state. doi:10.1016/S0013-7952(99)00090-3

Gupta, A.S. and Rao, S. K. (2001). Weathering indices and their applicability for crystalline rocks. *Bulletin of Engineering Geology and the Environment*, *60*(3), 201–221.

Gurocak, Z., & Kilic, R. (2005). Effect of weathering on the geomechanical properties of the Miocene basalts in Malatya, Eastern Turkey. *Bulletin of Engineering Geology and the Environment*, *64*(4), 373–381. doi:10.1007/s10064-005-0005-2

H.R.G.K. Hack. (1996). *Slope stability probability classification (SSPC)*. Delft Technical University.

Hack, R. (1998). *Slope Stability Probability Classification (SSPC) 2nd Edition* (pp. 1 – 258. ISBN:90 6164 154 3).

Hack, R. (2002). An evaluation of slope stability classification. In *ISRM International Symposium - EUROCK'2002, 25-27 November, 2002, Madeira, Portugal* (pp. 1–32).

Hack, R., & Price, D. (1997). Quantification of weathering. In Eds. Marinos et al (Ed.), *Proc. Engineering geology and the environment* (pp. 145 – 150). Retrieved from http://ezproxy.utwente.nl:2980/papers/1997/conf/hack_qua.pdf

Hack, R. & Huisman, H. (2002). Estimating the intact rock strength of a rock mass by simple means. In J. L. van Rooy & C. A. Jermy (Eds.), *Engineering geology for developing countries, 16-20 September 2002, Durban, South Africa* (pp. 1971 – 1977). ISBN: 0-620-28559-1. Retrieved from http://science.uwaterloo.ca/~mauriced/earth437/requiredreading/assignment_4_readingStrengthYield/Rock_Strength_by_Hack & Huisman.pdf

Hack, R., Price, D., Rengers, N. (2003). A new approach to rock slope stability - a probability classification (SSPC). *Bull Eng Geol Env*, *62*, 167–184. doi:10.1007/s10064-002-0155-4

Hampton, M. A., & & Griggs, G. B. (Eds.). (2004). *Formation , Evolution , and Stability of Coastal Cliffs – Status and Trends Formation , Evolution , and Stability of Coastal Cliffs – Status and Trends*.

Hay, R. L. (1959). Origin and weathering of Late Pleistocene ash deposits on St. Vincent, B.W.I. *The Journal of Geology*, *67*(1), 65 – 87. doi:10.1086/626558

Heath, E., Macdonald, R., Belkin, H., Hawkesworth, C., & Sigurdsson, H. (1998). Magmagenesis at Soufriere Volcano, St Vincent, Lesser Antilles Arc. *Journal of Petrology*, *39*(10), 1721–1764. doi:10.1093/petroj/39.10.1721

Heidari, M., Momeni, a. a., & Naseri, F. (2013). New weathering classifications for granitic rocks based on geomechanical parameters. *Engineering Geology*, *166*, 65–73. doi:10.1016/j.enggeo.2013.08.007

Hencher, S. (2008). The "new" British and european standard guidance on rock description. A critique by Steve Hencher. *Ground Engineering*.

Hencher, S. R., & McNicholl, D. P. (1995). Engineering in weathered rock. *Quarterly Journal of Engineering Geology and Hydrogeology*, *28*, 253–266. doi:10.1144/GSL.QJEGH.1995.028.P3.04

Hoek, E. (1983). Strength of jointed rock masses. *Geotechnique*, *23*(3), 187–223. doi:10.1680/geot.1983.33.3.187

Huisman, M. (2006). *Assessment of rock mass decay in artificial slopes* (pp. 1 – 281). Enschede, The Netherlands ISBN:9061642469. Retrieved from http://www.itc.nl/library/papers_2006/phd/huisman.pdf

Huisman, M., Nieuwenhuis, J. D., & Hack, H. R. G. K. (2011). Numerical modelling of combined erosion and weathering of slopes in weak rock. *Earth Surface Processes and Landforms*, *36*(13), 1705–1714. doi:10.1002/esp.2179

Jain, S. (2014). Weathering and mass wasting. In *Fundamentals of Physical Geology* (pp. 129 – 163). Springer India. doi:10.1007/978-81-322-1539-4_7

Kamh, G. M. E. (2005). The impact of landslides and salt weathering on Roman structures at high latitudes—Conway Castle, Great Britain: a case study. *Environmental Geology*, *48*(2), 238–254. doi:10.1007/s00254-005-1294-2

Kamh, G. M. E. (2011). Salt weathering , bio-deterioration and rate of weathering of dimensional sandstone in ancient buildings of Aachen City , Germany. *International Journal of Water Resources and Environmental Engineering*, *3*(June), 87–101 ISSN: 2141–6613.

Labus, M., & Bochen, J. (2012). Sandstone degradation: an experimental study of accelerated weathering. *Environmental Earth Sciences*, *67*(7), 2027–2042. doi:10.1007/s12665-012-1642-y

Lawrence, J. a., Mortimore, R. N., Stone, K. J., & Busby, J. P. (2013). Sea saltwater weakening of chalk and the impact on cliff instability. *Geomorphology*, *191*, 14–22. doi:10.1016/j.geomorph.2013.02.022

Lee, S.-G., & Hencher, S. R. (2009). The repeated failure of a cut-slope despite continuous reassessment and remedial works. *Engineering Geology*, *107*(1-2), 16–41. doi:10.1016/j.enggeo.2009.03.011

Lerman, A., & Meybeck, M. (Eds.). (1988). *Physical and Chemical Weathering in Geochemical Cycles* (pp. 1–355). Kluwer Academic Publishers.

Lindsay, P., Campbell, R. ., Fergusson, D. ., Gillard, G. ., & Moore, T. . (2001). Slope stability probability classification, Waikato Coal Measures, New Zealand. *International Journal of Coal Geology*, *45*(2-3), 127–145. doi:10.1016/S0166-5162(00)00028-8

Liu, Z., Deng, D., & De Schutter, G. (2014). Does concrete suffer sulfate salt weathering? *Construction and Building Materials*, *66*, 692–701. doi:10.1016/j.conbuildmat.2014.06.011

Lubelli, B., van Hees, R. P. J., & Groot, C. J. W. P. (2004). The role of sea salts in the occurrence of different damage mechanisms and decay patterns on brick masonry. *Construction and Building Materials*, *18*(2), 119–124. doi:10.1016/j.conbuildmat.2003.08.017

Marinos, V., Marinos, P., & Hoek, E. (2005). The geological strength index: applications and limitations. *Bulletin of Engineering Geology and the Environment*, *64*(1), 55–65. doi:10.1007/s10064-004-0270-5

Matsukura, Y., & Matsuoka, N. (1996). The effect of rock properties on rates of tafoni growth in coastal environments. *Zietschrift Fur Geomorphologie N.F.*, *106*, 57–72 ISSN: 00442798.

McLaren, S. J. (2001). Effects of sea spray on vadose diagenesis of Late Quaternary aeolianites, Bermuda. *Journal of Coastal Research*, *17*(1), 228–240 ISSN 0749–0208.

Meunier, J. D., Kirman, S., Strasberg, D., Grauby, O., & Dussouillez, P. (2014). Incipient weathering by Stereocaulon vulcani at Réunion volcanic island. *Chemical Geology*, *382*, 123–131.

Mottershead, D. (1989). Rates and patterns of bedrock denudation by coastal salt spray weathering: A seven-year record. *Earth Surface Processes and Landforms*, *14*. doi:10.1002/esp.3290140504

Mottershead, D. (2013). Coastal Weathering. In J. Shroder (Ed.), *Treatise on Geomorphology*. San Diego, CA. doi:10.1016/B978-0-12-374739-6.00064-6

Mottershead, D., Gorbushina, A., Lucas, G., & Wright, J. (2003). The influence of marine salts, aspect and microbes in the weathering of sandstone in two historic structures. *Building and Environment*, *38*(9-10), 1193–1204. doi:10.1016/S0360-1323(03)00071-4

Mustoe, G. E. (2010). Biogenic origin of coastal honeycomb weathering. *Earth Surface Processes and Landforms*, *35*, 424 – 434. doi:10.1002/esp.1931

Nazir, R., Momeni, E., Armaghani, D. J., For, M., & Amin, M. (2013). Correlation Between Unconfined Compressive Strength and Indirect Tensile Strength of Limestone Rock. *Electronic Journal of Geotechnical Engineering, 18*, 1821 – 1898.

Niini, N., Uusinoka, R., & Emekeokhale, S. (2001). Bedrock parameters of natural surfaces differing from those of excavated road cuts. *Bulletin of Engineering Geology and the Environment, 60*(2), 103–108. doi:10.1007/s100640000094

Pola, A., Crosta, G. B., Fusi, N., & Castellanza, R. (2014). General characterization of the mechanical behaviour of different volcanic rocks with respect to alteration. *Engineering Geology, 169*, 1–13. doi:10.1016/j.enggeo.2013.11.011

Price, D. G. (1995). Weathering and weathering processes. *Quarterly Journal of Engineering Geology and Hydrogeology, 28*, 243–252. doi:doi: 10.1144/GSL.QJEGH.1995.028.P3.03 v. 28 no. 3 p. 243-252

Price, D. G. (2009). *Eningeering geology.* (M. H. de Freitas, Ed.) (pp. 1 – 429. ISBN:9783540292494). Springer.

Proceq. (2006). Proceq Concrete Test Hammer; Operating Instructions.

Pye, K., & Mottershead, D. N. (1995). Honeycomb weathering of Carboniferous sandstone in a sea wall at Weston-super-Mare, UK. *Quarterly Journal of Engineering Geology, 28*, 333–347. doi:10.1144/GSL.QJEGH.1995.028.P4.03

Rad, S., Rivé, K., Vittecoq, B., Cerdan, O., & Allègre, C. J. (2013). Chemical weathering and erosion rates in the Lesser Antilles: An overview in Guadeloupe, Martinique and Dominica. *Journal of South American Earth Sciences, 45*, 331–344. doi:10.1016/j.jsames.2013.03.004

Rijkers, R., & Hack, R. (2000). Geomechanical analysis of volcanic rock on the island of Saba (Netherlands Antilles). In *GeoEngg2000 conference, IAEG, ISSFME,ISRM, Melbourne, Australia* (pp. 1–6).

Rivas, T., Prieto, B., Silva, B., & Birginie, J. M. (2003). Weathering of granitic rocks by chlorides: effect of the nature of the solution on weathering morphology. *Earth Surface Processes and Landforms, 28*(4), 425–436. doi:10.1002/esp.492

Rodriguez-Navarro, C., & Doehne, E. (1999). Salt weathering: influence of evaporation rate, supersaturation and crystallization pattern. *Earth Surface Processes and Landforms, 24*(3), 191–209. doi:10.1002/(SICI)1096-9837(199903)24:3<191::AID-ESP942>3.0.CO;2-G

Sancho, C., Fort, R., & Belmonte, a. (2003). Weathering rates of historic sandstone structures in semiarid environments (Ebro basin, NE Spain). *Catena, 53*(1), 53–64. doi:10.1016/S0341-8162(02)00197-2

Sari, M., & Karpuz, C. (2008). A new empirical failure model for the Ankara andesites. In *9th Regional Rock Mechanics Symposium* (pp. 245–255). Izmir, Turkey: Dokuz Eylul University.

Smith, A. L., Roobol, M. J., Mattioli, G. S., Fryxell, J. E., Daly, G. E., & Fernandez, L. A. (2013). *The Volcanic Geology of the Mid-Arc Island of Dominica* (Vol. 7, p. 249 doi:10.1130/2013.2496.). Geological Society of America. Retrieved from http://books.google.com/books?id=FbmkAQAAQBAJ&pgis=1

Smith, A. L., & Roobol, M J, Gunn, B. . (1980). *T h e Lesser Antilles - A Discussion of the Island Arc Magmatism. Bulletin of Volcanology* (Vol. 43).

Smith, B. J., & McGreevy, J. P. (1988). Contour scaling of a sandstone by salt weathering under simulated hot desert conditions. *Earth Surface Processes and Landforms*, *13*(8), 697–705. doi:10.1002/esp.3290130804

Sunamura, T., & Aoki, H. (2011). Application of an S-shaped curve model to the temporal development of tafoni of salt-weathering origin. *Earth Surface Processes and Landforms*, *36*(12), 1624–1631. doi:10.1002/esp.2175

Tating, F., Hack, R., & Jetten, V. (2013). Engineering aspects and time effects of rapid deterioration of sandstone in the tropical environment of Sabah, Malaysia. *Engineering Geology*, *159*, 20–30. doi:10.1016/j.enggeo.2013.03.009

Tating, F., Hack, R., & Jetten, V. (2014). Weathering effects on discontinuity properties in sandstone in a tropical environment: case study at Kota Kinabalu, Sabah Malaysia. *Bulletin of Engineering Geology and the Environment*. doi:10.1007/s10064-014-0625-5

Tating, F., Hack, R., Jetten, V. (2013). Weathering and deterioration as quantitative factors in slope design in humid tropical areas : case study Northern. In *Engineering in Exotic Environments . 28 September 2012. TUDelf, Netherlands* (pp. 22–28).

Tommasi, P., Verrucci, L., & Rotonda, T. (2015). Mechanical properties of a weak pyroclastic rock and their relationship with microstructure. *Canadian Geotechnical Journal*, *52*(April 2014), 1–13. doi:dx.doi.org/10.1139/cgj-2014-0149

Topal, T., & Sözmen, B. (2003). Deterioration mechanisms of tuffs in Midas monument. *Engineering Geology*, *68*(3-4), 201–223. doi:10.1016/S0013-7952(02)00228-4

Trenhaile, A. S. (2005). Modelling the effect of waves, weathering and beach development on shore platform development. *Earth Surface Processes and Landforms*, *30*(5), 613–634. doi:10.1002/esp.1166

Tuǧrul, A. (2004). The effect of weathering on pore geometry and compressive strength of selected rock types from Turkey. *Engineering Geology*, *75*(3-4), 215–227. doi:10.1016/j.enggeo.2004.05.008

Tugrul, A., & Gurpinar, O. (1997). A proposed weathering classification for basalts and their engineering properties (Turkey). *Bulletin of Engineering Geology and the Environment*, *55*, 139–149. doi:10.1007/BF02635416

USAID. (1991). *St. Vincent and the Grenadines Country Environmental Profile.*

Warkentin, B. P., & Yong, R. N. (1960). Shear strength of montmorillonite and kaolinite related to interparticle forces. *Clays and Clay MInerals*, *9*(1), 210–218. doi:10.1346/CCMN.1960.0090111

Wellman, H. W., & Wilson, a. T. (1965). Salt Weathering, a Neglected Geological Erosive Agent in Coastal and Arid Environments. *Nature*, *205*(4976), 1097–1098. doi:10.1038/2051097a0

Wells, T., Binning, P., Willgoose, G., & Hancock, G. (2006). Laboratory simulation of the salt weathering of schist: 1. Weathering of schist blocks in a seasonally wet tropical environment. *Earth Surface Processes and Landforms*, *31*(3), 339–354. doi:10.1002/esp.1248

Yokota, S., & Iwamatsu, A. (1999). Weathering distribution in a steep slope of soft pyroclastic rocks as an indicator of slope instability. *Engineering Geology*, *55*, 57–68.

Zedef, V., Kocak, K., Doyen, A., Ozsen, H., & Kekec, B. (2007). Effect of salt crystallization on stones of historical buildings and monuments, Konya, Central Turkey. *Building and Environment*, *42*(3), 1453–1457. doi:10.1016/j.buildenv.2005.12.010

Zuquim, M. &, & Rowland, J. (2013). Structural controls on fluid flow at the Onemana area, Coromandel Peninsula, New Zealand. In *New Zealand Geothermal Workshop 2013, Rotorua, New Zealand 17 - 20 November 2013.*

(http://www.uwiseismic.com/General.aspx?id=66) (viewed 10 August 2014)

http://www.columbia.edu/~vjd1/weathering.htm (viewed 16 February 2015)

9. APPENDIX

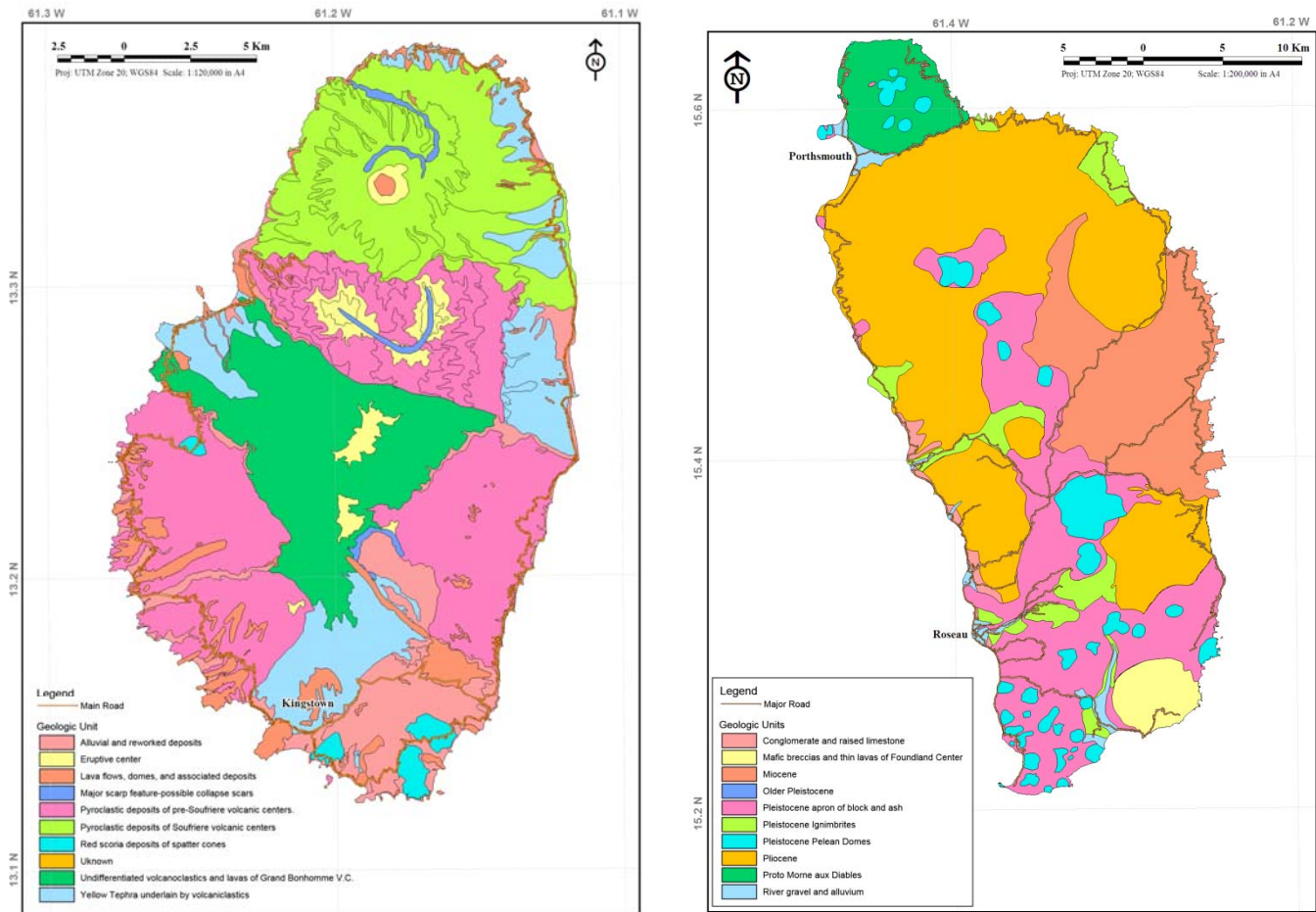## 9.1. General geologic maps of Saint Vincent and Dominica

Figure 42. General geologic maps available from literature. (a) Saint Vincent (b) Dominica

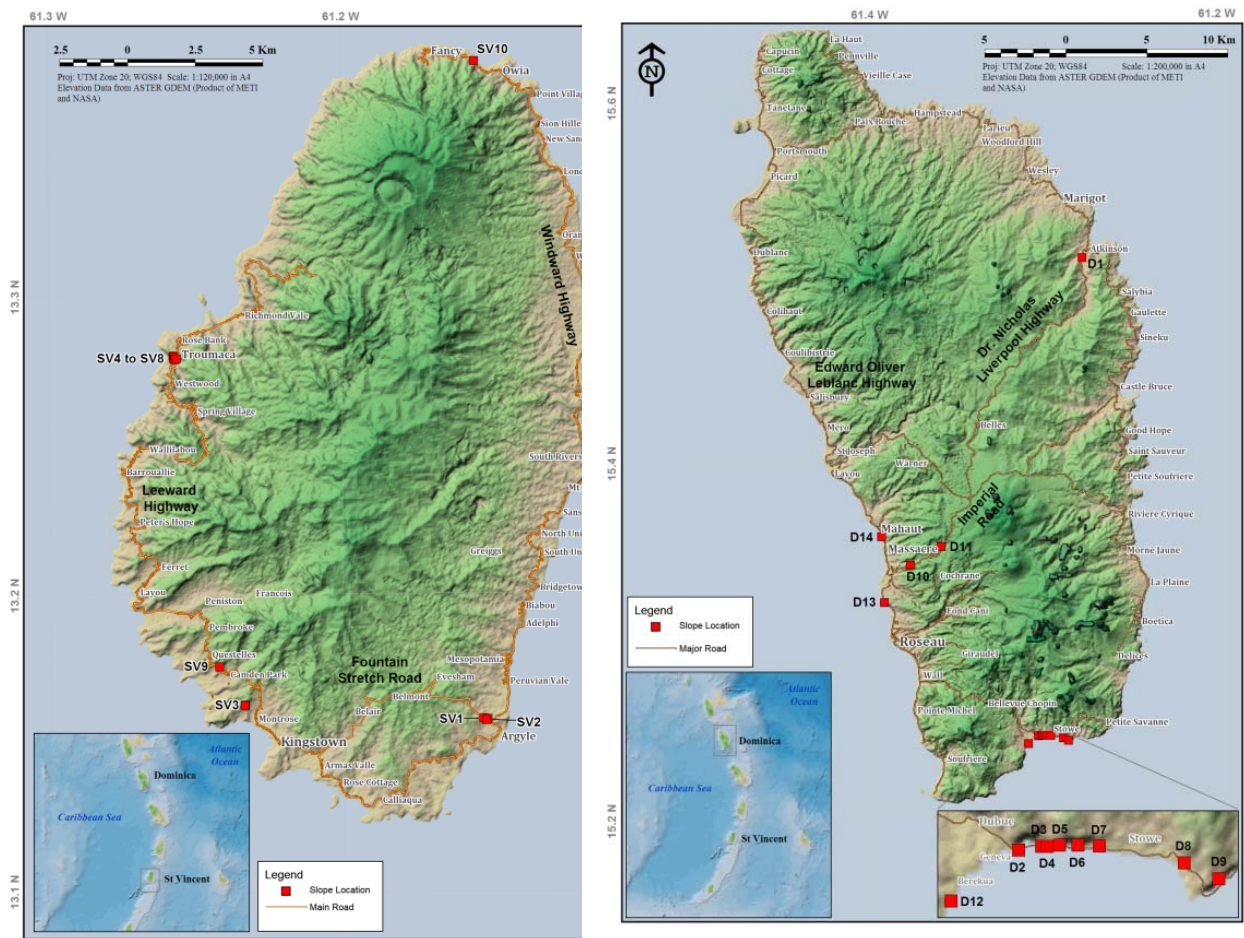## 9.2. Slope description and characterization

Figure 43. Location of investigated exposures in (a) Saint Vincent; (b) Dominica

9.2.1. Exposures in Saint Vincent

Abbreviations:

DS	Discontinuity spacing	Im	Infill material
Rl	Large-scale roughness	Ka	Karst
Rs	Small-scale roughness	term	termination

Exposure	GU	IRS (MPa)	Intact Rock Description	Rock mass properties		
				Weathering		Description of Discontinuities
				BS5930:1981	SSPC	
SV2 Location: Cut slope southeast of control tower of new airport, Argyle Year of excavation: 2013	SV2A Dimension of mapped exposure: L – 20 m H – 15 m	75	Same description of core stone in SV1A but the decomposed part is less than half of the whole rock.	Moderately weathered	0.90	J1 – 85/314 with DS of 0.13 m, slightly curved smooth undulating. J2 – 41/134, 1 m DS, straight rough planar. J3 – 70/258 also 1 m DS, straight, rough undulating and J4 – 52/122 with DS of only 0.04 m, slightly curved rough planar. For all sets, the infill is mainly fine non-smoothening material; no seepage observed
Slope orientation: 50/130 Whole exposure: L – 60 m H – 20 Remarks: Used as a reference slope for SV1	SV2B Dimension of mapped exposure: L - 35 m H – 10 m	8.75	The clasts have the same composition and weathering state. The matrix is greyish purple and is denser than its counterpart in SV1B.	Highly weathered	0.62	J1 – 45/015 has DS of 2 m, terminates within the rock, slightly curved, smooth undulating. J2 – 25/280 has DS of 0.17 m, terminates outside exposure and against other discontinuities and with slightly wavy rough undulating joint planes. J3 – 75/054 with DS of 0.5 m terminates within the exposure, slightly curved rough undulating. J4 - 80/054 is single but notably persisting up to the end of the exposure (bench), slightly curved smooth undulating. The infill material for all sets is fine soft sheared material; no seepage observed
	SV2C Dimension of mapped exposure: L – 20 m H – 15 m	8.75	It is moderately weak, greenish light grey with specks of lighter colour due to the plagioclase phenocrysts.	Highly weathered	0.62	J1 – 68/070 with DS of 1.2 m and terminates within the rock, slightly curved smooth undulating with fine soft sheared material; J2 – 28/132 with 1.4 m DS and terminates within the rock, rough undulating. J3 – 45/001 with very close DS (0.03 m) and terminates against other discontinuities, rough stepped. Both J2 and J3 are slightly curved with medium grained non softening infill materials; J4 – 75/340 with DS of 0.1 m and persistent to adjacent units, slightly curved smooth undulating and filled with fine soft sheared material; no seepage observed

Exposure	GU	IRS (MPa)	Intact Rock Description	Rock mass properties		
				Weathering		Description of Discontinuities
				BS5930:1981	SSPC	
	SV2D Slope orientation: 80/304 Dimension of mapped exposure: L – 24 m H – 15 m	3.125	Weak medium bedded (0.15 m), off-white to light brown, fine-grained tuff, includes 10 cm x 20 cm highly oxidized, medium-sand lenses.	Moderately weathered	0.9	B1 – 60/004, average thickness of 0.15 m, has erosional contact with adjacent unit, slightly curved rough stepped, J1 – 80/303 with DS of 0.01 m, term outside exposure, slightly curved smooth undulating with clay infill material; no seepage observed
SV3 Location: New Montrose, Kingstown Slope orientation: 45/128 Slope height: 120 m Date of excavation: 2006	SV3A Extent of exposure: 60 m x 8 m	150	Very strong, greenish grey, porphyritic basalt. Rock Group: Lava flows, domes and associated deposits	Slightly weathered	0.95	J1- 85/160; DS is 0.23 m; term. outside exposure; slightly curved, rough undulating; Only stained surfaces ; J2-70/130; DS: 0.5 m; term. within exposure; slightly curved, rough stepped; J3- 55/128; S; term. outside exposure; slightly curved, rough undulating ; All sets, only surface staining, no karst, no seepage
Slope orientation: 55/130	SV3B Extent of exposure: 8 m x 3 m	3.125	Block and ash flow with fresh basalt clasts tightly imbedded in moderately weathered but weak, yellowish brown, fine grained tuff matrix Rock Group: Lava flows, domes and associated deposits	Moderately weathered	0.9	Only apparent flow direction (45/010)
SV4 Location: Along Leeward Highway, Troumaca Year of excavation: 1993 Slope orientation: 82/272	SV4A Dimension of mapped exposure: L - 10 m H - 5 m	3.125	Weak; very thinly bedded, yellowish grey, coarse-grained tuff. It includes pumice layer interbeds with maximum thickness of 0.3 m Rock group: Yellow tephra underlain by volcaniclastics	Moderately weathered	0.9	B1:23/086, DS of 0.04 to 0. 0.5 m, term outside of exposure, slightly curved, rough planar with flowing material infill (unconsolidated pumice) resulting to cavities in between bedding planes; J1 – 75/202 with DS of 0.6 m, slightly curved, rough planar and with fine non- softening infill material; J2 – 80/126 has 0.15 m DS, slightly curved, rough planar with only stained joint plane surface, both joint sets terminate within the exposure; no seepage observed

Exposure	GU	IRS (MPa)	Intact Rock Description	Rock mass properties		
				Weathering		Description of Discontinuities
				BS5930:1981	SSPC	
Slope height: 6 m Whole Exposure L – 50 m H – 6 m	SV4B

Dimension of mapped exposure: L – 15 m H – 4 m | 3.125 | Weak, massive, light reddish brown, mixed fine- grain and granule-sized tuff

Rock group: Yellow tephra underlain by volcaniclastics | Highly weathered | 0.62 | J1 – 80/188 has DS of 0.5 m and term against other discontinuities, slightly curved, rough undulating; J2 – 85/200 with 0.5 m DS, term within the exposure, slightly curved, rough stepped; J3 – 66/170, single but highly persistent, straight, rough stepped; All sets: no infill materials, joint planes are damp probably due to earlier rain shower |
| **SV5** Location: Along Leeward Highway, Troumaca Slope orientation: 80/065 Slope height: 10 Date of excavation: 1993 | SV5A Extent of exposure: L - 10 m H - 3 m | 31.25 | Moderately strong and cemented, very thinly bedded, yellowish brown, fine grained tuff

Rock group: Yellow tephra underlain by volcaniclastics | Moderately weathered | 0.9 | B: 15/022; thickness - 0.01 m; term within exposure; straight, rough planar, Im non-cohesive black scoria; J1: 89/358; DS – 0.03 m; term against other discontinuity; slightly curved, rough stepped; no karst; J2: 78/104, DS is 0.1 m, slightly curved, rough undulating, fine, non-softening Im; All sets: dry |
| Slope orientation: 83/232 | SV5B Extent of exposure: L - 60 m H - 6 m | 8.75 | Moderately weak, thinly bedded, yellowish brown, lapilli tuff

Rock group: Yellow tephra underlain by volcaniclastics | Moderately weathered | 0.9 | B: 42/010, thickness - 0.2 m; term. within exposure and in contact with SV5A; straight, rough planar; no Im, only surface staining; J1: 85/186, DS – 0.2 m; term. within rock, slightly curved, rough stepped no Im, only surface staining; J2: 85/204, DS – 0.5 m, term. within rock, straight, rough undulating, no Im, only surface staining; All sets: no karst, dry |
| **SV6** Location: within narrow valley going down to Lower Troumaca Slope orientation: 86/250 | SV6A Extent of exposure: L - 10 m H - 3 m | 8.75 | Moderately weak lapilli tuff with pebble-sized scoria, pumice and andesite clasts in friable, brown, coarse grained matrix

Rock group: Yellow tephra underlain by volcaniclastics | Highly weathered | 0.62 | J1: 75/236; DS – 0.1 m, term. within exposure, straight, rough planar, coarse, non-softening Im; J2: 80/342, DS – 0.3 m, term within exposure, straight, smooth undulating, no Im; J3: 55/283, DS – 0.3 m, term. within exposure and against other discontinuities, straight, rough planar, non-softening fine Im; All sets: no karst, no seepage though rock is damp due to lush vegetation casting shadow over exposure |
| Slope height: 10 m Date of excavation: 1993 | SV6B Extent of exposure: L - 10 m H - 3 m | 3.125 | Clast-supported lahar deposits with dominantly cobble-sized clasts in weak, dark brown matrix

Rock group: Yellow tephra | Highly weathered | 0.62 | J1: 20/302; DS – 0.5 m; term within exposure, slightly curved, rough planar, clay Im; J2: 88/072, DS – 2 m, term within exposure, slightly curved, rough undulating, fine; J3: 70/238, S, term within exposure, slightly curved, rough undulating, non-softening Im; All sets: no karst, No seepage though whole exposure is damp; Erosional contact with SV6A marked by thin cemented layer. |

Exposure	GU	IRS (MPa)	Intact Rock Description	Rock mass properties		
				Weathering		Description of Discontinuities
				BS5930:1981	SSPC	
			underlain by volcaniclastics			
SV7 Location: Along Leeward Highway, Lower Troumaca Slope orientation: 89/024 Slope height: 20 m Date of excavation: 2009	SV7A Extent of exposure: L - 15 m H - 15 m	8.75	Matrix-supported, moderately weak, compacted, thickly bedded lapilli tuff. Clasts are angular, strong andesite fragments and scoria. Matrix is moderately weak, orange brown and fine grained Rock group: Yellow tephra underlain by volcaniclastics	Highly weathered	0.62	B1: 25/044; Ds is 1 m, term. within the rocks, curved, rough undulating; J1: 52/312, DS – 0.1 m, term. within rock, slightly curved, polished stepped, flowing Im; J2: 60/308, DS – 0.08 m, curved, rough undulating, non-softening coarse Im; F1: 75/350, DS – 1 m, term. outside rock, straight, rough planar, non-softening coarse Im; All sets: no karst, no dry
	SV7B Extent of exposure: L - 10 m H - 8 m	3.125	Clast-supported, moderately weak but compacted, reddish brown, tuff breccia Rock group: Yellow tephra underlain by volcaniclastics	Highly weathered	0.62	F1: 75/350, DS – 1 m, term. outside exposure, straight, rough planar; non-softening coarse Im; J2: 88/210, DS – 0.4 m, term. outside rock, straight, rough undulating, non-softening coarse Im; J3: 24/089, S, term. outside rock, straight, rough planar, non-softening fine Im; All sets: no karst, dry
SV8 Location: Lower Troumaca Slope orientation: 70/200 Slope height: 20 m Date of excavation: 1993	SV8A Ext. of exposure: L - 80 H - 15 m Mapped: L - 10 m H - 8 m	1.1	Matrix-supported, friable, very weak, fine-grained lapilli tuff. The clasts are gravel-sized and the matrix is greenish buff ash. Rock Group: Lava flows, domes and associated deposits	Moderately weathered	0.62	J1: 65/228, DS – 0.5 m, term. within the exposure, slightly curved, smooth undulating, flowing Im; J2: 60/288, Ds – 2 m, term. outside exposure, slightly curved, smooth undulating, clay Im; All sets: no karst, dry
	SV8B Extent of exposure: L - 10 m H - 15 m	1.1	Very weak; medium-bedded, greenish light grey, lapilli tuff. Only quartz and biotite are identifiable under the handles. Rock Group: Lava flows, domes and associated deposits	Moderately weathered	0.62	B1: 20/294, DS is 0.2 m, slightly curved, smooth undulating, clay Im; J1: 85/212 DS – 0.5 m, term. within the exposure, slightly curved, rough undulating, clay Im; J2: 87/152, S, term. against beddings, straight, rough planar, fine, non-softening Im; All sets: no karst; damp
SV9	SV9	31.25	Ash and block flow deposits with	Slightly	0.95	J1: 80/084, DS – 0.4 m; term. within the exposure, straight, smooth undulating,

Exposure	GU	IRS (MPa)	Intact Rock Description	Rock mass properties		
				Weathering		Description of Discontinuities
				BS5930:1981	SSPC	
Along Leeward Highway near Campden Park, Kingstown Slope orientation: 65/306 Slope height: 20 m Date of excavation: 2014	Ext. of exposure: L - 100 m H - 3 m		andesite clasts in moderately strong, brownish light grey tuff matrix Rock Group: Lava flows, domes and associated deposits	weathered		clay Im; J2: 45/340, DS – 0.05 m, term. within exposure; slightly curved, rough stepped, clay Im; J3: 70/014, DS – 0.2 m, term. within exposure; straight, rough stepped, clay Im; All sets: no karst
SV10 Location: Windward Highway between Fancy and Owia Year of excavation: 2010 Slope orientation: 74/312 Slope height: 20 m Whole exposure: L - 50 m H - 20 m	SV10A Dimension of mapped exposure: L – 15 m H – 5 m	75	Strong, light grey, porphyritic andesite with hornblende phenocrysts	Fresh	1	Discontinuities forming large to very large polyhedral blocks. J1 – 82/244, J2 - 80/150, DS of 1 m, slightly curved rough stepped and no infill material but stained joint planes; J3 – 40/0130 with DS of 0.5 m, wavy and rough stepped, with fine non-softening Im. All sets terminate within the exposure; no karst along developed discontinuity planes
	SV10B Dimension of mapped exposure: L – 15 m H – 8 m		Strong, light grey, porphyritic andesite with hornblende phenocrysts	Fresh	1	J1 – 30/048 has DS of 0.36 m, term against other joints, slightly curved; J2 – 70/324, DS is 0.05 m; Joint planes of both sets are rough stepped with no infill materials; J3 – 68/104 has DS of 0.15 m, J4 – 60/029 and J5 – 82/128, 0.25 m. J3, J4, J5 term within the exposure, slightly wavy, rough planar and no Im. The joints are very tight to very open.
	SV10C Dimension of mapped exposure: L – 15 m H – 20 m		Strong, light grey, porphyritic andesite hornblende phenocrysts	Fresh	1	J1 – 85/270 with DS of 0.23 m, term within the exposure, slightly curved, polished planar. J2 – 3/064 with DS of 0.17 m, term against other discontinuities, straight, smooth planar. J3 – 60/198, DS of 0.2 m, term within the exposure, straight, smooth undulating; J4 – 60/248, DS is 0.2 m, term within the rock, straight, smooth undulating; J5 – 75/060, single within the exposure but persistent All sets: No Im aperture is varying from open to very open, dry

9.2.2. Exposure in Dominica

Exposure	GU	IRS (MPa)	Intact Rock Description	Rock mass properties		
				Weathering		Description of Discontinuities
				BS5930:1981	SSPC	
D1 Along Dr. Nicholas Liverpool Highway Location: near, Marigot along Dr. Nicholas Liverpool Highway	D1A Mapped exposure: L – 40 m H – 4 m	31.25	Clast-supported volcanic breccia with fresh, strong, dark grey, porphyritic, generally fine-grained andesite clasts set in moderately strong, brown, coarse-grained andesitic matrix.	Moderately weathered	0.9	Three dominant discontinuity sets: J1-75/011, DS is 0.5 m and term against other discontinuities, wavy, smooth undulating; J2-35/136, DS of 0.2 m, term against other discontinuities, straight, rough undulating; J3-75/308, S, term within the exposure, slightly curved, rough undulating; All sets: fine non-softening Im, during fieldwork, water, probably surface run-off from previous rain, seen flowing from top of the slope
Year of excavation: 2011 Slope orientation: 86/158 Slope height: 20 m Total exposure dimension: L - 100 m H - 15 m	D1B Dimension of mapped exposure: L – 7 m H – 4 m	75	Strong, greenish light grey, porphyritic, basalt dike.	Slightly weathered	0.95	J1 – 63/008, DS of 0.2 m; J2-50/154 with DS of 0.5 m; J3 – 80/098 with DS of 0.1 m; all joints term within the unit, straight, rough stepped, fine non-softening Im; Water locally dripping from some discontinuity, discontinuity planes have iron staining.
	D1C Mapped exposure: L – 40 m H – 6 m		Matrix-supported volcanic breccia with fresh, strong, dark grey, porphyritic, generally fine grained andesite clasts with moderately strong, brown, coarse-grained andesitic matrix.	Moderately weathered	0.9	J1 – 85/266 with 0.1 m DS; J2 – 70/312 with DS of 0.07 m. Both sets term within the exposure, straight, rough planar, fine non-softening Im. Water flowing from top of the slope over about a 3 m- wide part of the exposure. Traces of water flow still visible in other dry parts. Usually found horizontally intertonguing with D1A.
	D1D Dimension of mapped exposure: L – 30 m H – 12 m		Volcanic breccia with clast and matrix same composition as in D1C except that the clasts are moderately weathered and the matrix is weak and generally highly friable.	Highly weathered	0.62	Has randomly oriented short discontinuities that terminate against each other. Tight opening. Clast-matrix interfaces are open (~ 2 mm wide).
D2 Location: Dubuc - Fond St. Jean Road	D2A Dimension of mapped	8.75	Brownish-grey ,very gravelly sand with many cobbles and some boulders; poorly sorted, subrounded to subangular dominantly andesite	Moderately weathered	0.9	Fault – 70/202, persistence >20 m, slightly curved, rough undulating with 15 cm opening and displacement of 20 cm; lenses of matrix-supported coarse sandstones demarcated by cemented silt-sized lamina boundaries, lenses extend to about

Exposure	GU	IRS (MPa)	Intact Rock Description	Rock mass properties		
				Weathering		Description of Discontinuities
				BS5930:1981	SSPC	
Year of excavation: ca. 1950 Slope orientation: 86/158 Slope height: 100 m Total exposure dimension: L - 200 m H - ~100	exposure: L – 20 m H – 20 m		and dacite clasts; matrix outermost surface can be scratched by pick of geologic hammer becoming highly compacted in fresh surface; lahar deposits associated with Pleistocene ash and block flow deposits			10 m with maximum thickness 0.3 to 0.5 m.
	D2B Dimension of mapped exposure: L – 150 m H – 10 m	8.75	Same general description with D2A but increased volume of boulder size clasts; soil type is cobble many boulder and much gravelly sand	Moderately weathered	0.9	Generally dense and massive with small lenses of fine sand (extend to only few centimetres)
	D2C Dimension of mapped exposure: L – 150 m H – 10 m	8.75	Same description in D2A	Moderately weathered	0.9	generally dense, three notable fine sandstone lenses, topmost lenses (about 9 m from base of slope) extends to about 30 m and thickness of 0.3 to 0.5 m and cut by J1 – 80/188 and J2 – 80/180, J1 is persistent to only up to 3 m, both sets appear to be slightly curved and rough undulating
	D2D Slope height: ~ 100 m Dimension of mapped exposure: L – 50 m H – max. 6 m	8.75	Brownish grey gravelly sand with some cobbles; cobbles and gravel clasts are subangular to subrounded, fresh to slightly weathered	Moderately weathered	0.9	dense; with apparent flow direction orientation (23/250), ~ 5 cm single interbed of fine sand at the base; cavities at the base of the slope, salt deposits in the surface
D3 Location: Dubuc - Fond St. Jean Road, Dubuc Year of excavation: ca. 1950 Slope orientation: 88/188; Slope height: 100 m		8.75	Cobbles and gravel clasts are subangular to subrounded, fresh to slightly weathered	Moderately weathered	0.9	J1 75/192, DS is 0.5m, slightly curved, rough undulating, fracture is open up to 10 cm max, no infill; no karst

Exposure	GU	IRS (MPa)	Intact Rock Description	Rock mass properties		
				Weathering		Description of Discontinuities
				BS5930:1981	SSPC	
~ 5 above msl Total exposure dimension: L - 100 m H - ~15 m						
D4 Location: Dubuc - Fond St. Jean Road, Dubuc Year of excavation: ca. 1950 Slope orientation: 80/178; Slope height: 100 m ~ 5 above msl Total exposure dimension: L - 100 m H - ~15 m			cobbles and gravel clasts are subangular to subrounded, fresh to slightly weathered	Highly weathered	0.62	No observable discontinuity
D5 Location: Dubuc - Fond St. Jean Road, Dubuc Year of excavation: ca. 1950 Slope orientation: 88/188; Slope height: ~100 m ~ 5 above msl Total exposure dimension: L - 30 m H - ~20 m			cobbles and gravel clasts are subangular to subrounded, fresh to slightly weathered	Moderately weathered	0.9	Fracture parallel to slope - 70/178 (single) roots coming out from discontinuity
D6 Location: Dubuc - Fond St. Jean Road, Dubuc Year of excavation: ca. 1950 Slope orientation: 85/202 Slope height: ~100 m 10 - 15 m from msl Total exposure dimension: L - 100 m H - ~6 m		8.75 (matrix)		Highly weathered	0.62	no structure recorded
D7 Location: Dubuc - Fond St. Jean Road, Dubuc Year of excavation: ca. 1950		8.75 (matrix)		Highly weathered	0.62	fracture - 75/198, single , slightly curved, rough undulating

Exposure	GU	IRS (MPa)	Intact Rock Description	Rock mass properties		
				Weathering		Description of Discontinuities
				BS5930:1981	SSPC	
Slope orientation: 85/138 Slope height: 100 m 10 - 15 m from msl Total exposure dimension: L - 100 m H - ~6 m						
D8 Location: Dubuc - Fond St. Jean Road, in Stowe Slope orientation: 85/250 Slope height: 10 m Date of excavation: 1960	SV8A Extent of exposure: 40 m x 60 m Mapped: 12 m x 6 m	3.125	Block and ash flow with dominantly fresh cobble-sized clasts supported by moderately weak reddish brown lapilli tuff	Highly weathered	0.62	J1: 25/154, DS – 1 m, slightly wavy, rough undulating, clay Im; J2: 80/250, DS – 0.08; persist to adjacent unit; straight, rough undulating; Both sets: clay Im, no karst; dry but whole exposure damp due to shadow of lush vegetation
	D8 Extent of exposure: L - 40 m H - 60 m	8.75	Tuff breccia with gravel-sized clasts set in moderately strong, reddish brown, coarse grained matrix	Highly weathered	0.62	J1: 75/062, DS – 1 m, term. within exposure, straight, rough planar; J2: 80/250, DS – 0.3, persist to adjacent unit, straight, rough planar; J3: 50/254, S, term. within unit, curved, smooth undulating; All sets: coarse soft-sheared Im, no karst
D9 Location: Dubuc - Fond St. Jean Road in Point Carib Slope orientation: 60/130 Slope height: 12 m Date of excavation: 1960	D9A Extent of exposure: L - 60 m H - 7 m	75	Strong dark grey porphyritic andesite	Slightly weathered	0.95	J1: 63/144; DS – 0.2 m; term. against other discontinuities, slightly curved, smooth undulating, clay Im; J2: 62/010, DS – 0.5 m; term against other discontinuities, slightly curved, rough undulating, clay Im; J3: 70/098, Ds – 0.5 m; term. against other discontinuities slightly curved, rough stepped, no Im, surface staining; J4: 70/198, DS – 0.5; term. outside exposure, slightly curved, rough stepped, no Im, surface staining; J5: 60/142, DS – 3 m; term, within the unit, no Im, surface staining ; All sets: no karst, dry
Slope orientation: 86/106	D9B Extent of exposure: 60 m x 7 m Mapped:	75	Strong dark grey porphyritic andesite	Slightly weathered	0.95	J1: 70/109, DS – 0.3 m, term within exposure, slightly curved, rough planar, no Im only surface staining; J2: 45/080, DS – 0.3; term. within exposure; curved, rough stepped, clay Im; J3: 86/106, 2 m, term. within exposure; curved, rough stepped, fine non-softening Im ; J4: 50/204, S; term. within exposure; curved, smooth planar, clay Im; All sets: no karst, dry

Exposure	GU	IRS (MPa)	Intact Rock Description	Rock mass properties		
				Weathering		Description of Discontinuities
				BS5930:1981	SSPC	
	15 m x 7 m					
Slope orientation: 70/134	D9C Extent of exposure: L -60 m H - 7 m Mapped: 15 m x 3 m	8.75	Clast – supported block and ash flow deposits with mainly cobble-sized clast set in coarse grained matrix	Highly weathered	0.62	J1: 75/079, DS – 0.3 m, term. within exposure, straight, rough undulating; J2: 79/274, DS – 0.1 m, term within exposure; straight, rough planar; All sets: clay Im, no karst, dry
D11 Location: Imperial Road Year of excavation: 2011 Slope orientation: 85/70 Slope height: 8	Dimension of mapped exposure: L – 100 m H – 7 m	1.1	Very weak, reddish-brown, fine-sand to clay tuff breccia	Completely weathered	0.35	J1: 80/288, DS is 5 m; J2: 79/132; J3:66/048; J4: 85/242. All sets: terminating outside the exposure; straight, polished planar, Im: clay, no karst, damp.
D12 Location: Pierre Charles Boulevard Year of excavation: 2000? Slope orientation: 63/130 Slope height: 15 Total exposure dimension: L - 100 m H - 8 m		8.7	Moderately weak, dense, light-grey, gravelly-coarse-sand-sized ignimbrite. Clasts are dominantly slightly weathered pumice	Moderately weathered	0.9	Massive; no observable discontinuity sets
D13 Location: Edward Oliver Leblanc Highway Year of excavation: 2000? Slope orientation: 85/234 Slope height: 45 m Total exposure dimension: L - 14 m H - 7.5 m		8.75	Moderately weak, yellowish-grey to grey, gravelly-coarse-sand-sized BAF, clasts are fresh to slightly weathered, angular, cobble to gravel-sized, andesite and dacites	Highly weathered	0.62	No observable discontinuity sets
D14 Location: Leeward Highway, Mahaut-Massacre boundary	D14A Dimension of mapped exposure:	75	Strong, grey, porphyritic andesite. In some faces, bout 5 mm-thick maroon of reddish brown discolouration coating was observed.	Fresh	1	With pillow structures. Four joint sets including pillow boundaries forming dominantly small, mixed tabular and columnar blocks : J1 - 50/140 with DS of 0.2 m, slightly curved, smooth planar; J2 – 20/359, 0.22 m DS, straight, rough

Exposure	GU	IRS (MPa)	Intact Rock Description	Rock mass properties		
				Weathering		Description of Discontinuities
				BS5930:1981	SSPC	
Year of excavation: 1960 Slope orientation: 65/192 Slope height: 20 Total exposure dimension: L - 50 m H - 10 m	L – 10 m H – 6 m					stepped; J3 – 70/252, 0.18 m DS, straight, polished undulating; J4 – 75/010 with DS of 0.15 m, straight, rough planar. All joint sets: term against other discontinuities
	D14B Dimension of mapped exposure: L – 8 m H – 2 m	75	Strong, greenish-brownish grey, porphyritic andesite.	Moderately weathered	0.9	With spheroidal weathering. Four joint sets forming small to very small polyhedral blocks: J1 – 89/348 with DS of 0.3 m, straight, rough planar with fine soil infill material; J2 – 80/064 with DS of 0.6 m , slightly curved, rough planar, fine soft-sheared Im; J3 – 61/012 with 0.5 DS , slightly curved, rough planar with fine soil Im ; J4 – 25/041 with 0.1 m DS, straight, rough planar with fine non-softening Im. The joint sets terminate against or crisscross with other discontinuities and have open apertures. All discontinuities dry.
	D14C Dimension of mapped exposure: L – 15 m H – 3 m	75	Strong, greenish grey, porphyritic andesite.	Slightly weathered	0.95	J1- 55/139, DS of 0.15 m, straight, smooth planar; J2 – 18/357, DS is 0.07 m, straight, rough stepped; J3 – 70/252 with DS of 0.1 m; J4 – 75/013 with DS 0.12 m; J5 – 42/135 with DS of 0.2 m; roughness of J3, J4 and J5 is straight, rough planar; All sets: fine non-softening Im, dry
	D14D Dimension of mapped exposure: L – 5 m H – 6 m on both sides of the whole exposure	75	Fragmented, strong, greenish-brownish grey, porphyritic andesite. Rock material makes about 70% of the rock mass but the matrix is highly weathered almost grading to residual soil.	Moderately weathered	0.9	Slumped blocks due to loss of matrix cohesion. Four dominant joint sets but many randomly oriented small joints present very small to small tabular blocks: J1 – 60/012 with 0.3 m DS, J2 – 83/064 with DS of 0.1 m, J3 – 87/348 with DS of 0.15 m and J4 – 25/041 with DS of 0.1 m; all sets: straight, rough planar; Im are fine non-softening for J1, fine softening for J2 and medium softening for J3 and J4. The joint openings are wide particularly in the slumped portion of the exposure. No seepage observed.

9.3.   Scatter plots of rock properties with SSPC WE of individual GUs

Table of references in the scatter plots

Lithology		Weathering degree (BS5930, 1981)		SSPC WE
And	Andesite	I	Fresh	1
Lavas	AP, BP, BM			
AP	Andesite	II	Slightly weathered	0.95
Bslt	Basalt	III	Moderately weathered	0.9
BP	Pillow basalts	IV	Highly weathered	0.62
BM	Massive basalts	V	Completely weathered	0.35
Vlcs	Volcanoclastics (block-and-ash flow (BAF) and (tuff breccias)			
Tuff	Tuff			
Mtrx	Matrix of Vlcs			
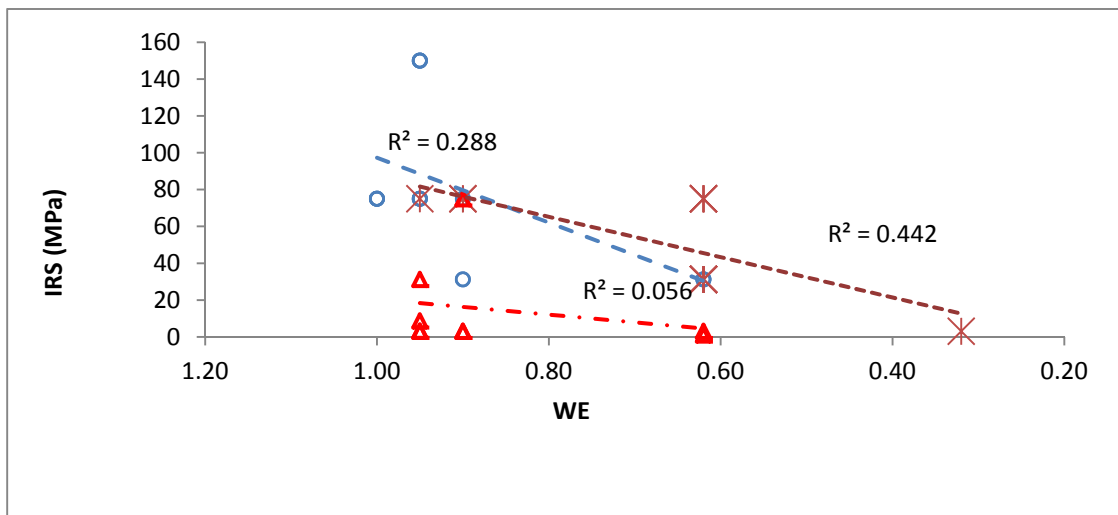
Figure 44. IRS vs. SSPC WE.
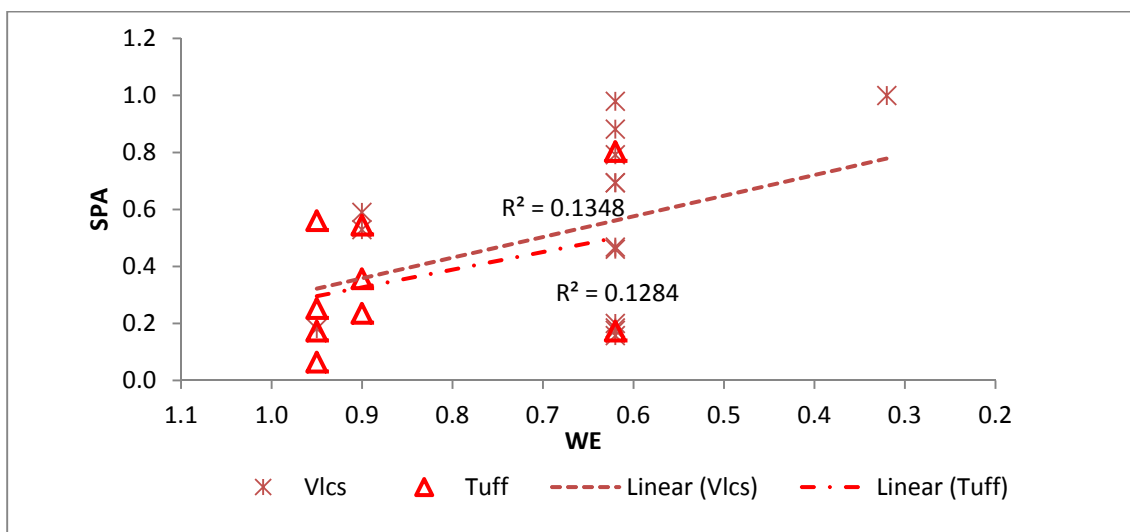
Figure 45. .SPA vs. SSPC WE.
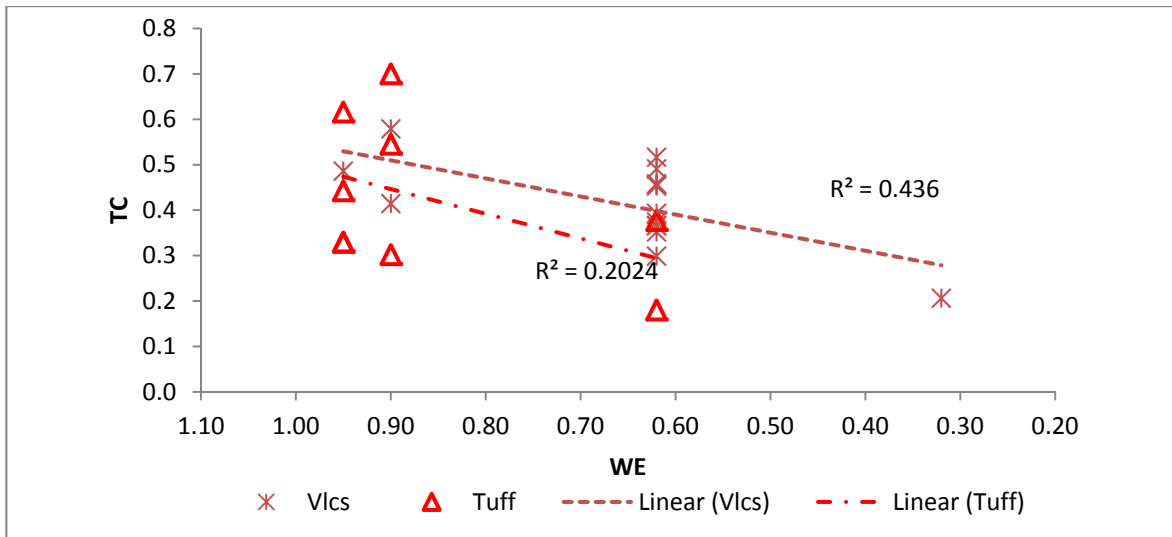
Figure 46. TC vs. WE.
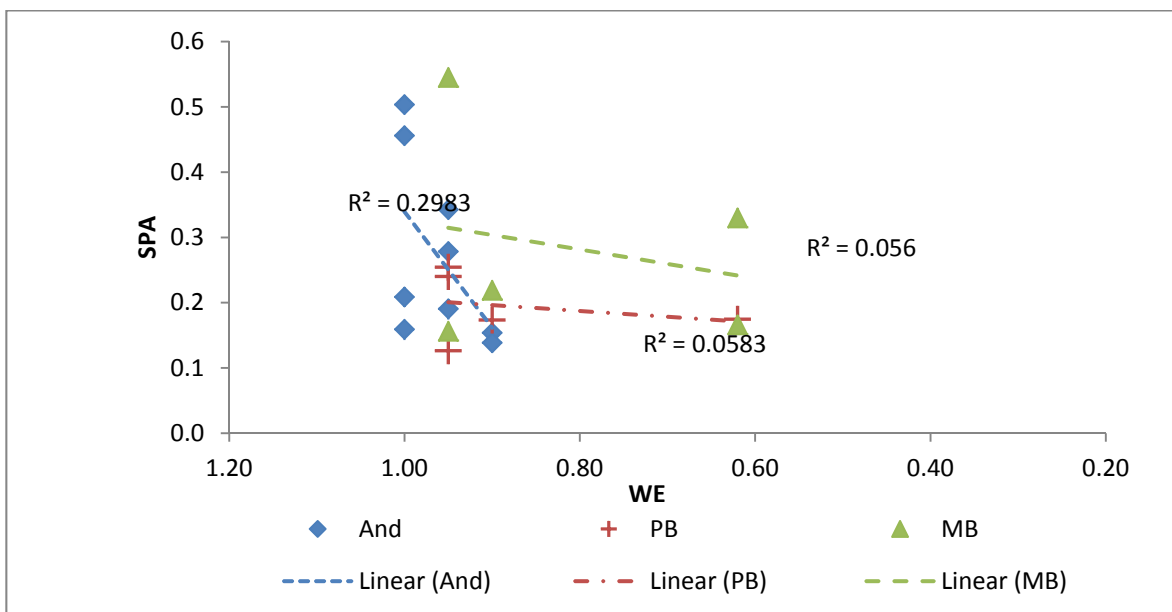
Figure 47. SPA vs. WE
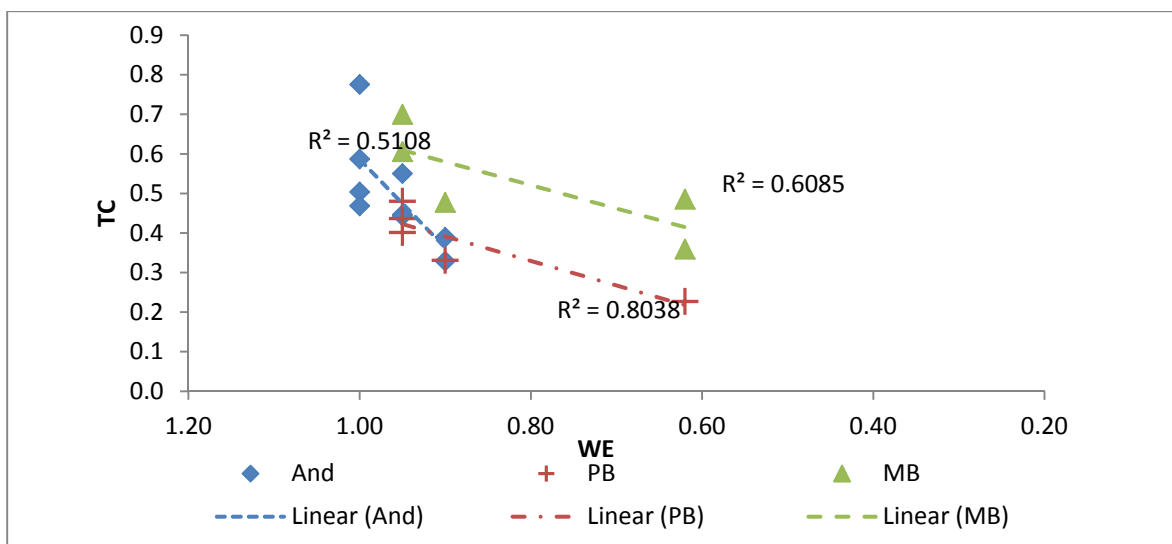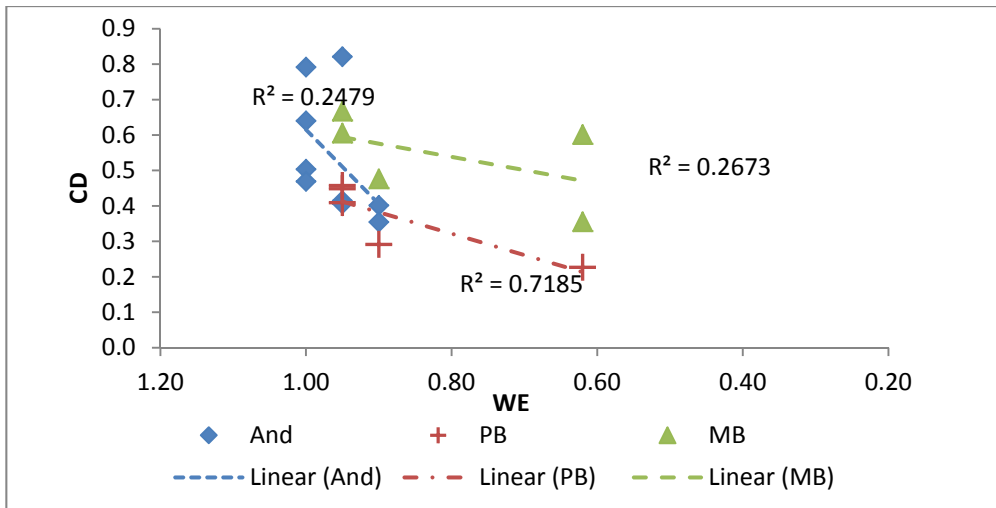
Figure 48. TC vs. WE. .
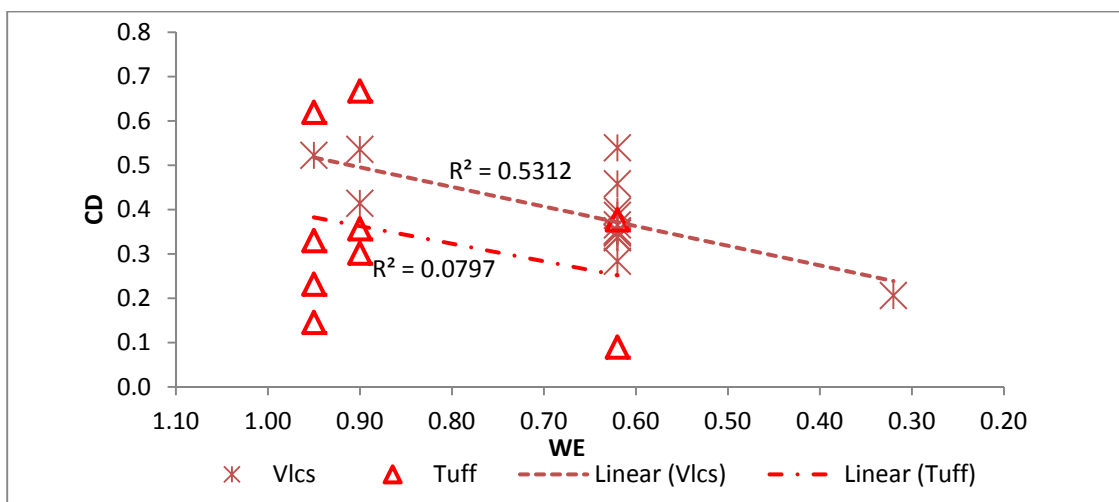
Figure 49. CD vs. WE .

Figure 50. CD vs. WE.

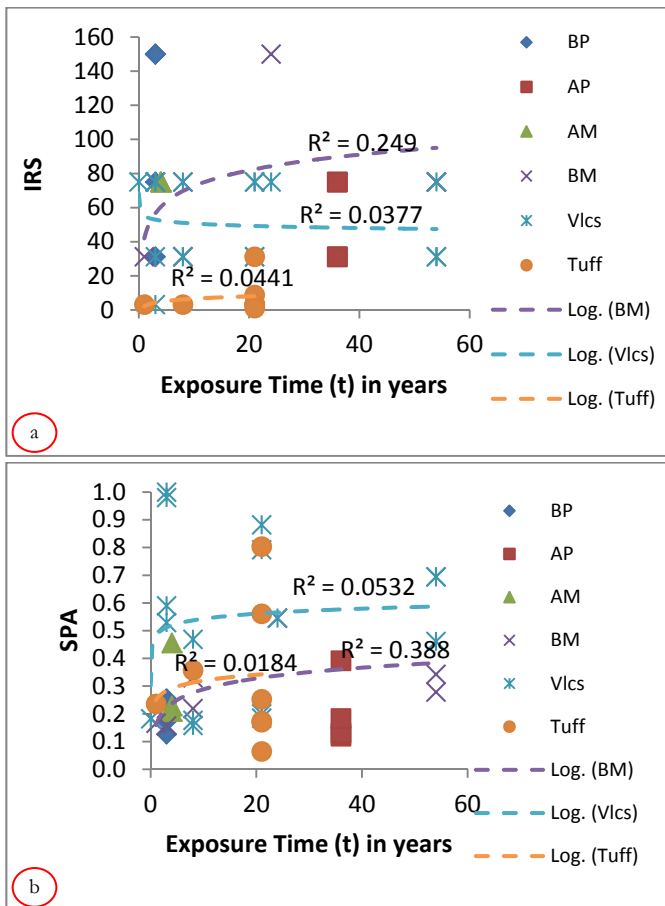## 9.4. Scatter plots of rock properties vs. time of exposure

Figure 51. Relationship of time with SPA and IRS. There is weak correlation of the IRS (a) and SPA (b)with exposure time. A slight reduction though is seen in the Vlcs.
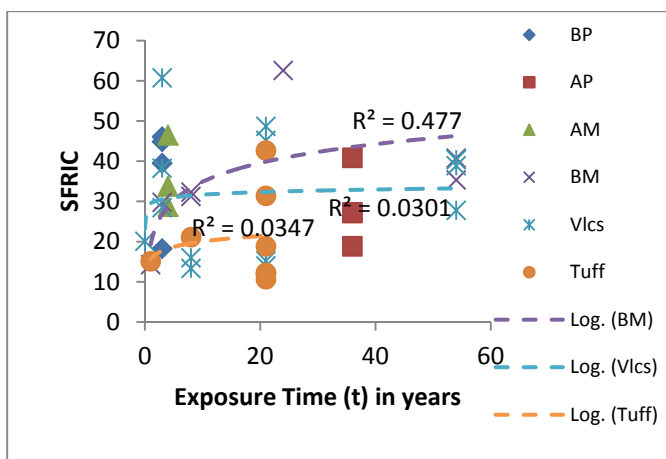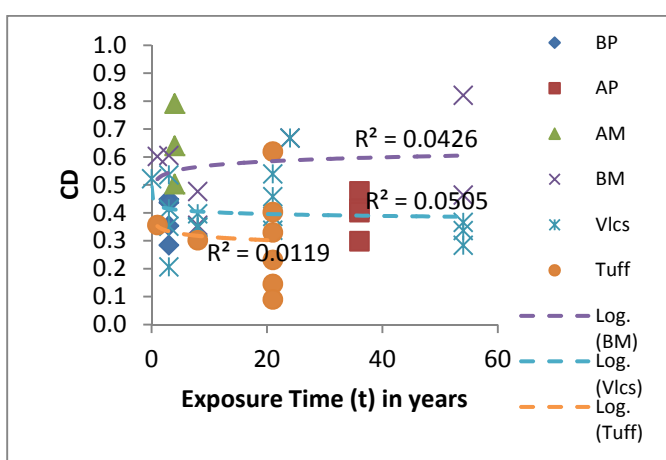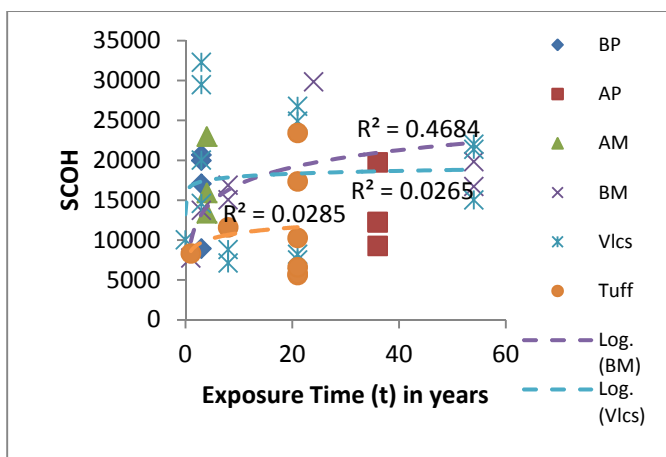
Figure 52. SFRIC vs. exposure time

Figure 53. CD vs. exposure time

Figure 54. SCOH vs. exposure time